First-Day Road Log: Mesa Portales And The Sierra Nacimiento Front Via Arroyo Chijuilla, The Piedra Lumbre Road, And San Miguelito Canyon

Kevin M. Hobbs, Jerry Kendall, Susan Lucas Kamat, K. Luke Martin, and Amanda Cantrell
2025, pp. 1-57. https://doi.org/10.56577/FFC-75.1

in:

Geology of the Eastern San Juan Basin - Fall Field Conference 2025, Hobbs, Kevin M.; Mathis, Allyson; Van Der Werff, Brittney;, New Mexico Geological Society 75 th Annual Fall Field Conference Guidebook, 227 p. https://doi.org/10.56577/FFC-75

This page is intentionally left blank to maintain order of facing pages.

FIRST-DAY ROAD LOG:

MESA PORTALES AND THE SIERRA NACIMIENTO FRONT VIA ARROYO CHIJUILLA, THE PIEDRA LUMBRE ROAD, AND SAN MIGUELITO CANYON

KEVIN M. HOBBS[1], JERRY J. KENDALL[2], SUSAN LUCAS KAMAT[3], K. LUKE MARTIN[1], AND AMANDA CANTRELL[4]

[1]New Mexico Bureau of Geology and Mineral Resources, 801 Leroy Place, Socorro, NM 87801; kevin.hobbs@nmt.edu
[2]Department of Earth and Planetary Sciences, University of New Mexico, Albuquerque, NM 87131
[3]New Mexico Environment Department Surface Water Quality Bureau, 1190 St. Francis Drive, Suite N4050, Santa Fe, NM 87505
[4]Badlands Scientific Expeditions, LLC, Edgewood, NM 87015

Assembly Point: Circle A Ranch entry road just west of main ranch house
Departure Time: 7:30 AM
Distance: 61.5 miles
Stops: 4

Views, landmarks, and outcrops are given using the clock system, where 12:00 is straight ahead, 3:00 is to the right, and 9:00 is to the left. Driving distances are given in imperial units.

SUMMARY

Day 1 of the field conference travels a counter-clockwise loop around Mesa de Cuba and Mesa Portales, the two stratigraphically highest of several sandstone-capped mesas marking the southern edge of the San Juan Basin near Cuba. Most of the drive is through regions of sedimentary rocks deposited at or near sea level in the Western Cordillera from the Mesozoic through the early Cenozoic. Now higher than 2 km (1.2 mi) above sea level, these sediments record a fascinating tale of tectonic evolution of the western part of our continent. Subsidence that accommodated sediment deposition was facilitated by a combination of crustal processes that we discuss throughout the day. Uplifts during the compression-dominated depositional history of these rocks provided a sediment source, but also led to unconformities that we discuss at Stops 2 and 3. The late Cenozoic uplift of the Colorado Plateau leads to today's high elevation, but tensional tectonics relating to the Rio Grande rift—just a few kilometers to our east—now changes the landscape. A unifying question for each of today's stops is "What can sedimentary rocks tell us about the tectonic history of a region?".

7:30 AM: Depart Circle A Ranch in caravan.

8:00–9:30 AM: Stop 1 involves a short walk into a disused stone quarry where excellent exposures of bedding structures can be found in the Paleogene San Jose Formation. Our goals here are to investigate these structures and put them into depositional and deformational context.

10:00–11:30 AM: Stop 2 again involves a short walk. Several interesting geologic features are on wondrous display here: silcretes, a small-offset fault, the Nacimiento Formation-San Jose Formation contact, and the black mudstones of the Ojo Encino Member of the Nacimiento Formation. At this stop, our goals are to discuss the uncertainty surrounding the age of the lower San Jose Formation, to inspect a small basin-internal fault and discuss its implications, to visit an excellent example of a Nacimiento Formation silcrete and discuss the paleogeographic and paleoenvironmental inferences one makes from it, and finally to view and wonder at artists' interpretations of these landscapes.

12:15–1:45 PM: Stop 3 visits the western edge of Mesa Portales in Cañon Jarido. Here, we view the contact between the uppermost Cretaceous unit (Kirtland Formation) and lowermost Paleogene unit (Kimbeto Member of the Ojo Alamo Formation) in this corner of the San Juan Basin. These units record a major shift in the tectonic history of the basin that can be elucidated with careful inspection. Nearby fossil localities in uppermost Cretaceous rocks recently have afforded new discoveries about the dinosaurs that made the basin their home in the late Mesozoic. These units also were the subject of a paleontological controversy in the early 21st century that will be discussed in précis.

3:00–5:00 PM: Stop 4 has two substops. At Stop 4A, a broad vista provides an overview of the 5-km (3.1-mi)-thick Phanerozoic section in the San Juan Basin (complicated by some pesky faults!). With this view before us, we discuss the continental-scale implications of these sedimentary units, and how modern understanding of the tectonic development of North America has been built by the gradual increase of knowledge provided by the works of generations of scientists. At Stop 4B, an outcrop of the Entrada Sandstone-Todilto Formation contact brings us back to the rocks. The paleoenvironmental and paleotectonic implications of this contact are discussed. Then, these units' utility as reservoirs for oil, gas, water, and carbon is applied to what we observe in outcrop.

6:30 PM: New Mexico Geological Society banquet at Circle A Ranch (held outdoors, dress appropriately).

[Waypoint]
Miles since last entry
Mileage Description

Waypoint 1.01 [36.0864°, −106.9314°]

0.0 Assemble caravan on Los Pinos Road (the road providing access to Circle A Ranch) just uphill from the blue gate at the entrance to Circle A. You are parked upon a mountain-front terrace deposit of the Pleistocene(?) Rio de los Pinos that extends from the foot of the Sierra Nacimiento, 2 km (1.2 mi) northeast of here, to U.S. Route 550, approximately 6 km (3.7 mi) southwest of here. This terrace is the most extensive in the Rio de los Pinos drainage, but there are at least two others: a higher, older terrace caps discontinuous mesas on the north side of the drainage (Fig. 1.01); and a lower, younger terrace is preserved on inset surfaces farther downstream. This terrace deposit contains poorly to moderately sorted sand through boulders and is at least 7 m (23 ft) thick (Fig. 1.02 and 1.03). The terraces of the Sierra Nacimiento mountain front are largely unstudied; their ages, thicknesses, composition, paleoclimatic and/or neotectonic significance, and relationships to downstream terraces of the Rio Puerco are poorly documented. Just to the northwest, this terrace has been removed by erosion, exposing a small badlands valley that the Circle A Ranch dwellers call "Little Grand Canyon" (Fig. 1.04). The badlands expose the interbedded sandstones and mudstones of the Regina Member of the San Jose Formation. The well-expressed bedding of that unit, combined with the excellent unvegetated outcrops in the "Little Grand Canyon," allow determination of low dip angles of less than 5° here. About 2 km (1.2 mi) to the east, uplift along the Nacimiento fault results in a vertical to overturned Mesozoic section.

ZERO ODOMETER as you pass the blue gate leaving Circle A Ranch.

0.15
0.15 Road to the left (northeast) leads to the Los Pinos Trailhead, from which one can make a short, steep hike through dense spruce and fir forests to the San Pedro Parks and headwaters of the Rio Puerco. However, public access to that trailhead was stolen in the mid-2010s by a landowner who gated the road, cutting off ingress to public lands. This is a disturbing and increasingly common trend in New Mexico.

0.25
0.4 Cattle guard. High fence and driveway to right (west).

0.2
0.6 Pavement begins.

0.2
0.8 Cross Rito de los Utes. A large narrowleaf cottonwood (T'iis, *Populus angustifolia*) on the right; many more can be found about the Circle A Ranch. The narrowleaf

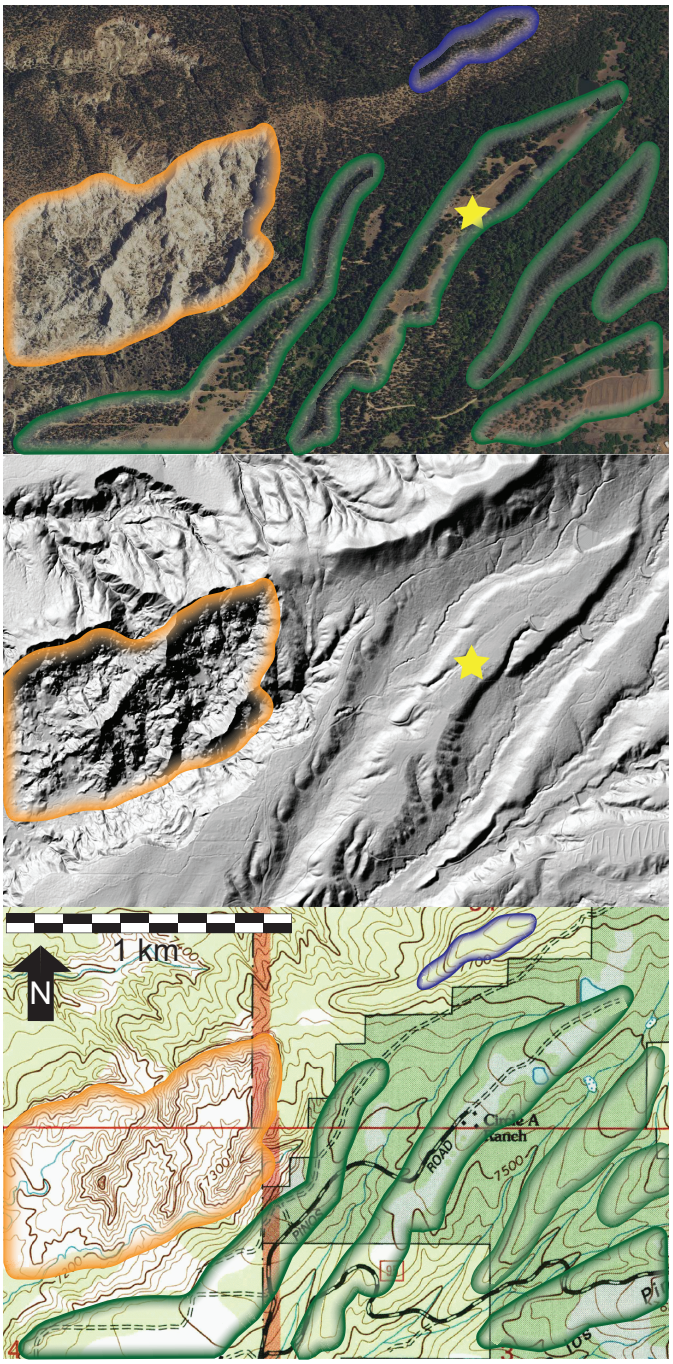

Figure 1.01. Aerial photograph (top), hillshade DEM (middle), and USGS topographic map (bottom) of the mountain front around Circle A Ranch and upper Rio de los Pinos. Blue outline marks the highest terrace-pediment deposit of the area. Green outlines mark the more extensive terrace-pediment deposits of the Rito Leche surface of Bryan and McCann (1936); Circle A Ranch is built upon this terrace. The orange outline marks the deeply eroded area known as "Little Grand Canyon" where an unnamed tributary to Arroyo San Jose has removed all surficial deposits and exposed badlands in the San Jose Formation. Yellow star marks the ranch house at Circle A Ranch. Contour interval in bottom image is 20 ft. Scale and orientation are identical in all images.

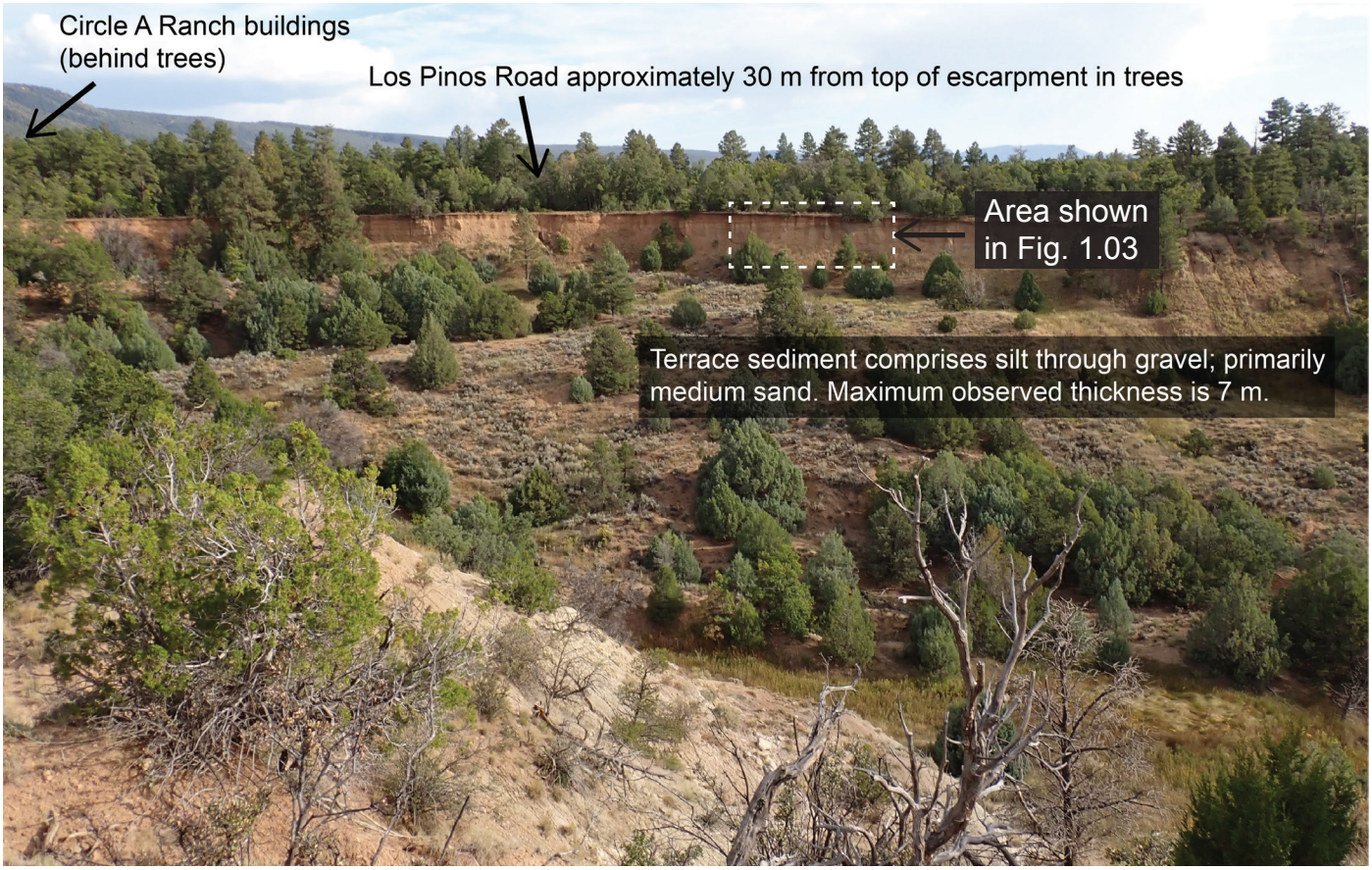

Figure 1.02. Photograph looking southeast from within the "Little Grand Canyon" toward the Los Pinos Road where it enters Circle A Ranch. The continuous medium brown cliff outcrop consists of >7 m (>23 ft) of poorly consolidated deposits of the Rito Leche terrace of Bryan and McCann (1936). Circle A Ranch and most of the inhabited and/or irrigated properties along the Sierra Nacimiento mountain front between 2,195 m and 2,350 m (7,200 ft and 7,700 ft) elevation are upon similar deposits.

Figure 1.03. Annotated photograph showing a darker deposit filling a paleochannel (outlined with dashed white line) within terrace deposits seen in Figure 1.02. The paleochannel's maximum thickness is approximately 2.2 m (7.2 ft). The darker deposit consists of clay through fine sand, leading to the interpretation that the Sierra Nacimiento mountain front experienced episodes of relative quiescence and/or low fluvial energy during development of its geomorphic surfaces. These finer-grained deposits, combined with the low relief atop mountain-front terraces, have allowed successful agriculture here for centuries.

Figure 1.04. View to the northwest from the Los Pinos Road near the entrance to Circle A Ranch showing the badlands of the "Little Grand Canyon." The community of La Jara occupies the grassy area in the distance, about 3 km (1.9 mi) away. The black arrows indicate surfaces of the Rito Leche terrace—the same one shown in Figure 1.02 and upon which Circle A Ranch is built. The dashed white line marks the uphill projection of that surface. Note that there exists San Jose Formation bedrock above that projected line, indicating that the upper portions of outcrop here would have formed a remnant highland during the active episode of Rito Leche terrace development.

cottonwood is a close cousin to the more familiar Rio Grande (*P. deltoides wislizensi)* and Fremont cottonwood (*P. fremontii*) common along New Mexico's major waterways, but is relegated to higher elevations. The genus is promiscuous, and hybridization occurs where species' ranges overlap.

0.2

1.0 Road bends to the left. A good roadcut outcrop of San Jose Formation feldspathic arenite is on the inside of the turn. Note the contorted bedding, to be discussed at Stop 1 (Fig. 1.05). Note also the sandiness of this deposit (Fig. 1.06)—it wasn't derived from the crystalline rocks of the Nacimiento Uplift just 5 km (3.1 mi) to the east!

0.3

1.3 For such a small road, here is an impressive roadcut through a thick sandbody of the San Jose Formation. Note also the thick accumulation of silt through medium sand on the north side of this outcrop. At this high point, the road leaves the Rio de los Pinos drainage and enters the valley of the Rio Puerco, which here is a verdant, tranquil stream that is often less than 2 m (7 ft) wide.

Figure 1.05. Roadcut exposure of contorted bedding in an arenite of the San Jose Formation along the Los Pino Road. Scale marker is 17 cm (7 in) in total length.

Figure 1.06. Photograph of arenite texture in the same roadcut exposure as shown in Figure 1.05. Mudclasts like these are the most common pebbles in the San Jose Formation at this location. Pebbles of minerals or crystalline rock are nearly nonexistent.

0.3

1.6 At left, a good view to the east of the lowest sandstone of the San Jose Formation, about 100 m (330 ft) from the road, and of black mudstones of the upper Nacimiento Formation (about 1 km [0.6 mi] distant), a Paleocene fluvial siliciclastic unit that underlies the San Jose Formation (Fig. 1.07). Note that bedding here dips north, parallel to the mountain front and the basin-bounding Nacimiento fault. The broadening of the valley before you likely is due to the more easily erodible character of the Nacimiento Formation relative to the San Jose Formation.

0.3

1.9 At the 25 MPH Speed Limit sign on the right, a cliff of amalgamated sandstones is formed by the Cuba Mesa Member of the San Jose Formation. Typically (but not always!) the thickest sandbody within the formation, the Cuba Mesa Member is often used as a marker in subsurface logs (e.g., Smith and Lucas, 1991; Smith, 1988). The Cuba Mesa Member lacks any biostratigraphic or geochronologic indicators; its Eocene age is assumed based on lithostratigraphic comparison with the overlying fossiliferous Regina Member. However, its long-assumed Eocene age is questioned by some recent workers (e.g., Zellman et al., 2024; Hobbs and Gillam, 2025a) and further work on the unit is ongoing after a three-decade hiatus. This cliff will be visible on the right for the next mile (1.6 km) or so.

To the left, a gravel-capped terrace of the Rio Puerco stands 10 m (33 ft) above the valley floor 350 m (1,100 ft) to the southeast. This is the lowest extensive fluvial terrace in this reach.

0.3

2.2 Camino del Rio Puerco enters at left. Ahead lies the verdant irrigated valley of the upper Rio Puerco (Fig. 1.08).

0.2

2.4 On the skyline atop the Cuba Mesa Member of the San Jose Formation and among pines at 2:00, note the architectural statement that puts Cuba in the same company as Edinburgh, Neuschwanstein, Mont Saint-Michel, and Kilkenny (Fig. 1.09). If only the San Juan Basin contained iconic 12th and 13th century architecture which one could replicate…

At 9:00 to 10:00, mudstones of Nacimiento Formation persist on a low terrace mesa underneath a thin layer of Sierra Nacimiento-derived gravel.

0.3

2.7 Pass through a copse of narrowleaf cottonwoods along the Rio Puerco. The river is deflected westward here to work its way around the low mesa of Nacimiento Formation mudstones projecting into the valley.

0.8

3.5 Behind the house with a red roof on the right, a 40-m (131-ft)-tall terrace deposit rests atop Nacimiento

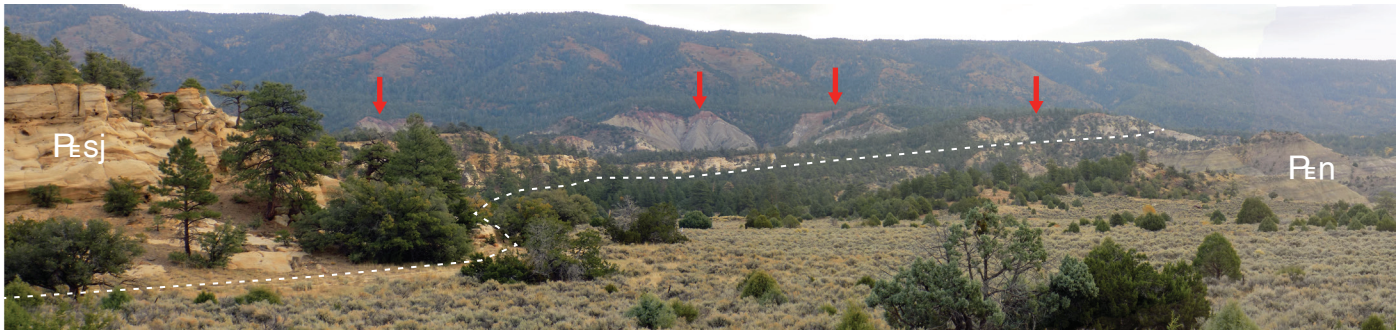

Figure 1.07. View to the southeast from the Los Pinos Road of the Nacimiento (PEn)-San Jose (PEsj) Formation contact (dashed white line). Strata in the foreground are dipping north 5 to 9°, oblique to view angle. Red arrows mark high terrace-pediment deposits derived from reddish Permian and/or Triassic sedimentary rocks.

Figure 1.08. The upper Rio Puerco Valley along the Los Pinos Road, with rounded hills of Nacimiento Formation mudstones and sandstones capped by thin terrace gravels in the background. On the skyline, the highlands of the Sierra Nacimiento rise to elevations of over 3,200 m (10,500 ft), more than a kilometer higher than the irrigated valley floor here.

Figure 1.09. The Cuba castle. Due to its defensible location atop a bluff of the Cuba Mesa Member of the San Jose Formation, the castle has never been breached by marauders.

Formation fluvial sedimentary rocks. The orange sandstone near the top of the terrace is thin and discontinuous, meaning it likely belongs to the Nacimiento Formation, not the San Jose Formation, whose basal sandstones tend to be thicker and more laterally continuous.

0.3

3.8 The road here bends to right around a gravel-capped mesa of Nacimiento Formation; this is the same terrace as seen 0.3 miles (0.5 km) back (Fig. 1.10). On the other (northwest) side of this mesa, the Cuba Drive-in Theater operated in the late 20th century.

0.4

4.2 Terminus of Los Pinos Road at U.S. Route 550.

REZERO ODOMETER at stop sign.

0.0 Turn right (north) on U.S. Route 550.

0.1

0.1 The contact between the drab and muddy Nacimiento Formation and the yellow sandstones of the lower San Jose Formation is visible at 1:00. From 2:00 to 3:00, high terrace gravels of an ancient Rio Puerco cap mudstone mesas of the Nacimiento Formation. The north end of Mesa de Cuba makes up the western skyline from 8:00 to 10:00. Cuba's former drive-in theater occupied the flat lot halfway up the hill at right.

0.6

0.7 At 1:00, near the crest of the hill and behind Jersey barriers, steeply west-dipping normal faults cut beds in the basal San Jose Formation (which is the Cuba Mesa Member in this part of the basin). Note also the increase in fault-parallel fractures in the footwall to the right of the fault (Fig. 1.11). There are what seem to be younger surficial sediments in the hanging wall near the top of the outcrop. Is this truly a fault, as mapped by Woodward et al. (1972), or just a gravity slump? Bedding in sandstones near the highway at the foot of this outcrop is strongly backrotated.

0.7

1.4 Bridge crosses Rito de los Pinos, which heads at 3,100 m (10,200 ft) elevation in the Sierra Nacimiento 11 km (6.9 mi) northeast of here and flows through the Circle A Ranch. To the left, Lapis Lane leads toward large cottonwoods nearly hiding a house (Fig. 1.12), where the wife-and-husband pair of artist and writer Martha Simpson and novelist William Eastlake lived in the 1950s and 1960s. Eastlake (1917–1997), a Purple Heart veteran of the Battle of the Bulge, is perhaps best known as the author of the war novel *Castle Keep*, which was

modified for the big screen and starred Burt Lancaster, Bruce Dern, and Peter Falk. For the San Juan Basin geologist, Eastlake's *Checkerboard* trilogy of *Go in Beauty* (1956), *The Bronc People* (1958), and *Portrait of an Artist with Twenty-six Horses* (1963) are must-reads on account of their significant passages describing the beauty of these landscapes and their inhabitants. Eastlake was among the first EuroAmerican authors to write Navajo characters as fully formed, intelligent, emotional humans rather than the cardboard cutouts of the "white man's Indian" that typifies much of western literature. Martha Simpson (1898–1984) was an accomplished and multifaceted artist and writer. Her 1965 cookbook *Rattlesnake Under Glass: A Roundup of Authentic Western Recipes* won the 1966 New Mexico Press Zia Award. It contains recipes for "Santa Fe

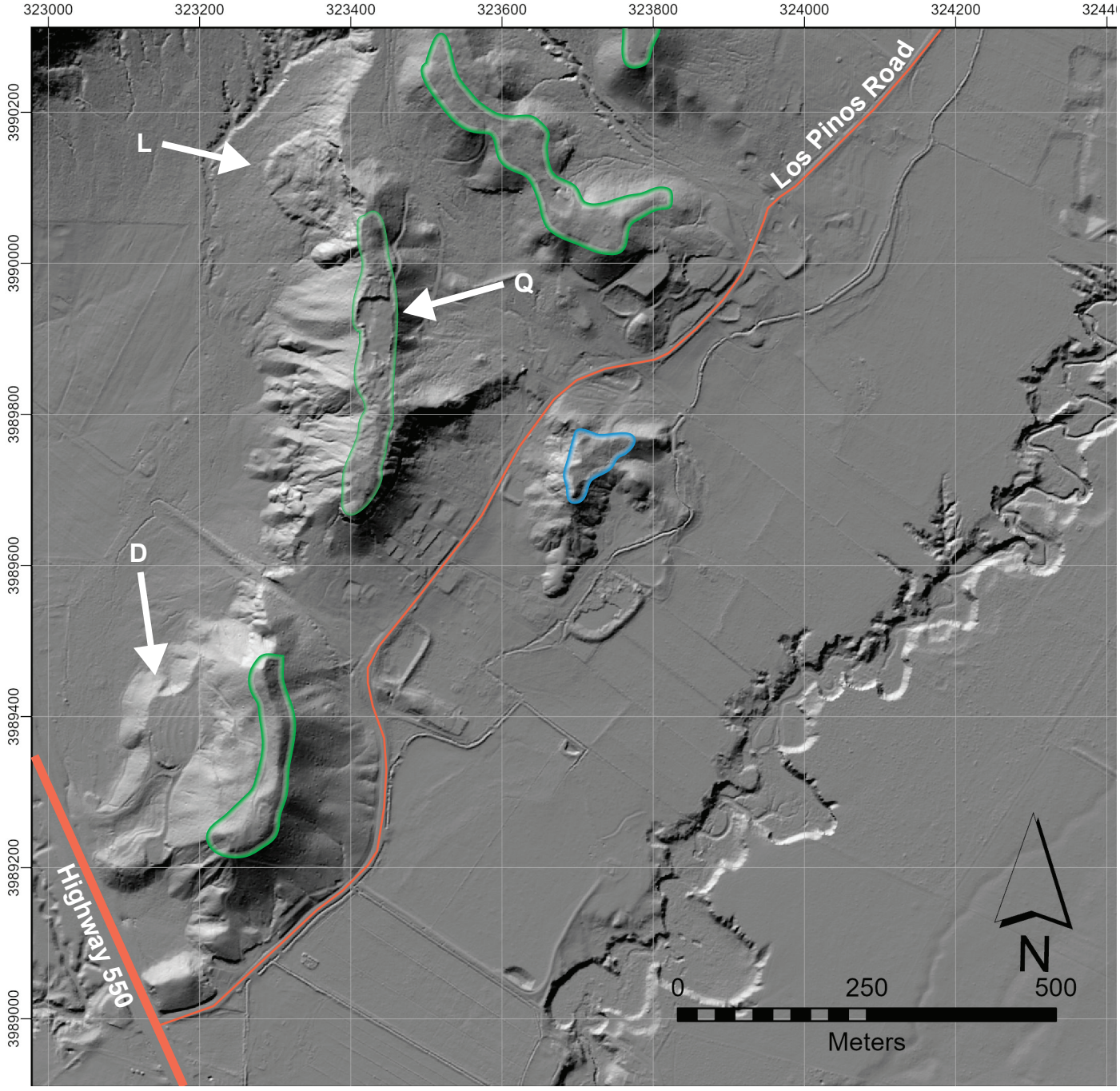

Figure 1.10. Annotated shaded relief map showing the Rio Puerco Valley near the junction of Los Pinos Road and U.S. Route 550. Green outlined areas represent the 45–49 m (148–160 ft)-high terraces that likely correspond to the Rito Leche surfaces of Bryan and McCann (1936). Blue outlined area is a lower gravelly terrace that stands some 24 m (79 ft) above the modern Rio Puerco. Note the sinuosity of the incised Rio Puerco at center right. L = a 1-ha (2.4-ac) lobate landslide emanating from a gravel-capped sandstone mesa. This landslide is not present on a 1954 aerial photograph, but is visible in a 1996 photo. Its vertical drop is approximately 30 m (100 ft), with a 95 m (311 ft) maximum horizontal runout. Q = disused gravel quarry. D = site of the former drive-in movie theater. The screen was on the east side facing to the west. Berms that helped aim car windshields up toward the movie screen are arranged in arcs and are still visible in this hillshade imagery.

Figure 1.11. Fault in basal San Jose Formation at mile 0.7 on the east side of U.S. Route 550. White line marks fault surface. Note intense fault-parallel fracture sets in footwall at top right. The drab mudstones at bottom right are within the uppermost Nacimiento Formation.

Figure 1.12. The Eastlake house.

Cock" and "Sandoval County Beer," neither of which are to be served at this conference.

At this house, Eastlake and Simpson frequently entertained the paleontologist George Gaylord Simpson (Martha's brother), the science popularizer and eugenicist Sir Julian Huxley, and University of New Mexico alumni Robert Creeley (Black Mountain poet) and Edward Abbey (anarchist writer). As of 2024, the house is in poor condition, except for its well-made fireplace and chimney constructed entirely of boulders of fossil wood from the San Jose Formation (Fig. 1.13). Each May, sharp-eyed travelers on U.S. Route 550 can spot prodigious blossoms of a large lilac on the house's east side next to the chimney.

0.4

1.8 Roadcut outcrops of the Cuba Mesa Member of the San Jose Formation on both sides of highway.

0.2

2.0 At left, an alluvial valley of Arroyo San Jose opens before you. The fine-grained alluvium is at least 18 m (59 ft) thick, based on exposures in the incised arroyo on the far (west) side of this valley.

0.3

2.3 At right, note the interbed of gray mudstone within the yellow arenites of the San Jose Formation (Fig. 1.14).

0.3
2.6 Note gravel-capped terraces on both sides of highway.

0.4
3.0 **State Road 96 turns off to right; stay straight on U.S. Route 550.**

Figure 1.13. Eastlake house chimney made from logs of petrified wood from the San Jose Formation. A signature in the mortar reads "B. Montoya, April 16, 1954."

0.3
3.3 Roadcuts on both sides of highway expose reddish mudstones of the Regina Member of the San Jose Formation. The Regina Member also contains thick yellow sandstones nearly identical to those of the basal Cuba Mesa Member of the San Jose Formation.

0.6
3.9 At 3:00, a scenic view up the valley of Arroyo San Jose (Fig. 1.15), after which is named the San Jose Formation. The southeast corner of the Jicarilla Apache Nation is near the center of this valley about 1 km (0.6 mi) from the highway. That nation stretches to the Colorado border 100 km (62 mi) north of here.

0.6
4.5 Dirt road at left provides access to the top of Mesa de Cuba, whose western and southern exposures will be prominently visible at mile 14 to 15 of this road log.

1.5
6.0 On right, a large pullout with a historic marker explaining the geology of San Juan Basin (Fig. 1.16). Who needs college?

0.8
6.8 Colorful outcrop of Regina Member mudstones at 3:00.

0.5
7.3 Roadcut outcrop exposes the low-angle plane beds that typify many of the San Jose Formation's sandstones (Fig. 1.17). Above them, near the top of the outcrop, soft-sediment deformation structures (SSDSs) appear.

0.6
7.9 **Turn left (south) on BLM Road 1101 (Chijuilla Road).** This turn can be easy to miss; it steeply descends from U.S. Route 550 just before a guardrail on the south side of the highway.

Figure 1.14. Gray mudstone within the Cuba Mesa Member of the San Jose Formation pinching out to the right (south) in a roadcut on the east side of U.S. Route 550. Pinch out is just above white arrow.

Figure 1.15. View to the north from U.S. Route 550 at mile 3.9 into the upper Arroyo San Jose valley. The black pin marks the southeastern corner of the Jicarilla Apache Nation. The community of La Jara is at far right. The low badlands hills on the skyline at left and center contain the type section of the Regina Member of the San Jose Formation.

Figure 1.16. New Mexico Official Scenic Marker #22 explaining San Juan Basin geology on the north side of U.S. Route 550.

0.1

8.0 Cross cattle guard. Pavement ends. Immediately after cattle guard, take a hard right onto a faint two-track road. Follow this two track for 0.5 miles across the small valley and onto the low hill to the west.

Waypoint 1.02 [36.0673°, −107.0743°]

0.5

8.5 STOP 1. Park in a small clearing of the foot of hill. Walk uphill about 100 m (330 ft) to the southwest into a disused stone quarry for outcrops of San Jose Formation arenites and discussion of their sedimentary structures. This quarry appeared active in a 1954 aerial photograph. The date of its abandonment is unknown.

Introduction to Paleoseismites

Seismites are sedimentary beds and/or structures that have deformed due to seismic shaking. The term is more specifically applied to coseismic deformations that occur as a result of overpressurization of pore water that caused sediment liquefaction. Deformation occurs prior to lithification when sediment is still unconsolidated or poorly consolidated. Therefore, a seismite is a type of soft-sediment deformation structure (SSDS). The phenomenon occurs when force is applied to saturated sediment, causing the pore water to attempt to flow to areas of lower pressure (usually upward and toward the ground surface). The repeated application of force in seismic compression waves creates conditions in which pore water cannot flow out before the next cycle of force. This causes pore water pressure to increase to a point that it exceeds the force between individual sediment particles that keep them in contact with each other. These particle-to-particle contacts are the means by which unconsolidated sediment transfer forces. When these contacts are removed—even temporarily—the sediment loses its strength (i.e., the ability to transfer stress) and behaves practically equivalent to a liquid (i.e., liquefaction).

Seismites first were described in relatively young sediments whose deformation could be linked to observed seismic events. Their preservation in the rock record—as paleoseismites—has been noted for decades, but was relatively unstudied until the late 20th century. The main difficulty in interpretation of paleoseismites is the inability to observe or measure the seismic shaking that is assumed to have formed them. Attempts at categorizing the necessary causative factors for seismites, as well as tests for distinguishing seismites from small SSDSs that do not have a seismic origin, have somewhat formalized the study and interpretation of these features in the rock record (Table 1). Some SSDSs, including sand blows, upward-propagated clastic dikes, and thixotropic bowls, are strongly linked to seismicity with few other known genetic origins (Li et al., 1996; Mahindra and Bagati, 1996; Obermeier, 1996). Seismites are most likely to form during seismic shaking from earthquakes with magnitudes M_W >5.5 in silt and sand (Wheeler, 2002). Their frequency and size decrease with distance away from earthquake hypocenters (Obermeier, 1996; Montenat et al., 2007).

Paleoseismites record syndepositional tectonism prior to lithification. Recent work shows they can record fold growth and the onset of orogenic episodes (Obermeier, 1996; Bartholomew et al., 2002; Obermeier et al., 2002; Jackson et al., 2016). Given seismites' formation prior to lithifaction—and often when sediments are at Earth's surface—the timing of seismicity can be assumed to be the same as the age of the sediments in which they formed (Jackson et al., 2016, 2019). Planar paleoseismites—primarily clastic dikes—are known to form parallel to preexisting fracture avenues reflecting the local stress field at the instant of paleoseismites formation (Jackson et al., 2019). The trends of clastic dikes interpreted as paleoseismites often are compatible with independently derived shortening directions in orogenic settings (Jackson et al., 2019; Hobbs and Thacker, 2021).

Paleoseismites in San Juan Basin Sedimentary Rocks

Recent investigations in the eastern and central San Juan Basin have documented SSDSs interpreted as paleoseismites in the Paleogene Ojo Alamo and San Jose Formations (Hobbs and Thacker, 2021, 2022). Observed structures include clastic dikes, convolute bedding, obliterated bedding, diapir-like structures, sand blows, and potential thixotropic bowls (Fig. 1.18). These features are most common in the eastern San Juan Basin between Mesa Portales and the central Jicarilla Apache Nation, where they are observed in the Ojo Alamo Formation sensu Baltz (1967) and the Cuba Mesa and Regina Members of the San Jose Formation. Soft-sediment deformation structure become less common to the west, with none known west of −107.45°. The northernmost known San Juan Basin SSDS is at 36.48°, although difficulty with land access farther north

Figure 1.17. Roadcut outcrop of the Regina Member of the San Jose Formation at mile 7.3. The middle of the outcrop (between the white dashed lines) exhibits low-angle very-thin plane beds, the most common bedform in the arenites of the San Jose Formation. Thin white lines are parallel to bedding. Above the plane beds, soft-sediment deformation structures (SSDSs) disrupt bedding similar to what will be inspected at Stop 1.

TABLE 1. Summary of suggested tests of soft-sediment deformation structures of possible seisimic origin

Test name	Critical observation	Limitations
1. Sudden formation	Structure formed suddenly than by any nonseismic alternative	May be unable to rule out nonseismic origins without further evidence
2. Synchroneity	Nearby structures of same type formed at times indistinguishable from each other	May be unable to rule out nonseismic origins without further evidence; dating and/or correlation lack resolution to distinguish synchroneity from near-synchroneity
3. Zoned distribution	Indicators of strength of shaking decrease outward from a central area	Cannot rule out seismic origin
4. Size	Structure cannot be larger than all similar structures known to have been formed by historical earthquakes	Maximum sizes are unknown; cannot rule out seismic origin for small structures
5. Tectonic setting	Seismic shaking strong enough to form the structure occurs more often than any nonseismic alternative in modern analogs	Threshold seismic factors for formation remain largely unknown
6. Depositional setting	Seismic shaking by itself forms similar structures in modern settings	Difficulty in recognizing some newly formed structures in the field

Modified from Wheeler, 2002.

than that prevents further investigation. Potential paleoseismite SSDSs have not been reported in the Late Cretaceous Kirtland Formation that underlies the Ojo Alamo Formation nor in the Paleogene Nacimiento Formation that lies between the Ojo Alamo and San Jose Formations.

Given that Paleogene units in the San Juan Basin were deposited by fluvial systems in an active broken-foreland basin during the Laramide orogeny, and given that paleoseismites are more numerous in the eastern San Juan Basin and become less numerous and then absent toward the central and western basin, it follows that a seismic source in the Paleogene must have been located at or near the basin's eastern margin. Fortunately for this discussion, the basin's southeastern margin is marked by one of the largest-displacement and longest Laramide faults in the Four Corners: the Nacimiento fault system. This system stretches approximately 100 km (62 mi) along the west face of

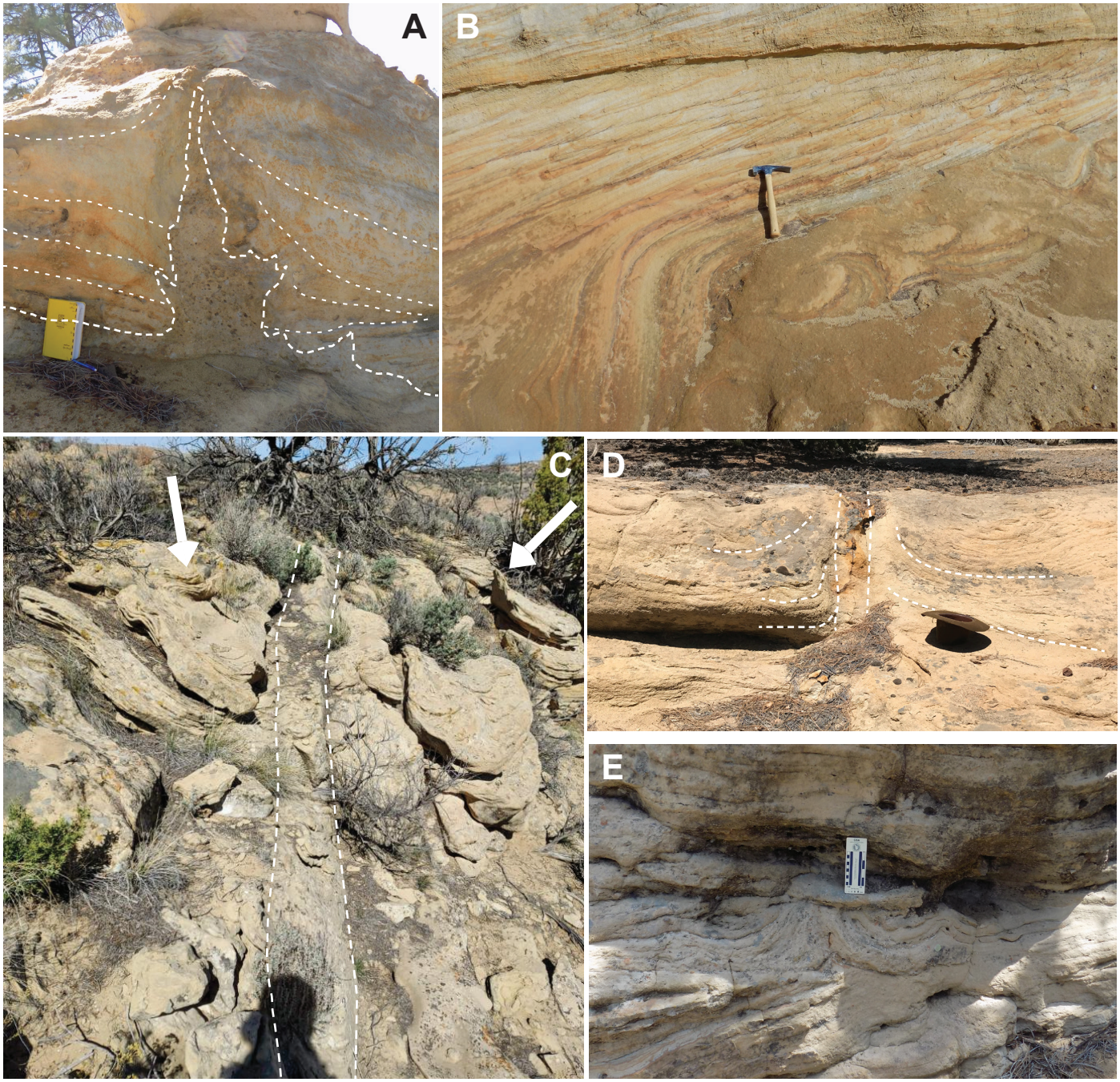

Figure 1.18. Field photographs of paleoseismites in San Juan Basin Paleogene sedimentary rocks. A: San Jose Formation injectite. Mud-clast conglomerate injected 70 cm (28 in) into overlying arenite. Field book is 19 cm (7.5 in) tall. B: Contorted and overturned bedding in an arenite of the Regina Member of the San Jose Formation. Hammer is 31 cm (12 in) long. C: Clastic dike (within dashed lines) with upturned adjacent beds (white arrows) in the Regina Member of the San Jose Formation. Dike is 25 cm (10 in) wide, trends 148°, and is finer-grained that surrounding arenite. D: Clastic dike with upturned adjacent beds in the Ojo Alamo Formation at Mesa Portales. Hat is 30 cm (12 in) wide. Dike is 22 cm (9 in) wide and trends 160°. E: San Jose Formation convolute beds truncated by overlying beds, indicating that deformation occurred when sediment was at or very near the surface. Black scale bars are 10 cm (3.9 in) long.

the Sierra Nacimiento and has a throw of at least 3.7 km (2.3 mi) and a dextral offset of between 2 and 30 km (1.2 and 19 mi) (Woodward et al., 1992; Pollock et al., 2004). The presence of paleoseismites in the Ojo Alamo and San Jose Formations is a potential indicator of earthquakes with magnitudes M_W >5.5 in eastern San Juan Basin in the early Paleogene. A clastic dike on the central Jicarilla Apache Nation (Fig. 1.18C) is 54 km (33 mi) from the Nacimiento-Gallina fault system, suggesting a paleoearthquake magnitude of at least M_W >6 based on modern observations of seismites formation (table 2 in Wheeler, 2002) and assuming a paleohypocenter on the Nacimiento-Gallina fault system.

Unexplored and unanswered questions abound with regards to paleoseismites in Paleogene San Juan Basin rocks: was the Nacimiento-Gallina fault system the seismic source, or was there some other unknown source in the subsurface? Why are paleoseismites present in the Ojo Alamo and San Jose Formations yet absent in adjacent formations? Can synchroneity of formation ever be proven (or even suggested) in 65-million-year-old paleoseismites? What are the tectonic and sedimentary implications of strong syndepositional seismicity in the Paleogene San Juan Basin? Further work and a more diverse suite of research expertise are needed to address these questions and to discover others (a statement that surely is true of every topic relating to every field in natural science!).

At Stop 1, exposures of the San Jose Formation showcase arenites of the Regina Member. The typical planar nature of bedsets is on display in loose blocks near the northern end of the quarry. On the quarry's western wall, one can observe excellent exposures of some of the less common primary sedimentary structures of the San Jose Formation, including planar and trough cross-beds and climbing cross-laminae (Fig. 1.19). On the southern and eastern quarry walls, look for SSDSs (Fig. 1.20). Can these be called paleoseismites with any confidence? Why or why not? One wonders if the quarrymen were disappointed by the presence of highly contorted bedding in their quarry…? Zellman et al. (2024) provided the first and most exhaustive investigation of San Jose Formation sedimentary architecture in decades. Their work—especially their tables 1 and 2—offers a well-documented, clearly illustrated, and reasoned interpretation of observed fluvial bedforms and lithosomes that should be considered by anyone working in not just the San Juan Basin, but in any fluvial sedimentary systems.

8.5 **Return to vehicles, turn around, and retrace route for 0.5 miles back to BLM Road 1101.**

0.5

9.0 **TURN RIGHT (SOUTH), back onto BLM Road 1101. Watch for livestock.**

0.9

9.9 Sage (Ts'ahtsoh, *Artemisia tridentata*)-covered Chijuilla Valley spreads out on your right; on the skyline at left are orange sandstones of the Regina Member of the San Jose Formation. The impoundment at right was built sometime after 1954, during a midcentury fit of pond construction for livestock grazers in this part of the San Juan Basin.

0.8

10.7 A lone cottonwood at right.

0.3

11.0 Cattle guard.

0.2

11.2 Culvert over Arroyo Chijuilla. To the left, a bedrock exposure on the arroyo floor hints at the maximum thickness of the alluvium in this valley (Fig. 1.21). To the right, an upstream gabion structure is an attempt to prevent farther downcutting. Arroyo Chijuilla flows south for 17 km (10 mi) from here, passing between Mesa de Cuba and Mesa Portales before joining the Rio Puerco at Llano de Chino 11 km (6.6 mi) south of Cuba.

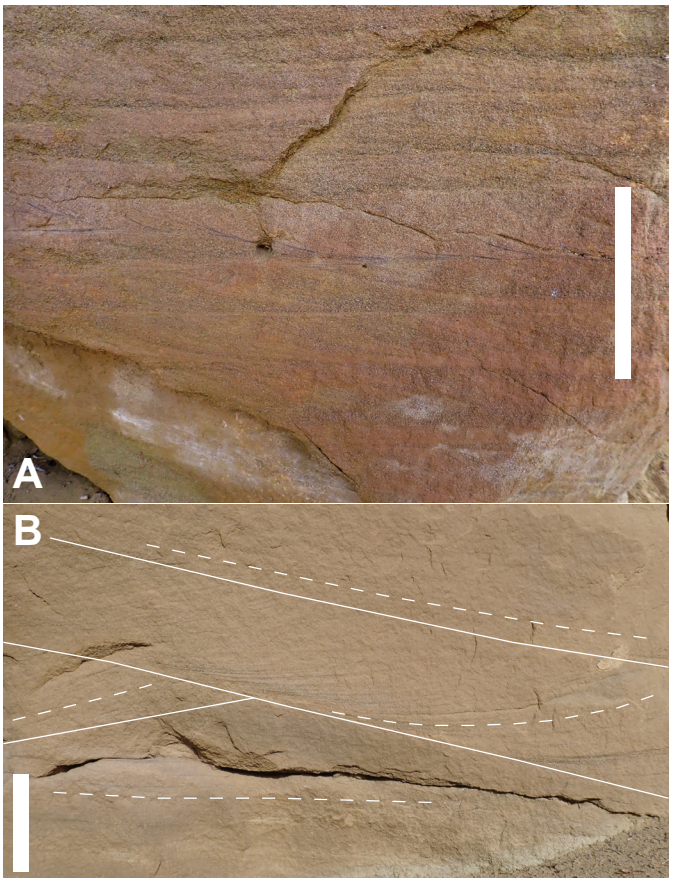

Figure 1.19. Primary sedimentary structures in the San Jose Formation at Stop 1. Scale bars in photographs are 10 cm (3.9 in) long. A: Tabular cross-laminae with planar and parallel bounding surfaces. Close inspection can be required in order determine whether individual laminae intersect the lower bounding surface at an angle or with a tangential toe-in. Note: the contrast in this photo has been digitally manipulated to make grains and bedforms more visible. B: Scour-and-fill structures with climbing cross-laminae. Solid white lines mark first-order bounding surfaces; dashed white lines mark bedding orientation within a depositional unit.

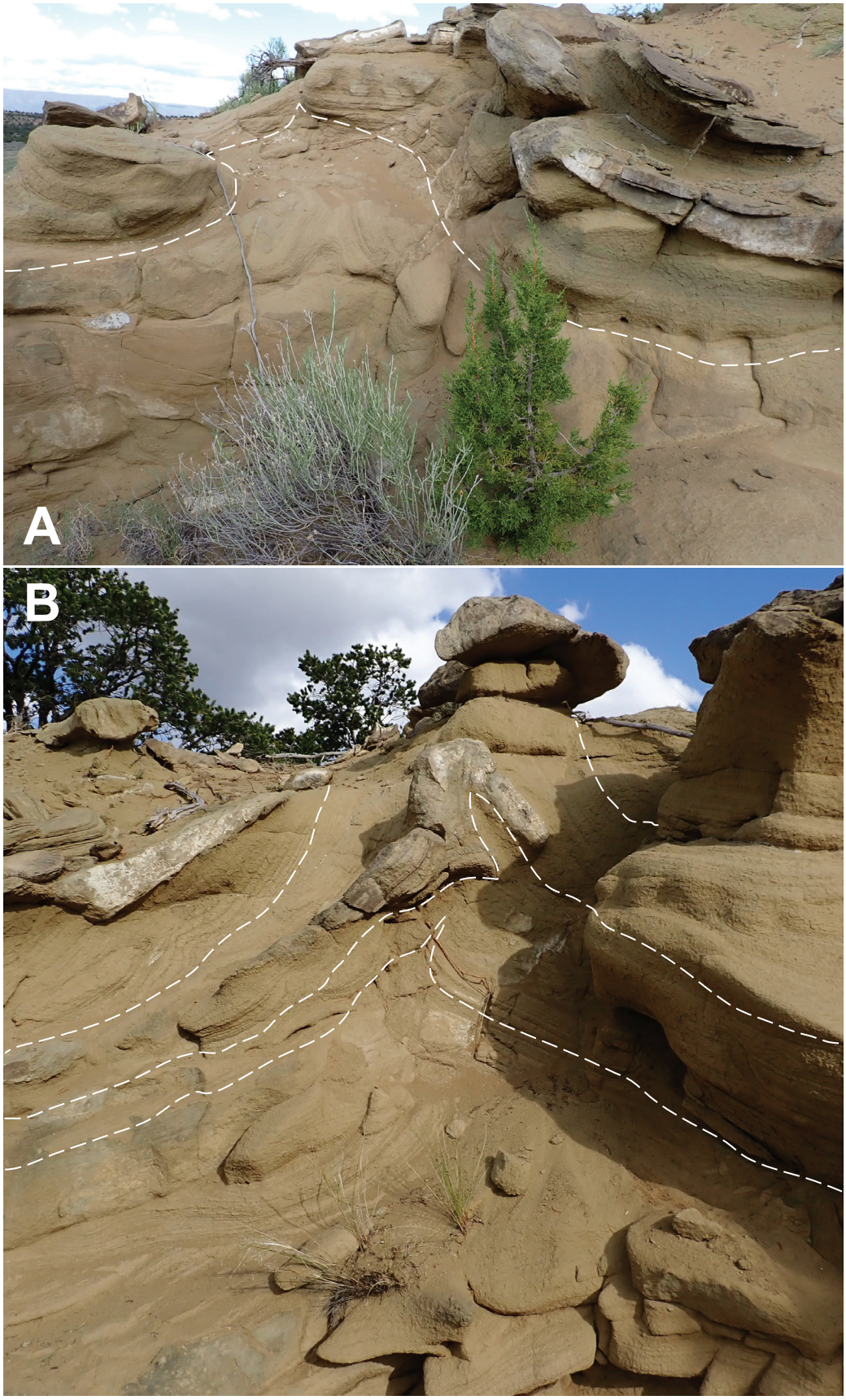

Figure 1.20. Soft-sediment deformation structures (SSDSs) in the San Jose Formation at Stop 1. A: Contorted bedding. Dashed white line follows a bedding surface. Outcrop is 2.5 m (8.2 ft) tall. B: Possible injectite. Like many such structures at Stop 1 and elsewhere in similar outcrops in eastern San Juan Basin, there are small faults within this structure that truncate bedding. Dashed white lines follow bedding surfaces. Outcrop is 3 m (10 ft) tall.

0.1
11.3 Road bends to the right (west); livestock pens to the left.

0.7
12.0 At 3:00, a distinctive short tower of yellow sandstone (most likely Regina Member) rises above the ponderosa pines (Ńdíshchíí', *Pinus ponderosa*; Fig. 1.22). At the foot of this feature among the piñon (Chá'oł, *Pinus edulis*) and juniper (Gad, *Juniperus* spp.) lie the remains of a homestead (Fig. 1.23). As of 2024, there persist a few well-built but roofless log structures and a root cellar at this site.

0.2
12.2 **Stay straight at road intersection.**

0.3
12.5 Crest of hill; road starts downhill. For the next 3 miles, Mesa Chijuilla is on the right. Here, there are good exposures of the red and grayish-red muddy sandstones of the Regina Member of the San Jose Formation from 2:00 to 3:00.

1.2
13.7 Just after a cattle guard, the road descends through good outcrops of San Jose Formation sandstone (Fig. 1.24). Can you tell if this is the basal Cuba Mesa Member or a sandbody within the Regina Member?

Figure 1.21. Arroyo Chijuillla downstream of BLM Road 1101 at mile 11.2. White arrow marks an outcrop of San Jose Formation arenite in arroyo floor.

0.3
14.0 Black mudstones at 3:00. This road is usually well-maintained because it provides access to wells in the Rio Puerco well field whose wells are set in fractured sandy strata of the lower Mancos Shale (the Sanostee/Sanastee sandstone and/or Hospah sandstone, both informal names used by industry).

0.4
14.4 **Stay right (southwest) at road intersection.** At 12:00 lies an extensive outcrop of black mudstones of the upper Nacimiento Formation, which will be discussed at Stop 2 (Fig. 1.25). As you continue around the bend, the promontory at 1:00 showcases yellowish-brown sandstones of the basal Cuba Mesa Member of the San Jose Formation overlying the drab gray and white mudstones and sandstones of the upper Nacimiento Formation (Fig. 1.26). At 9:00, note the shallow north dip of the pine-covered Mesa de Cuba, whose upper surface is a rough dip slope (Fig. 1.27).

0.3
14.7 Just at a small two track to the right (west), you pass through the 36th parallel. You are at the same latitude as Kitty Hawk, North Carolina; the Strait of Gibraltar; Rhodes, Greece; K2 in Kashmir, Pakistan; Tokyo, Japan; Badwater Basin, California; Kolb Rapid at Mile 205 on the Colorado River in Grand Canyon, Arizona; Fajada Butte in Chaco Canyon, New Mexico; and Calle Lopez in Española, New Mexico.

Waypoint 1.03 [35.9954°, −107.0823°]

0.4
15.1 **STOP 2. Just before the cattle guard at the foot of a hill, turn left (south) on dirt road that parallels a barbwire fence; proceed 100 m to first intersection and make a hard left to circle back toward BLM Road 1101 and park (Fig. 1.28). On foot, cross BLM Road 1101 and head for the Nacimiento Formation outcrops about 200 m to the north** for discussion of the Paleocene-Eocene boundary, silcretes, and basin-internal faulting.

Figure 1.22. A resistant outcrop of Regina Member sandstone rises above the Arroyo Chijuilla valley at mile 12.0.

The Paleocene-Eocene Boundary in the San Juan Basin

The nature of the contact between the Nacimiento and San Jose Formations has been studied, debated, interpreted, and left alone for decades (e.g., Simpson, 1948; Baltz, 1967; Cather et al., 2019; Zellman et al., 2024). Here in the southeastern San Juan Basin, most workers interpret the boundary as a slight angular unconformity (Baltz, 1967; Smith and Lucas, 1991; Williamson and Lucas, 1992; Cather et al., 2019). But some interpret the contact as conformable (e.g., Barnes et al., 1954; Stone et al., 1983; Zellman et al., 2024). Recent work in the northern San Juan Basin affirms previous interpretation that the contact there is conformable (e.g., Smith and Lucas, 1991; Cather et al., 2019; Hobbs and Gillam, 2025a, 2025b).

Whether the contact (in this case, a lithostratigraphic boundary) is conformable or unconformable, the Paleocene–Eocene boundary (chronostratigraphic) in the San Juan Basin section is largely unaddressed. Chronologic constraints in the Nacimiento and San Jose Formations come from biostratigraphy (e.g.,

Figure 1.23. Log cabin remains just off the road log route at mile 12.0.

Figure 1.24. Sandstone outcrop just off the road log route at mile 13.7.

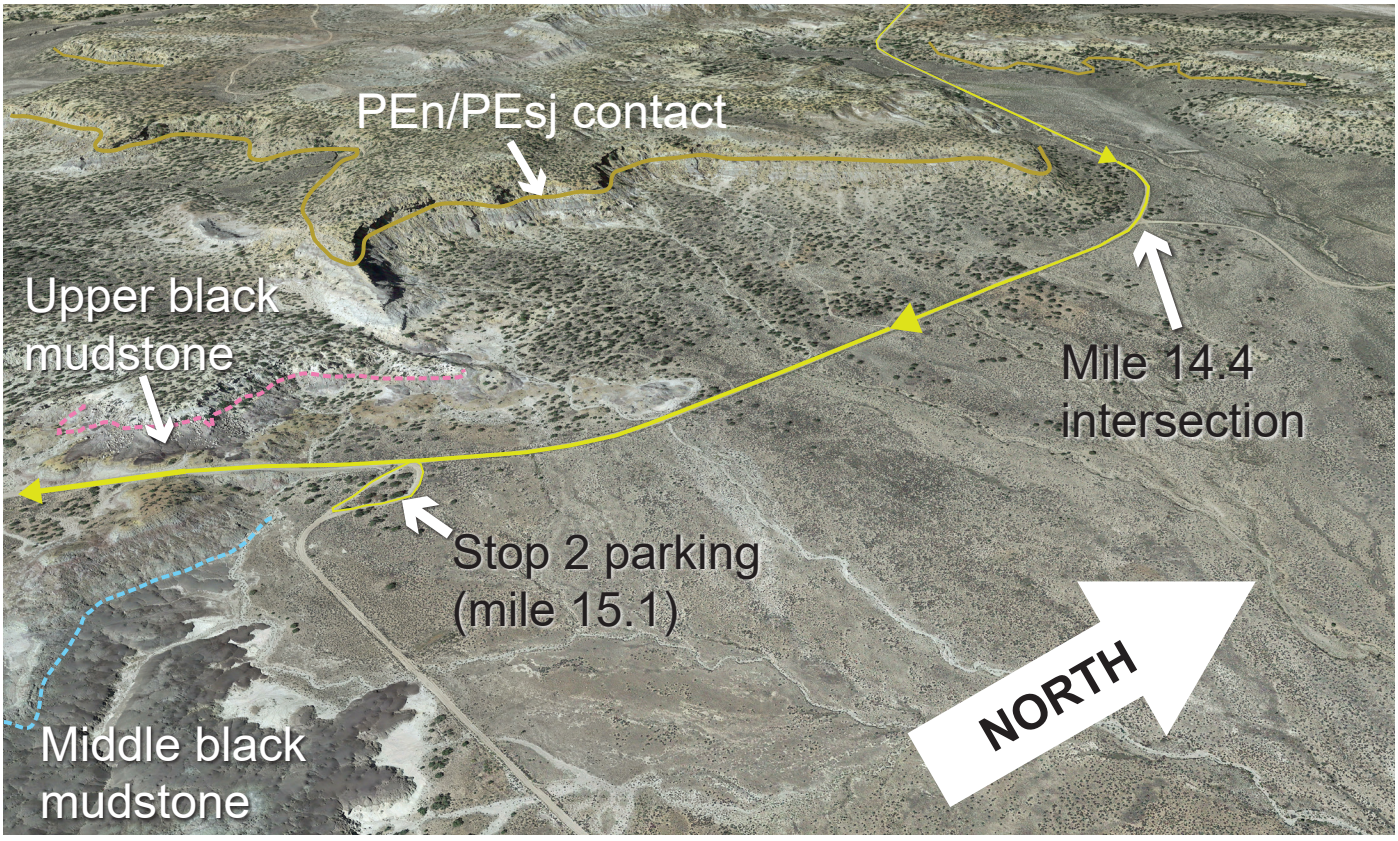

Figure 1.25. Oblique aerial view of the area around Stop 2. The road log route along BLM Road 1101 is marked by the yellow line. Mesa Chijuilla at top center is capped by the San Jose Formation (PEsj), whose lower contact with the Nacimiento Formation (PEn) is marked by the orange line. The middle black mudstone (whose top is denoted by dashed blue line) and upper black mudstone (whose top is denoted by dashed pink line), two easily traceable informal horizons within the Paleocene Nacimiento Formation, are on display here. The middle black mudstone is traceable for at least 75 km (47 mi) to upper Blanco Wash near Nageezi in San Juan County.

Figure 1.26. Southern promontory of Mesa Chijuilla above Stop 2. Gently northwest-dipping beds of drab-colored sandstones and siltstones of the upper Nacimiento Formation underlie light yellowish brown to pale brown cliff-forming arenites of the Cuba Mesa Member of the San Jose Formation.

Figure 1.27. View to the east from Stop 2 area toward the west face of Mesa de Cuba. Note the shallow north dip. The Sierra Nacimiento makes up the skyline. BLM Road 1101 in foreground.

Smith and Lucas, 1991; Flynn et al., 2020), detrital grain dating (e.g., Pecha et al., 2018; Cather et al., 2019), and magnetostratigraphy (e.g., Leslie et al., 2018; Flynn et al., 2020). Detrital sanidine evidence suggests that the Ojo Encino Member of the Nacimiento Formation was deposited after 64.4 ± 0.2 Ma (Cather et al., 2019). Multiple methods suggest that the Ojo Encino Member was deposited approximately 61.7 Ma. Williamson and Lucas (1992) propose that the overlying Escavada Member (uppermost Nacimiento Formation) potentially was deposited as recently as 58.9 Ma, although this requires projection of magnetostratigraphic interpretations across the San Juan Basin. The Regina Member of the San Jose Formation contains a rich Eocene paleofauna (Simpson, 1948) widely accepted to biostratigraphically constrain those beds to approximately 53 Ma (Smith and Lucas, 1991). The stratigraphic horizons to which these age constraints are applied are separated by a minimum of 90 m (295 ft; Lucas et al., 1981) and potentially >240 m (>790 ft; Zellman et al., 2024) of strata whose exact ages are unknown. These strata include the upper Ojo Encino Member and the Escavada Member of the Nacimiento Formation and the Cuba Mesa Member and lower Regina Member of the San Jose Formation. Therefore, the chronostratigraphic gap between the middle Nacimiento Formation and the middle San Jose Formation encompasses at least 5.9 My. The Paleocene–Eocene boundary, at 56.0 Ma, lies somewhere in that interval.

Many San Juan Basin researchers wonder what happened—and when—in that ≥5.9 My interval. It is plainly evident that during that interval, a considerable volume of sediment was deposited in the southern San Juan Basin, including, at a minimum, the entirety of the uppermost Nacimiento Formation and lowermost San Jose Formation. During the approximately 62 Ma to 53 Ma time interval, the Paleocene–Eocene Thermal Maximum (PETM) occurred at 56.0 Ma (McInerney and Wing, 2011). The PETM was a global climate event that caused average annual temperature increases of 5° to 8° C, caused by the release of thousands of gigatons of carbon into Earth's atmosphere (McInerney and Wing, 2011; Haynes and Hönisch, 2020); it is the best-known historic analogue for current anthropogenic global climate changes. As of 2024, there exists no evidence for San Juan Basin sedimentary rocks that match the 56 Ma age of the PETM. However, the rocks in the upper Nacimiento and lower San Jose Formations have received less intense study than sub- and superjacent strata due to their dearth of known paleontological specimens. New and current research into the interval (e.g., Zellman et al., 2020, 2024; Hobbs and Gillam, 2025a, 2025b) seeks to improve understanding of the Paleocene–Eocene transition in the San Juan Basin and link the sedimentary record with climatic and tectonic events.

Silcretes

Silcretes are indurated silica-cemented sediments and soils containing >85 wt% SiO_2 (Summerfield, 1983; Nash and Ullyott, 2007). Most silcrete research has focused on those from Australia and southern Africa where they form from the long-term accumulation of silica in duricrusts in stable landscapes (e.g., Thiry et al., 2006), and from Cenozoic deposits of western Europe where they represent paleosol duripans or more recent groundwater precipitation horizons (e.g., Huggett and Longstaffe, 2016). More localized silcrete formation is known from North America (e.g., Wehrfritz, 1978; Nimlos and Ortiz-Solorio, 1987; Williamson et al., 1992), South America (e.g., Batezelli and Ladeira, 2016), southwest Asia (Khalaf, 1988), and New Zealand (Lindqvist, 1990). Silcretes are known in rocks ranging in age from Precambrian to recent (Mustard and Donaldson, 1990; Dubroeucq and Thiry, 1994), but the majority are hosted by Cenozoic sediments (Nash and Ullyott, 2007).

Silcrete mineralogic composition is dominated by opal, chalcedony, and quartz (Nash and Ullyott, 2007). Matrices are composed of opal, chalcedony, and microquartz (<20 μm). Grain overgrowths and large void-fillings are commonly

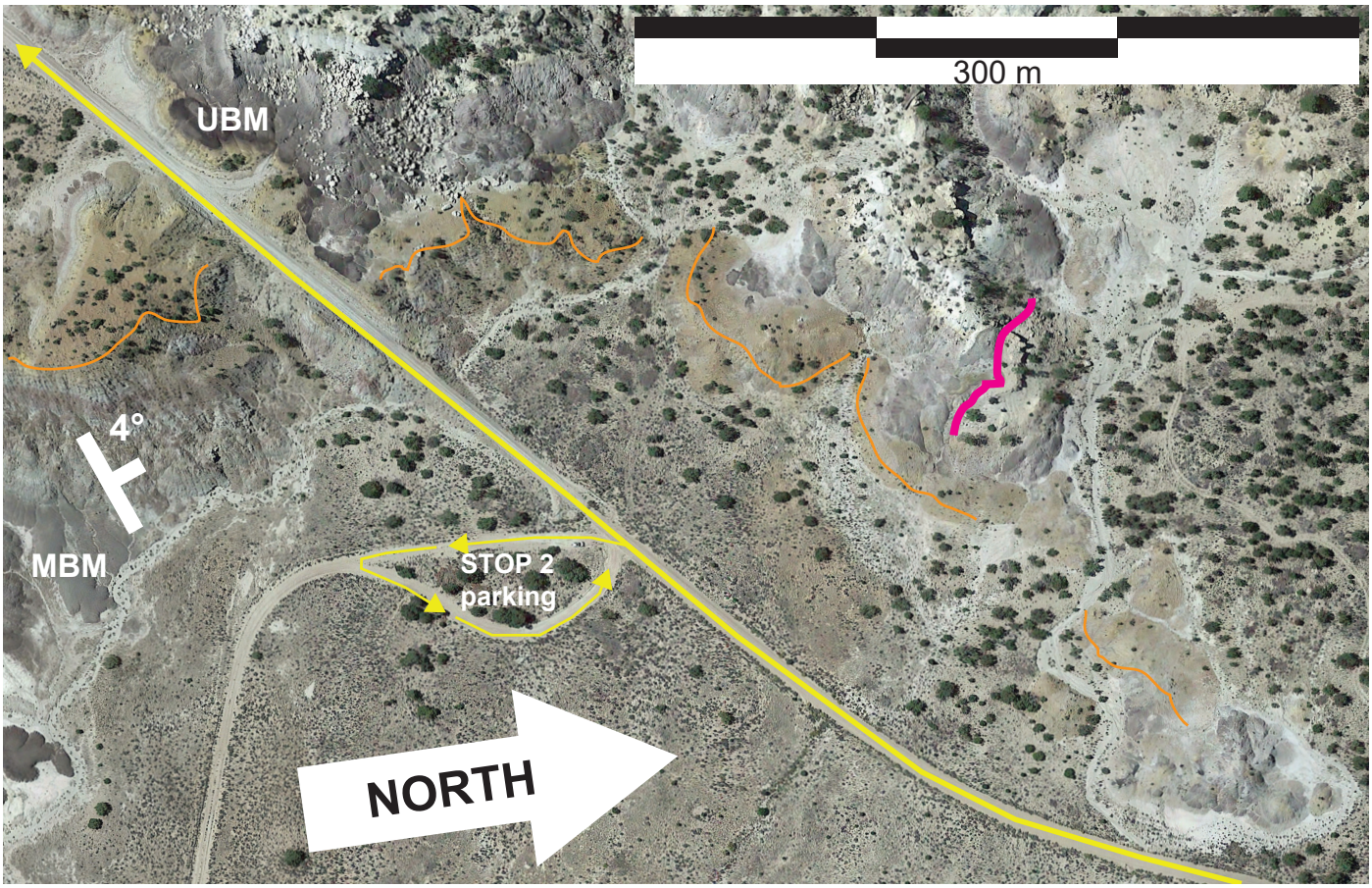

Figure 1.28. Annotated aerial photograph of Stop 2 area. Orange line marks the outcrop of a silcrete. Pink line marks the approximate trace of a fault. MBM = middle black mudstone. UBM = upper black mudstone. Paleogene units in this area dip shallowly to the northwest. Yellow line marks BLM Road 1101 and road log route.

megaquartz (>20 μm). The detrital component of silcretes is usually quartz (Nash and Ullyott, 2007). There is a well-documented sequence of silica ordering in silcrete cements, with amorphous opal being replaced progressively by chalcedony, microquartz, and megaquartz (Thiry and Milnes, 1991). This sequence is present in pedogenic silcretes, where more ordered silica is present near the top of the profile (Ballasteros et al., 1997), and in groundwater silcrete vug fills, where silica order increases toward the center of voids (Thiry and Milnes, 1991). Alumina content is usually <1 wt%, with higher concentrations reported in some pedogenic silcretes (Nash and Ullyott, 2007). The silica in most silcretes is derived from weathered silicate minerals, which requires solute silica in surface and subsurface waters. Silica solubility is affected by a number of factors, but under most conditions is greatest in waters with pH >9 (Dove and Rimstidt, 1994). Under most surficial and shallow groundwater conditions, quartz remains relatively insoluble, making quartzose sediments unlikely sources for solute silica in surface and subsurface waters (Nash and Ullyott, 2007). Argillization and clay diagenesis are important silica sources (Birkeland, 1974; Wopfner, 1983) and usually occur in low pH environments associated with high bioactivity or precipitation of metal oxyhydroxides. Silica can have biogenic sources in monocotyledonous plants and diatoms. Pedogenic and evaporitic silcretes involve vertical translocation of silica, resulting in vertical gradations in silica form and/or content (Nash and Ullyott, 2007).

Nacimiento Formation Silcretes

The Nacimiento Formation contains numerous 10–50 cm thick, weathering resistant, indurated silica-rich beds. These beds are interbedded with assorted facies, including sandstone, mudstone, and paleosols. Rains (1981) applied the term silcrete to these beds. Due to their resistance to weathering relative to subjacent and superjacent rocks, silcretes are noticeable features in the landscape as they cap mesas, form prominent bluffs and breakaways in hillslopes, and create talus-mantled slopes and plains below vertical outcrops (Fig. 1.29). Despite their prominence in the landscape and their abundance in the Nacimiento Formation, these silcretes remain poorly understood.

Three studies have investigated Nacimiento Formation silcretes, and all conclude that they likely formed via pedogenic or supergene processes as opposed to groundwater diagenesis (Rains, 1981; Williamson et al., 1992; Hobbs, 2016). The exact method of Nacimiento Formation silcrete formation, however, remains poorly understood. These silcretes are homogeneous, decimeters-thick beds with uneven bases and sharp planar tops (Fig. 1.30). Root traces and/or tubular trace fossils are present in approximately 20% of silcrete beds in the

Figure 1.29. Landscape view of upper Blanco Wash near Nageezi, where silcretes partially control landscape development. Many of the cliffs, mesas, and hoodoos in the image are capped by silcretes. Where silcretes form talus beneath outcrops, they commonly take on a medium orange color that makes them distinguishable from a distance (marked by white arrows).

San Juan Basin. Sub- and superjacent beds show no noticeable depletion or enrichment in silicon, aluminum, or base cations. Silcretes usually are parallel with underlying units, but can be found crosscutting lower units (Fig. 1.31). Grains within silcretes include moderately to well-sorted, fine-grained sand to silt, and contain strain-free monocrystalline quartz with minor amounts of microcrystalline quartz, chalcedony, feldspar, lithic fragments, and accessory minerals. Grains make up 35–60% of the rock. Tephra shards are common (Fig. 1.32), making up 9–20% of the rock by volume. Tephra shards were identified on the basis of biconcave shapes, arcuate clast margins, Y-shaped clasts, or preserved whole vesicles, all indicative of vesicularity. Many clasts are elongate and very angular. These have the same mineral and chemical composition as clasts that meet the criteria for shards, but one cannot be certain of their origin. By not counting them as shards, there likely exists an underestimate of the total percentage of shards in these silcretes. Silcretes are cemented by cryptocrystalline and microcrystalline silica matrix that is 40–65% of the rock by volume (Fig. 1.33). Unlike many pedogenic and groundwater silcretes, there is no observed progression of silica ordering (e.g., from low-order amorphous silica to high-order quartz) in grains, matrix, or vug fills of Nacimiento Formation silcretes. Clays make up <2% of the matrix and are often associated with bioturbation features. Unfilled pores make up <2% by volume of Nacimiento Formation silcretes, making these the lowest-porosity facies in the San Juan Basin Paleogene section. By standard sedimentary classification, Nacimiento Formation silcretes are classified as silica-cemented submature quartz wackes. By the pyroclastic classification of Schmid (1981), Nacimiento Formation silcretes are tuffites. Using the micromorphological classification of Summerfield (1983), Nacimiento Formation silcretes are F-fabric silcretes (matrix-supported).

Silcrete Origin in the Paleogene San Juan Basin

Hobbs (2016) proposed that the alteration and cementation of eolian-deposited silica-rich tephra were responsible for Nacimiento Formation silcretes. The abundance of very angular tephra shards (Fig. 1.32) suggests limited fluvial transport of these clasts after deposition. The nearest known igneous eruptive centers in the early Paleocene are ≥100 km (≥ 62 mi) from these silcretes (Cunningham et al., 1994), and tephra shards are likely to be destroyed or rounded if fluvially transported such a distance (Cas and Wright, 1988). The textural uniformity

Figure 1.30. A typical Nacimiento Formation silcrete outcrop. Note the uneven but sharp lower contact and sharp, planar upper contact. For scale, dog is 1 Labrador tall.

(fine sand to silt), sorting, lack of fluvial bedding structures, and stratigraphic relationships of these silcretes also suggest an ash-fall origin. Some silcretes can be observed on either side of sand-filled channel cut structures, suggesting that the silcrete formation is related to original bed composition instead of a later water table position. The "bifurcating" silcretes of Rains (1981; Fig. 1.31) are in fact the result of erosion of a lower ash-fall deposit by a channel cut and the subsequent deposition of a later ash-fall deposit that draped topography.

Even if the original bulk chemical composition of Nacimiento Formation eolian pyroclastic deposits is assumed to be as silica-rich as the most silicic shards observed in recent volcanic eruptions (75 wt% SiO_2, 13 wt% Al_2O_3, 12 wt% other; Shane, 1991), then postdeposition removal of aluminum and base cations is still required in order to attain the bulk chemical compositions observed in Nacimiento Formation silcretes (Table 2). This is problematic for the interpretation of Nacimiento Formation silcretes, as the geochemical stability of silicic pyroclastic materials is well documented. At low pH, silicon is relatively immobile, but base cations are more mobile. Due to the presence of Nacimiento Formation silcretes immediately above and below arkosic sandstones with unaltered

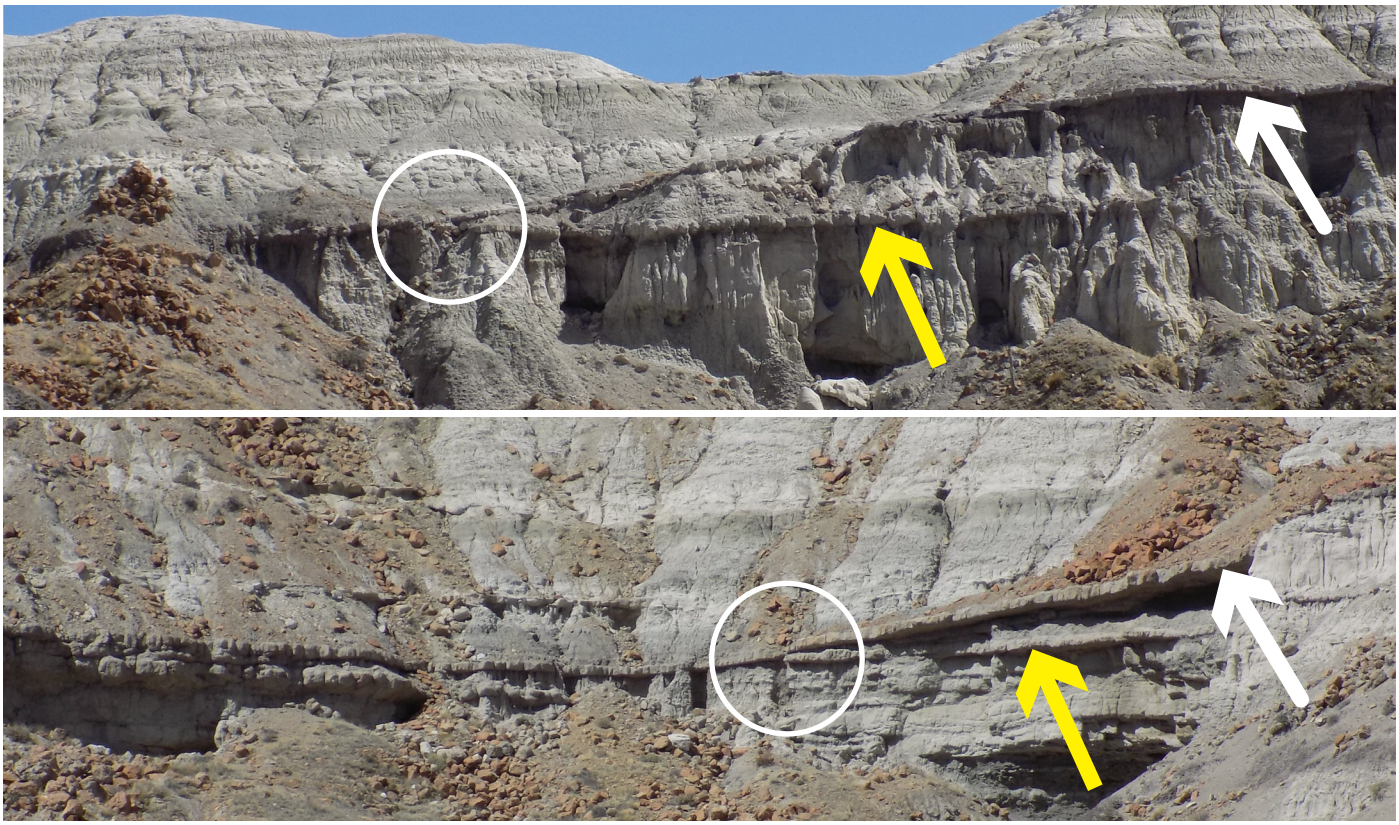

Figure 1.31. Two examples of Nacimiento Formation silcretes cutting across underlying beds. In both cases, the underlying beds include a silcrete (marked by yellow arrow). White arrows mark younger silcretes that were deposited and/or formed in disconformable contact with underlying beds. White circles are centered on intersections of upper and lower silcretes. Both outcrops are in the Torreon Wash drainage on Ceja Pelon Mesa.

TABLE 2. Bulk Geochemical Composition of San Juan Basin Silcretes

Sample	Wt% Na_2O	Wt% MgO	Wt% Al_2O_3	Wt% SiO_2	Wt% P_2O_5	Wt% K_2O	Wt% CaO	Wt% TiO_2	Wt% MnO	Wt% Fe_2O_3	Total
BDNZ-24	1.852	0.402	13.134	79.059	0.019	3.132	0.472	0.717	0.017	1.196	100.0
ESCA-05	0.099	0.357	5.892	90.622	0.012	0.532	0.391	1.118	0.008	0.968	100.0
CROW-06	0.253	0.199	3.829	93.597	0.010	0.150	0.224	1.062	0.011	0.665	100.0
CROW-082	0.224	0.151	5.275	92.229	0.013	0.103	0.143	1.070	0.014	0.779	100.0
CROW-05	0.145	0.178	7.867	89.619	0.015	0.081	0.118	1.054	0.010	0.910	100.0
ANSI-01	0.297	0.194	4.022	91.191	0.019	1.599	0.197	1.009	0.018	0.991	99.5
JACA-17	0.220	0.246	5.009	90.879	0.013	0.816	0.431	1.150	0.013	0.897	99.7
Average	0.441	0.247	6.433	89.599	0.015	0.916	0.282	1.026	0.013	0.915	99.887

from Hobbs (2016)

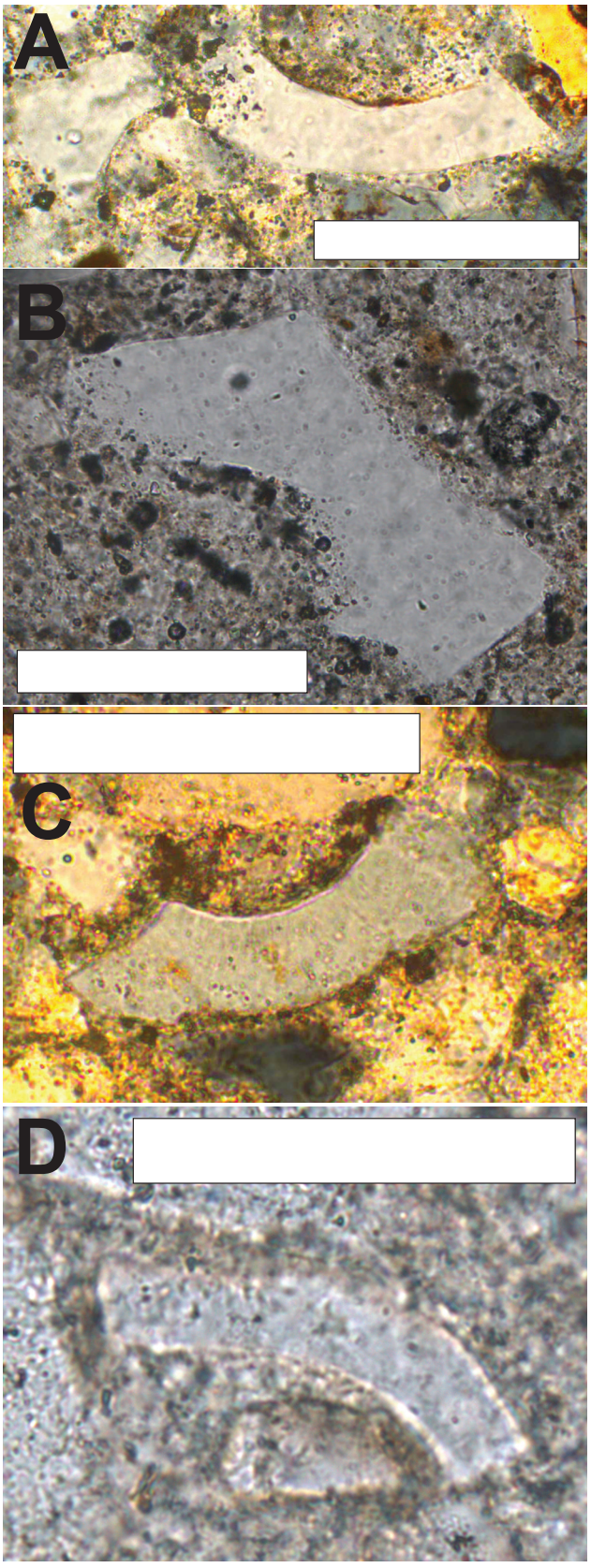

Figure 1.32. Plane-polarized light photomicrographs of tephra shards in Nacimiento Formation silcretes. White scale bars are 0.1 mm in each image. A: Sample ANSI-01 from Kutz Canyon. B: Sample CROW-06B from upper Blanco Wash (the area in Fig. 1.19). C: Sample OJEN-03 from Ojo Encino Wash. D: Sample ESCA-02 from upper Escavada Wash.

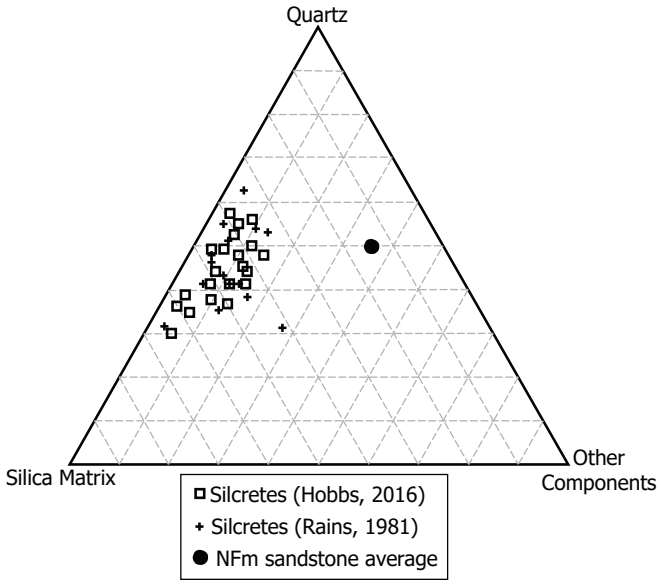

Figure 1.33. Ternary diagram showing relationships among quartz grains, silica matrix, and all other components in Nacimiento Formation silcretes and average Nacimiento Formation sandstone. NFm = Nacimiento Formation. Modified from Hobbs (2016).

feldspars, the lack of remarkable loss or gain of aluminum or base cations in those sandstones, and the distinct boundaries between silcretes and subjacent and superjacent beds, it seems unlikely that low pH groundwater could have caused the leaching observed in silcretes. If it had, greater alteration of adjacent units and less distinct lithologic boundaries would be expected. Instead, the chemical environments and processes responsible for silcrete formation must have been strictly confined to the eolian pyroclastic deposit beds themselves. A potential explanation is that porosity and permeability conditions within the eolian pyroclastic deposits allowed acidic meteoric waters long enough residence time to leach most aluminum and base cations from the initially glassy pyroclasts and interstitial ash. Plants colonized these deposits, as is evidenced by preserved roots traces, and their contribution of organic acids and ligands likely increased aluminum solubility (Drever and Stillings, 1997), an effect seen in modern plant-rich soils (Johnson et al., 1981). Modern soil formed in acidic materials or under acid-producing plant communities can create spodic horizons wherein aluminum and base cations are removed. While Nacimiento Formation silcretes lack the accumulation of aluminum and base cations deeper in the profile as observed in modern Spodosols, perhaps similar interactions among acidic materials, plant communities, and aluminum-humus complexes allowed for the nearly complete removal of most nonsilica elements from these horizons relatively rapidly after deposition.

Paleoenvironmental Implications of Nacimiento Formation Silcretes

The presence of numerous ash-fall deposits in the Nacimiento Formation demands a reconsideration of possible paleoenvironmental implications. Nacimiento Formation paleoclimatic conditions have been assumed as having high

mean annual precipitation and temperatures, due in part to the interpretation of crocodilian and palm fossils as indicators of humid paleoclimate conditions. The abundance of preserved ash-fall deposits in the Nacimiento Formation suggests that there was sufficient precipitation during Nacimiento Formation deposition to prevent the eolian erosion of these deposits; rapid colonization by plants likely aided in this preservation process. Ash-fall deposits in other Cenozoic fluvial basins have been interpreted as having been deposited under subhumid to semiarid conditions and as having significant impacts on paleobiota and paleolandscape development (Hunt, 1990). These silcretes prove that mineral material was delivered to the aggradational early Paleocene San Juan Basin via nonfluvial means. Nacimiento Formation silcretes also show that portions of the Nacimiento Formation depositional system underwent periods of quiescence during which eolian pyroclastic deposits could not only accumulate, but also be colonized by biota and preserved in the geologic record.

Basin-Internal Faults

> "High-angle faults of irregular strike are especially numerous in the Chama and Puerco platforms on the east side of the [San Juan] basin. The throw on these faults is small in relation to their length."
>
> V.C. Kelley, 1st NMGS Fall Field Conference Guidebook, 1950 (Kelley, 1950)

Since New Mexico Geological Society's first president Vin Kelly penned those words 74 Fall Field Conferences ago, many subsequent geologic mapping efforts in the San Juan Basin have revealed short (<10 km), often high-angle (>75°) normal faults (Fig. 1.34). These faults generally are too small to be captured on statewide or basin-wide geologic compilation maps, but are revealed in many areas within the basin by most field mapping efforts at the 1:100,000 scale or larger. Although the tectonic significance of basin-interior normal

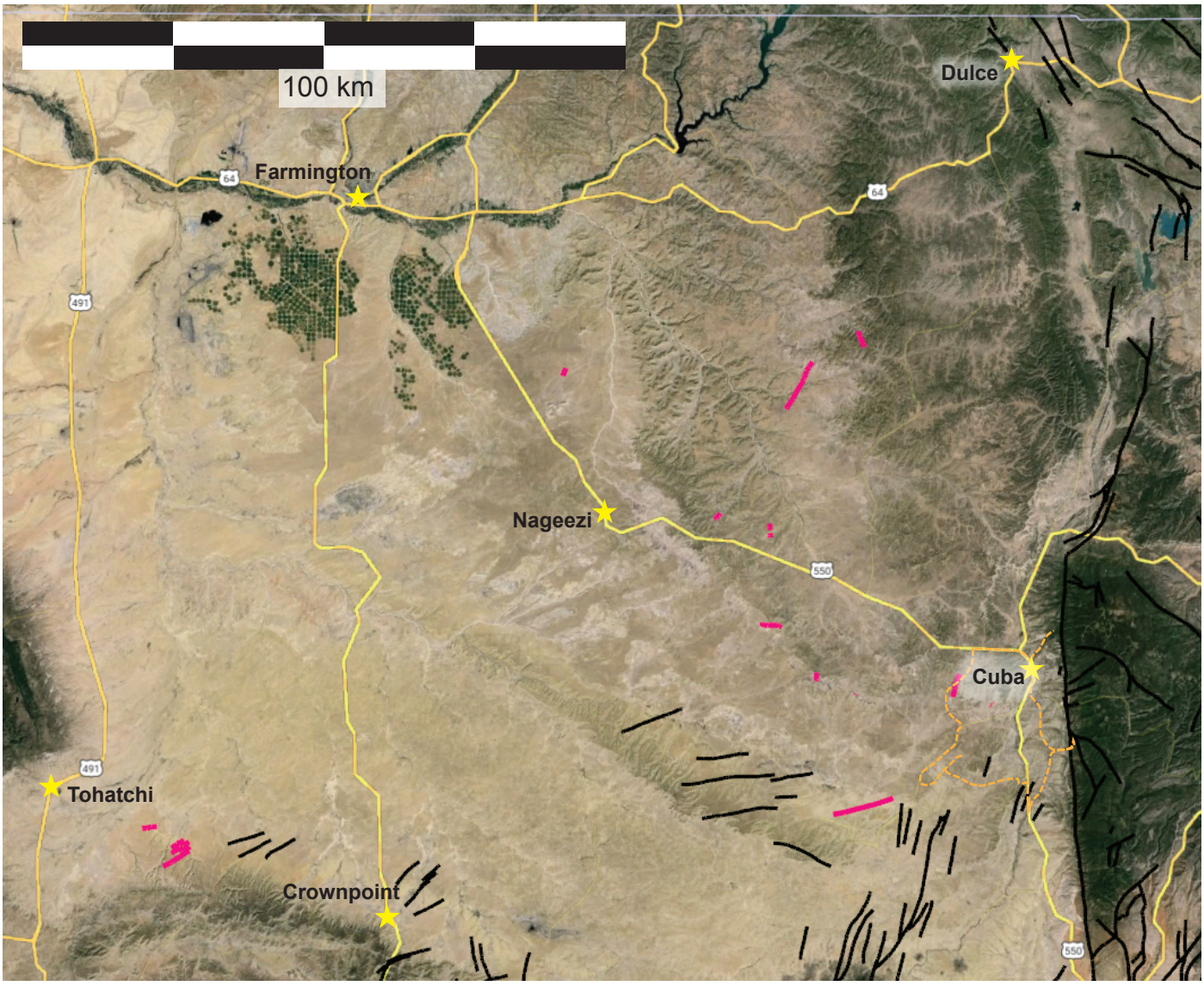

Figure 1.34. Aerial photograph of the San Juan Basin in New Mexico. Black lines show faults mapped at the 1:500,000 scale on the New Mexico State Geologic Map (NMBGMR, 2003). Pink lines show unmapped or newly mapped high-angle normal faults in the basin interior. Orange dashed line shows the route of the Day 1 road log.

faults is almost certainly of lesser importance than the larger-scale compressional and/or transpressional tectonics more plainly manifest in San Juan Basin deformation structures like the Nacimiento fault, it nonetheless deserves consideration. At present, however, it remains largely unaddressed.

Recent STATEMAP mapping on the Chaco Canyon 30x60-minute quadrangle (Hobbs and Pearthree, 2021) and the Coyote Canyon 15-minute quadrangle (Hobbs and Krupnick, 2024), and geologic mapping related to hazards analysis on the southern Jicarilla Apache Nation (Hobbs and Pearthree, 2023) presented opportunities for detailed documentation of several San Juan Basin-interior high-angle normal faults (e.g., Fig. 1.35). In each of these locations in the central and southern San Juan Basin, normal faults are found in Cretaceous and Paleogene siliciclastic sedimentary units. Where fault planes can be measured, their dips range from 56° to 88°. Fault offset is as much as 27 m (89 ft) and approaches zero at fault tips, where faults merge into joints traceable for up to hundreds of meters. Most observed fault planes do not preserve reliable kinematic indicators, but where striations are observed, they indicate dip-slip motion. Timing of fault motion is constrained only by crosscutting relations, with maximum ages of deformation provided by the ages of Late Cretaceous, Paleocene, or Eocene sedimentary rocks cut by faults, and minimum ages provided by undeformed Pleistocene or Holocene surficial sediments that overlie faults. San Juan Basin normal faults often are isolated; where they occur in proximity to one another, the sense of motion on each subparallel fault is the same (e.g., all faults in an area are down-to-the-south), suggesting a distributed fault zone as opposed to a series of grabens and horsts. Within individual quadrangles or similarly sized areas of study, the faults reported here sometimes have systematic orientations, especially near the eastern and western basin margins. In general, however, the wide range of fault orientations does not indicate a basin-wide uniform stress orientation leading to San Juan Basin normal faulting.

The formative stress(es) that caused San Juan Basin-interior normal faults are not understood. Several possible culprits include tension relating to late Cenozoic Rio Grande rift development just east of the basin, flower structures relating

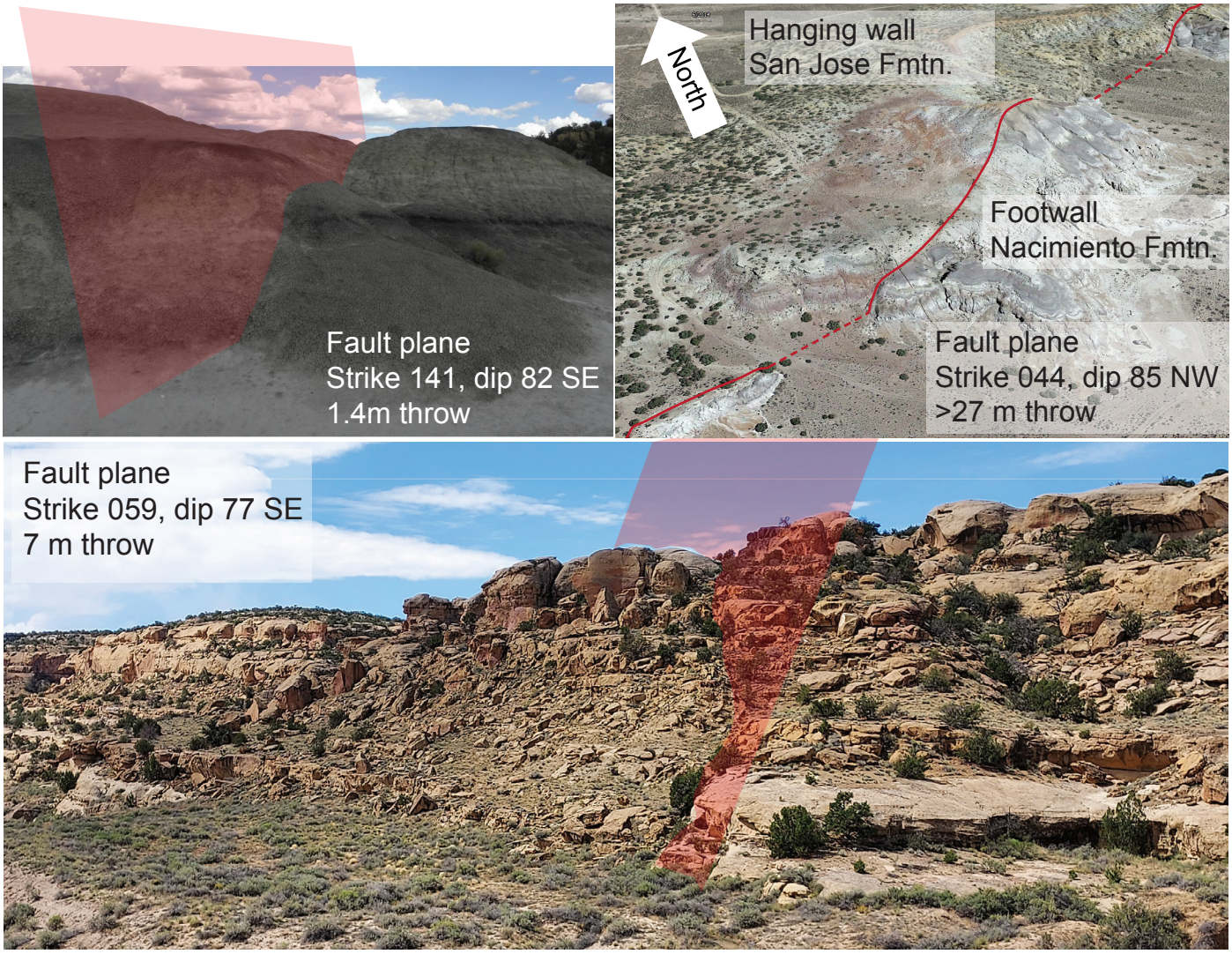

Figure 1.35. Field photographs of small-offset high-angle normal faults in the San Juan Basin. Top left: Fault cutting mudstones in the Ojo Encino Member of the Nacimiento Formation at Mesa de Cuba. Top right: Fault cutting the Nacimiento-San Jose Formation contact in Johnson Canyon near Lybrook. Bottom: Fault cutting the Point Lookout Sandstone in Peach Spring Canyon near Brimhall, Navajo Nation.

to unknown lateral shear in the basin subsurface, subsurface dissolution of lower soluble strata, and/or differential compaction faults. Each of these possibilities has arguments for and against it. The Rio Grande rift, for instance, is a known nearby source of tension with proven effects reaching into the Colorado Plateau. The orientation of these basin-interior normal faults, however, does not align with known stress vectors from rift-related extension, nor does the steep nature of these faults accommodate extension in any considerable way. When considering flower structures as a formative factor, one can argue that the scale, orientation, and steep fault planes of the en echelon faults observed in interior San Juan Basin all match with those observed in known flower structures elsewhere on Earth. However, there exist no known strike-slip faults capable of producing such structures in the San Juan Basin. Subsurface dissolution must be considered on account of the presence of soluble units in the San Juan Basin subsurface (in particular, the Jurassic Tonque Arroyo Member of the Todilto Formation) that are linked to collapse faults on Laguna Pueblo farther south in San Juan Basin. The offset of the largest normal faults observed in the basin's interior, however, is several times greater than the thickness of soluble units, and those soluble units are often >2 km (>1.2 mi) beneath strata that are faulted; it is unlikely that a few meters of offset will be transmitted over such distances. Differential compaction faults, a well-documented occurrence in thick sedimentary sequences such as those in the San Juan Basin, typically exhibit systematic orientations with respect to facies changes, depositional slope, or basement structures, and they typically form in high density fault arrays (not singly, as do many San Juan Basin normal faults; Xu et al., 2015).

What, then, to make of these faults? Even without a known—or even plausible—causative factor, the existence of these faults should be considered by any professional whose work might be affected by faults' properties. As the San Juan Basin's unconventional reservoirs are exploited, thinner and thinner target strata are sought. The presence of meters-scale faults in the subsurface should be of highest interest to geosteering crews. The same can be said for workers in ongoing carbon sequestration projects in San Juan Basin: what are the potential effects of faults such as these on the permeability of reservoirs and traps? For the hydrogeologist, what effects do they have on aquifer connectivity, recharge, etc.? Finally, for the good old generalist geologist, these faults represent an unknown piece of the geologic history of the region. Is that not reason enough for further inspection?

Further work with more mapping and basin-wide documentation and analysis is needed to understand more fully the causes, timing, and tectonic and/or basin evolution significance of the faults reported here. As San Juan Basin siliciclastic sedimentary units are further exploited as reservoirs for oil and gas, as aquifers, as repositories for produced water, and as targets for carbon sequestration, small-offset faults like these potentially serve as traps, leaks, or zones of increased permeability due to fault-zone fracturing, yet are unlikely to be recognized or documented in the subsurface. Characterization of these faults through geologic mapping is a first step to increasing understanding of the prevalence and significance and can shed light on why there are widespread (though small) extensional features throughout the otherwise compressional San Juan Basin.

At Stop 2, at least one fault causes easily visible offset in Nacimiento Formation sandstones (Fig. 1.36). Slickenlines indicate dip-slip motion (Fig. 1.37).

Artists and Nacimiento Formation Mudstones

> "As you come to it over a hill, it looks like a mile of elephants—gray hills all about the same size with almost white sand at their feet. When you get into the hills you find all the surfaces are evenly crackled so walking and climbing are easy."
>
> Georgia O'Keeffe (O'Keeffe, 1976)

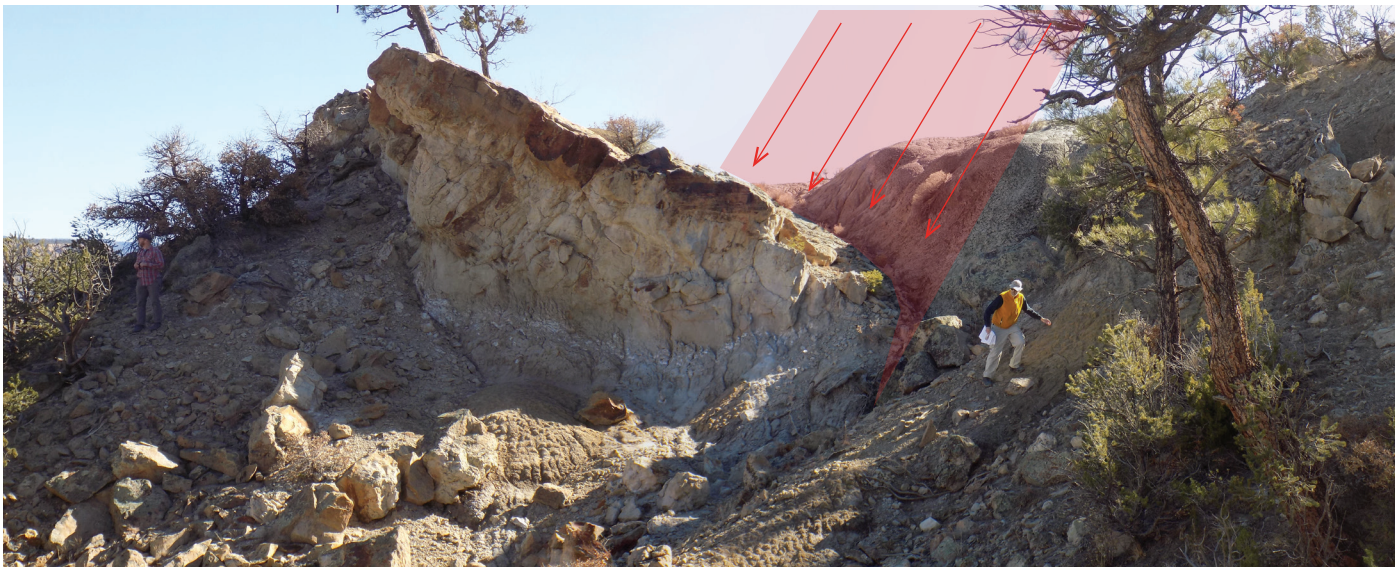

Figure 1.36. Annotated photograph of a fault exposed in Nacimiento Formation sedimentary rocks at Stop 2. Red shaded area is approximate location of fault plane; arrows indicate interpreted sense of motion. View is to the southeast; fault strikes approximately 300° and dips northeast.

Figure 1.37. Slickenlines on fault surface at Stop 2. Pen is placed approximately parallel to slickenlines and is 14.5 cm (5.7 in) long.

New Mexico's landscapes have inspired artists since before geology was a science. Geologic processes and products are so wonderfully displayed in New Mexican landscape, history, and culture, that artists' works often provide the geologist with an outsider's perspective on what we study. At Stop 2, one can view a small portion of such an example: the black mudstone landforms of the Ojo Encino Member of the Nacimiento Formation. These landforms crop out sporadically over a 75-km (45-mi) belt from Mesa de Cuba, just east of here, to upper Blanco Wash near Nageezi. Their slopes—capped by popcorn-like crunchy clay clods when dry, and a sticky, greasy, and near frictionless mire when wet—are steep at the base and become shallower uphill. This convex-up nature has befuddled at least one cliffed-out field geologist. The complexity of light and shadow on these nearly colorless hills, combined with their apparent but deceiving softness, made them a favorite subject of several of New Mexico's best-known artists of the 20th century.

Georgia O'Keeffe (1887–1986) made at least nine full-sized paintings of these hills, going so far as to name them "the Black Place." O'Keeffe's "Black Place" paintings (Fig. 1.38, 1.39) are held by several major museums within and outside New Mexico. Given the distance from her Abiquiu home, the painter would make days-long excursions to the San Juan Basin to study and paint here. Copious amounts of frozen venison and bacon, a ramshackle tent, and plenty of coffee—which the San Juan Basin winds apparently blew right out of its mug—were among her only supplies other than paints, brushes, and canvas (Fig. 1.40; O'Keeffe, 1976).

The ever-changing light conditions and moisture content of Nacimiento Formation mudstones makes them a challenging but attractive subject for photographers. Among these photographers are Maria Chabot, Todd Webb, and Eliot Porter. Chabot (1913–2001), a longtime assistant to O'Keeffe and an advocate for Native American arts and artists in New Mexico, documented many of her and O'Keeffe's trips to the Black Place (Fig. 1.41) with early morning or late evening photographs. Todd Webb (1905–2000), a Guggenheim Fellowship and National Endowment for the Arts recipient, visited the Black Place at least twice, including with O'Keeffe in 1963. Best known for his portraits and architecture photographs, Webb's photos of the Black Place are a departure from his normal subjects but capture well the fractal nature of drainage patterns in mudstone slopes (Fig. 1.42). Revered New Mexico photographer Eliot Porter (1901–1990) captured Nacimiento Formation mudstones on film for at least four decades. Porter was an early and vocal advocate for the use of color photography as an art form. He adopted Kodachrome film in the late 1940s and was the first color photographer to open an exhibition at the Metropolitan Museum of Art in New York. It seems strange, then, that he returned to the Black Place so often. The viewer wonders if some his San Juan Basin photographs were

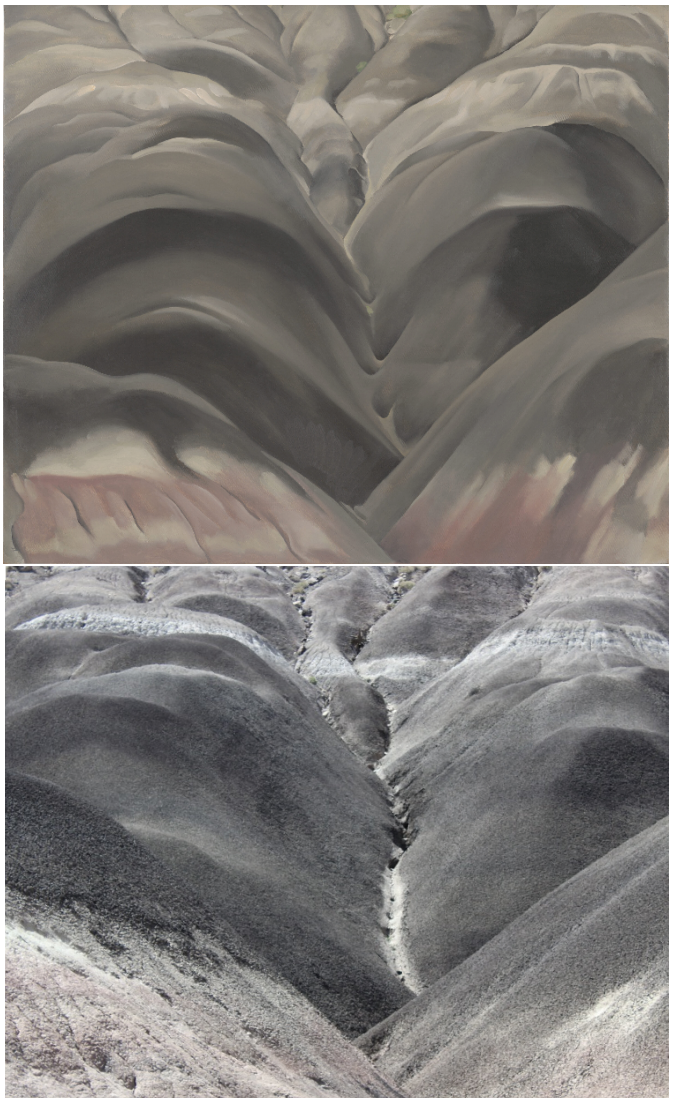

Figure 1.38. Top: "The Black Place I," painted by Georgia O'Keeffe in 1944. Held by the San Francisco Museum of Modern Art. Bottom: Field photograph of the outcrop depicted in O'Keeffe's "The Black Place I." Darkest-colored strata are organic-rich siltstones and mudstones. Lighter-colored strata are wackes and siltstones of arkosic composition.

even shot on color film (Fig. 1.43). The landscape in places lacks chroma altogether—perhaps this provided Porter with a challenge that is hard to find in other subjects?

15.2 Return to vehicles. Turn left (south) back onto BLM Road 1101, crossing cattle guard and climbing hill.

Figure 1.39. "The Black Place II," painted by Georgia O'Keeffe in 1944. Held by the Metropolitan Museum of Art.

0.2

15.4 At 1:00, the thin gray mudstone above the road is probably the "upper black mudstone"—an informal horizon name—of the Ojo Encino Member of the Nacimiento Formation. At 9:00, a shallowly north dipping silcrete caps a small mesa with hoodoos (Fig. 1.44).

0.6

16.0 Crest of hill. On a clear day, Mount Taylor (Tsoodził) can be seen just right of 12:00.

0.8

16.8 Road bends to left; outcrop on left has strong brown rounded concretions capping hoodoos of yellow sandstone horizons within the Nacimiento Formation. Concretions like these are common in the Paleogene units of the San Juan Basin and are related to groundwater mineralization. They are slightly enriched in iron and magnesium oxides.

0.3

17.1 Descend. Road crosses a steeply dipping down-to-the-west fault. At this location, this fault is not shown on maps, but is perfectly aligned with a down-to-the-west normal fault mapped by Fassett (1966) on Fork Rock Mesa 3 km (1.8 mi) south of here.

Figure 1.40. Artist Georgia O'Keeffe among Nacimiento Formation mudstones in 1944. At right, enjoying breakfast at the Black Place. At left, scouting with a Siamese cat. Pet animals like these often accompanied O'Keeffe on her painting trips. The painter noted that the cat would be shut safely in the cab of her Ford Model A at night while at the Black Place for protection from coyotes (O'Keeffe, 1976).

0.5

17.6 Road continues due south through a broad valley formed in the muddy middle and lower Nacimiento Formation. At 11:00 to 12:00, the tree-covered skyline is the crest of Mesa Portales, a shallowly north dipping mesa whose top is a dip slope of the Ojo Alamo Formation.

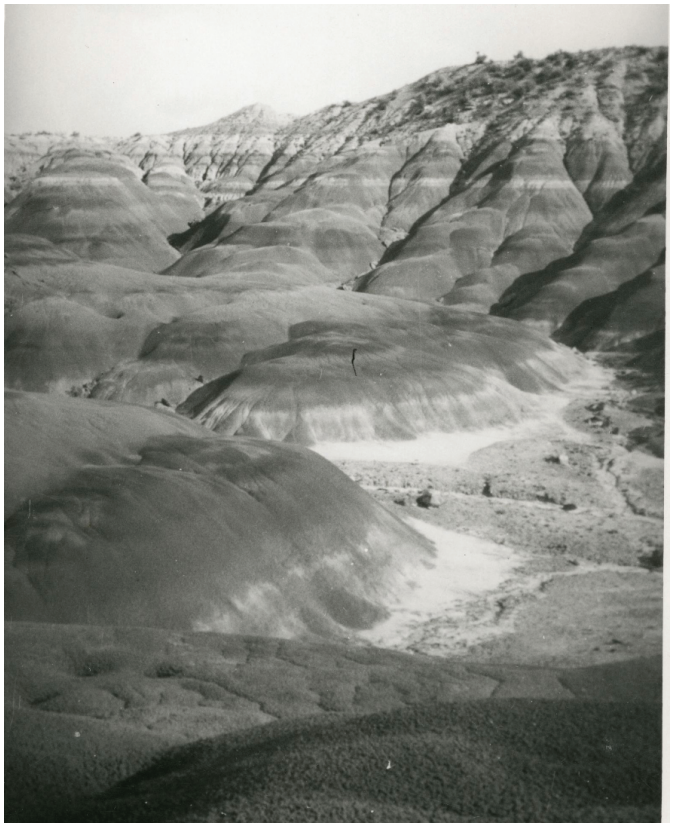

Figure 1.41. Untitled photograph from near "the Black Place" by Maria Chabot, 1944.

Figure 1.42. "O'Keeffe's Black Place—New Mexico—1957" by Todd Webb.

0.4

18.0 Road passes through the San Ysidro valley, largely blanketed with vegetation-stabilized eolian cover. This eolian unit is 0.5 to 8 m (1.6 to 26 ft) thick, contains a weakly developed pedogenic carbonate horizon, and still expresses eolian depositional morphology. Some of these

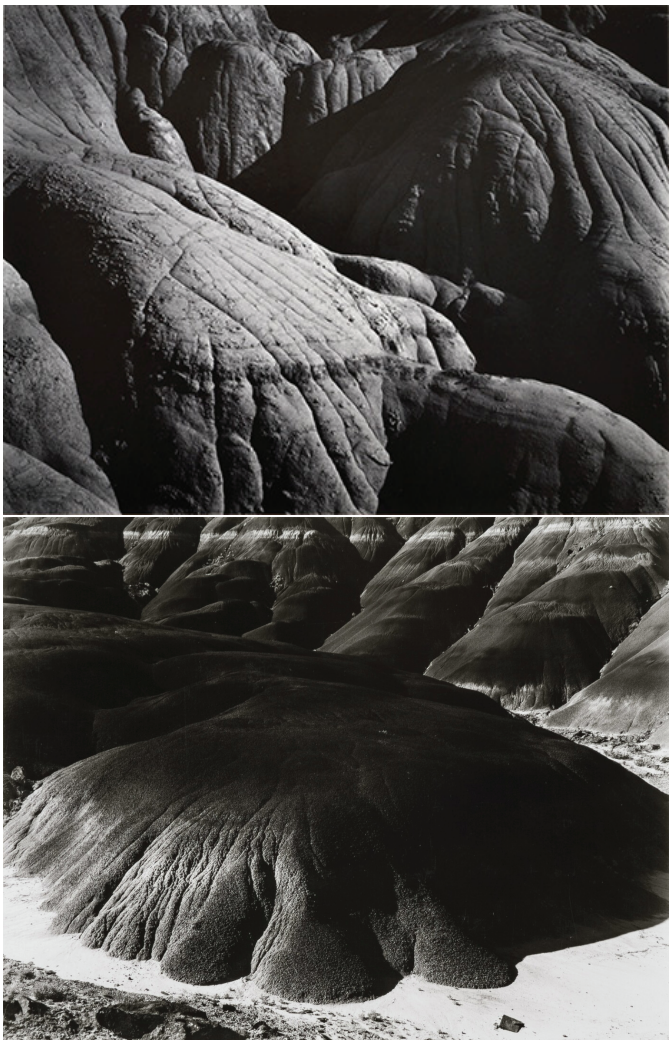

Figure 1.43. Top: "White Formations, Black Place, New Mexico, August 25, 1948," by Eliot Porter. Bottom: "Black Place, New Mexico, August 25, 1948," by Eliot Porter.

Figure 1.44. A silcrete-capped hoodoo formation just southwest of Stop 2. The upper black mudstone is visible in the right background.

landforms are best observed via remote sensing, such as in Figure 1.45, showing blowout depressions on either side of the road here.

0.3

18.3 **Road terminates at a T intersection. Turn left (east) onto the poorly marked and oft-washboarded Road 57 (Valle San Ysidro Road).**

0.2

18.5 **Road terminates at paved State Road 197.** Before the turn, the south end of Mesa de Cuba is visible at 9:00; the Sierra Nacimiento makes up the entire eastern skyline; and the dip slope of Mesa Portales is in front of you from 10:00 to 12:00. **Turn right (west) onto State Road 197.**

1.4

19.9 In a broad curve to the right, cross under powerlines. The road at left provides access to the northern dip slopes of Mesa Portales. **Stay on State Road 197.**

1.1

21.0 Cliffs in the distance at 12:00 are the thick arkosic arenites of the Ojo Alamo Formation.

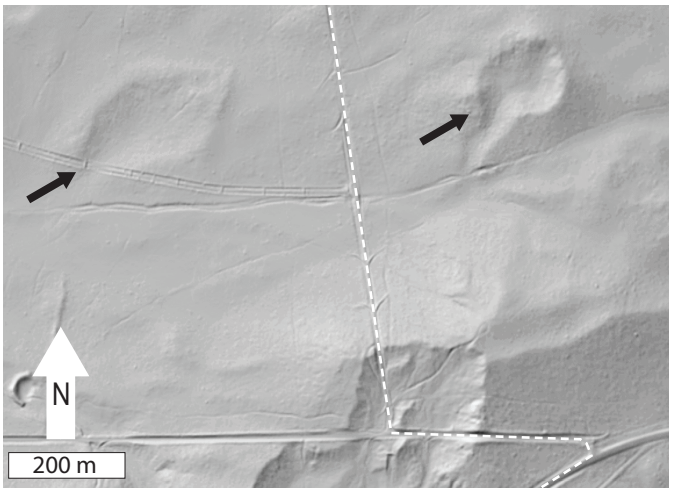

Figure 1.45. DEM-derived hillshade of the San Ysidro Valley near mile 18.0. BLM Road 1101 marked by dashed white line. Black arrows point to eolian blowout depressions in the eolian sand sheet covering most of this valley.

1.0

22.0 After a curve to the left, there is a good view of the Mt. Taylor (Tsoodził) volcanic field, including the northern end of Mesa Chivato and several volcanic necks, dead ahead.

0.7

22.7 Road begins a sweeping curve to the right, **begin slowing for upcoming turnoff.**

0.2

22.9 **Halfway through the curve, turn left (southeast) onto BLM Road 1102 (North Piedra Lumbre Road).**

Waypoint 1.04 [35.9079°, −107.1308°]

0.0

22.9 **Immediately after cattle guard, turn left (east) onto a two-track road to the north side of an earthen berm.**

0.6

23.5 Road heads due east up Cañon Jarido toward the center of Mesa Portales. Note the gentle north dip on top of the mesa.

0.5

24.0 Cattle guard.

1.0

25.0 Road crosses under powerlines. From 9:00 to 1:00, the gray mudstones of the Late Cretaceous Kirtland Formation are seen underlying thick, orange, laterally continuous arenites of the Ojo Alamo Formation. Just left of 12:00, notice thick orange sandstone at the same level of adjacent muds in the Kirtland Formation. This sandstone, well below the mesa-capping sandstone, is within the Kirtland Formation (Fig. 1.46). Hobbs and Fawcett (2021) describe the petrographic differences between the sandstones of the Kirtland and Ojo Alamo Formations.

Waypoint 1.05 [35.9090°, −107.0882°]

Figure 1.46. Panoramic photograph of Mesa Portales on the north side of Cañon Jarido near Stop 3. The dashed white line approximately marks the contact between the underlying Cretaceous Kirtland Formation and the overlying Paleogene Ojo Alamo Formation. Red arrow marks a discontinuous sandstone within the Kirtland Formation. White arrow marks the same stratigraphic level where no sandstones are present. The Ojo Alamo Formation at Mesa Portales is characterized by laterally continuous feldspathic arenites like these.

0.6

25.6 STOP 3. Just before the road passes into a copse of junipers, unload passengers and walk northeast about 100 m (330 ft) for a discussion of the Cretaceous–Paleogene transition in the San Juan Basin, recent paleontological discoveries in the Kirtland Formation on Mesa Portales, and the Ojo Alamo Sandstone.

The Cretaceous-Paleogene Boundary in the San Juan Basin

Sedimentary rock units bracketing the Cretaceous–Paleogene (K–Pg) boundary in the San Juan Basin have been the subject of investigation since the late 19th century (e.g., Cope, 1885), largely fueled by the abundance and diversity of dinosaur (e.g., Brown, 1910; Gilmore, 1916; Osborn, 1923; Wiman, 1930) and mammal (e.g., Sinclair and Grainger, 1914; Gilmore, 1916; Flynn, 1986; Williamson, 1993) fossils that provide some of the best-preserved and most geochronologically constrained records of animal life immediately before and after the end-Cretaceous extinction event at 66.043 ± 0.043 Ma. The K–Pg boundary in most of the San Juan Basin lies at the base of the Kimbeto Member of the Ojo Alamo Formation (Fig. 1.47). The unit underlying the Kimbeto Member has been called the Naashoibito Member since the middle 20th century, with some workers placing it as the uppermost member of the underlying Kirtland Formation (previously called the Kirtland Shale; e.g., Baltz, 1967) and others placing it as the lowermost member of the overlying Ojo Alamo Formation (e.g., Powell, 1973; Cather et al., 2019). Abundant biostratigraphic evidence (e.g., Williamson and Weil, 2008; D'emic et al., 2011) and geochronological data (Heizler et al., 2014) collected from within the Naashoibito Member suggest it is Maastrichtian in age (72.1 to 66.043 Ma), although there has been a controversial debate on stratigraphic and geochronological interpretation of the Naashoibito Member (see Fassett, 2009; Lucas et al., 2009; Fassett, 2013) in the 21st century. The Naashoibito Member overlies an unconformity of at least 3 My duration that removes the top of the Campanian and base of the Maastrichtian. There is another unconformity between the Naashoibito Member and the Kimbeto Member, although its duration is perhaps as little as 2 My. Arguments for placing the Naashoibito Member in the Kirtland Formation rest primarily on its Cretaceous age (thus preventing the Ojo Alamo Formation from being both Cretaceous and Paleogene). Arguments for placing the Naashoibito Member in the Ojo Alamo Formation include the fact that (1) the unconformity beneath it likely is larger than the one below it, and (2) nomenclatural convention following these units' first lithologic description by Bauer (1916; Fassett et al., 1987).

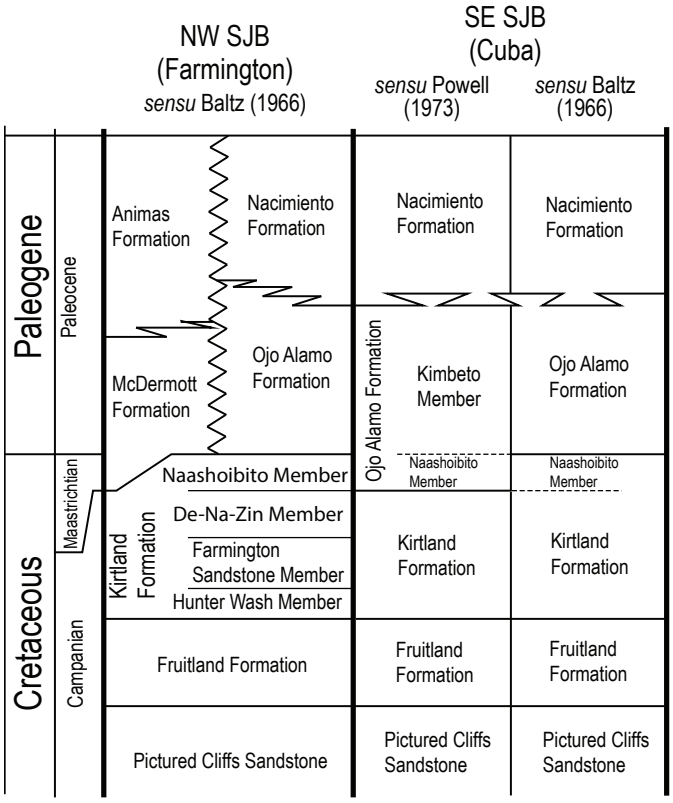

Figure 1.47. Simplified stratigraphic chart showing different nomenclatures of units bracketing the Cretaceous–Paleogene boundary in the San Juan Basin in New Mexico. Modified from Hobbs and Fawcett (2021).

Whichever formation one chooses to place the Naashoibito Member in, its paleontologic record, sedimentary architecture, and stratigraphic relationships all add to the complexity of the K–Pg boundary in the San Juan Basin. The Kirtland Formation, Ojo Alamo Formation, and Nacimiento Formation all record the tectonic evolution of the basin during the Laramide orogeny. Hobbs and Fawcett (2021) compared the mineralogical and geochemical compositions of sandstones from these formations, showing that earlier interpretations of regional paleogeographic rearrangement across the K–Pg boundary (Fig. 1.48) are supported by new data. Sandstone detrital grain compositional data show slight shifts in interpreted provenance types based on the methods of Dickinson et al. (1983), with a trend more toward a recycled orogen provenance through time (Fig. 1.49). Feldspar composition show a more striking change across the K–Pg boundary, with potassium feldspars becoming predominant in sandstones in the Paleogene Ojo Alamo Formation (Fig. 1.50)

In the southern San Juan Basin, including here at Stop 3, the long-held assumption that the Maastrichtian is absent (e.g., Fassett, 1966; Hobbs and Fawcett, 2021) is being challenged by recent paleontological discoveries. The *Torosaurus* described below and in a manuscript by Cantrell and Suazo (this volume), as well as recent discoveries of *Alamosaurus* nearby, suggests that Maastrichtian sediments are preserved in the area around Mesa Portales below the Kimbeto Member of the Ojo Alamo Formation. *Torosaurus* is known only from the Maastrichtian, with the oldest-known reliably dated specimen at younger than 69 Ma (Mallon et al., 2022). Detrital grain geochronology is currently underway to gather more evidence on the age of dinosauriferous strata near Cuba.

A note on terminology: The International Union on Geological Sciences (IUGS) in 1989 removed the term "Tertiary" as a descriptor for the geologic time period between the Cretaceous and the Quaternary. It was replaced by the Paleogene (spanning from the end of the Cretaceous to the beginning of the Neogene) and the Neogene (spanning from the end of

the Paleogene to the beginning of the Quaternary) Periods, although this remains contested (Knox et al., 2012). After nearly four decades, the term "Tertiary" remains in informal use. We use the IUGS-, USGS-, and NMBGMR-recommended terms "Paleogene" and "Neogene" instead.

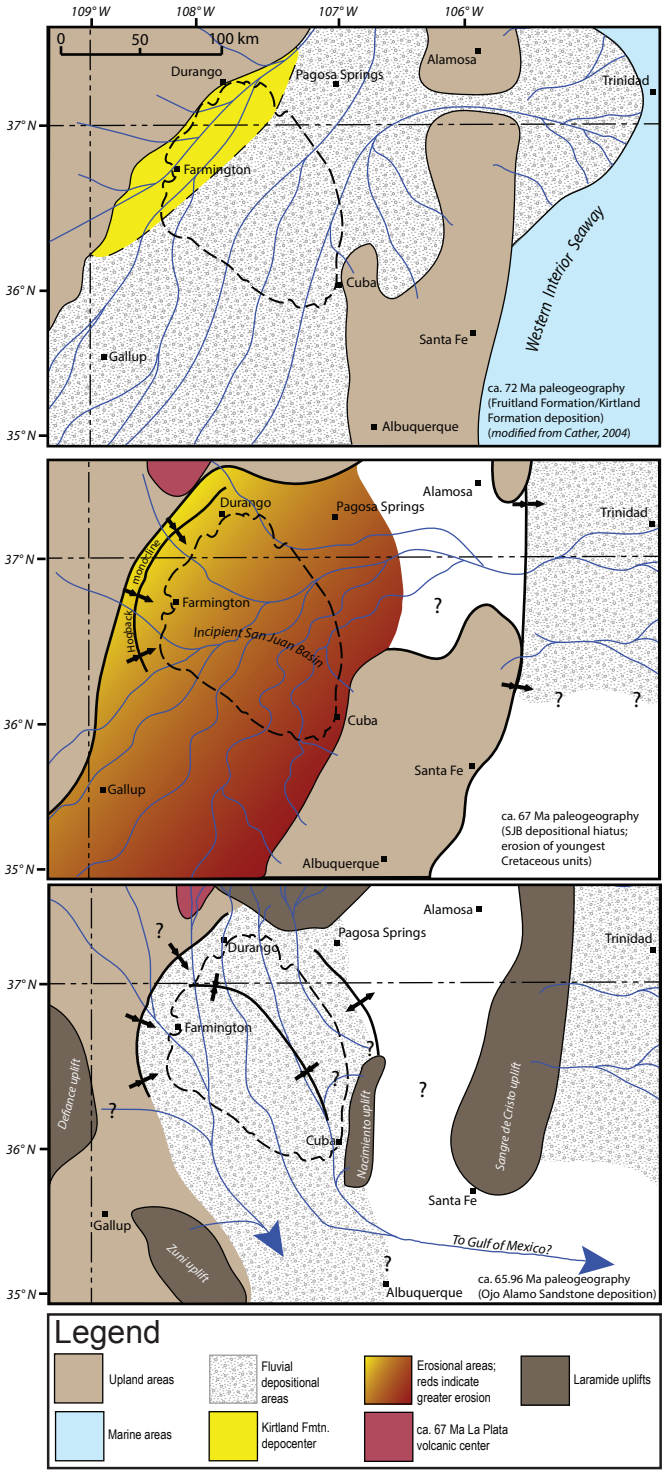

Figure 1.48. Paleogeographic maps showing Campanian (top), Maastrichtian (middle), and Paleocene (bottom) interpretations of the San Juan Basin region. Note that recent paleontological discoveries in the southeastern San Juan Basin, especially the *Torosaurus* (Cantrell and Suazo, this volume), might prove the middle (Maastrichtian) map incorrect. Modified from Hobbs and Fawcett (2021).

Recent Dinosaur Discoveries in the Southeastern San Juan Basin

Recent efforts by paleontologists to locate vertebrate fossils west of Cuba, New Mexico, near State Road 197, have led to the discovery of several important specimens. The most notable find is an 75% complete skeleton of an exceptionally large ceratopsian dinosaur, *Torosaurus* sp. (Fig. 1.51). This specimen was discovered in geologic units mapped as the Late Cretaceous (Campanian) Kirtland Formation. Other important finds from the area include *Alamosaurus* sp., *Triceratops* sp., *Edmontonia* sp., *Brachychampsa* sp., unidentified tyrannosaur and hadrosaur specimens, as well as several fish and turtle specimens. The *Torosaurus* sp. skeleton is on permanent display at the Museum of Evolution near the town of Maribo in Lolland, Denmark. A cast of the *Torosaurus* sp. skeleton is on permanent display at the University of New Mexico's Silver Family Geology Museum in Northrop Hall.

Vans proceed for another 0.3 mi before turnaround.

0.3

25.9 **Turn around just past retention dam and before cattle guard in meadow to right of road. Retrace route back to Stop 3, pick up passengers, then return west for 2.6 miles back to BLM Road 1102.**

2.9

28.8 **Road terminates. ZERO ODOMETER and turn hard left on BLM 1102.** For the next 11 miles, we follow a portion of the route of the 1977 NMGS Fall Field Conference, which covered 528 miles of San Juan Basin roads from Farmington to Crownpoint, Thoreau, Borrego Pass, Hospah, Red Mountain, Pueblo Alto, Torreon, La Ventana, Cuba, Llaves, El Vado, Dulce, Chromo, Chimney Rock, Ignacio, Navajo Dam, Aztec, and back to Farmington.

0.8

0.8 **Stay straight.** Road to the right goes to Media well field. This field was first drilled in 1953 in a shallow anticline discovered by surface mapping (Ostrander, 1957). The field's wells produced oil from the Jurassic Entrada Sandstone, which here exists about 1.6 km (1 mi) below ground surface. The discovery well in the Media well field reached "granite" (a catch-all term for crystalline rock used by drillers) at a depth of 2,952 m (9,684 ft), equivalent to approximately 850 m (2,800 ft) below sea level. At this latitude, crystalline rocks are found as high as 2,830 m (9,300 ft) elevation in the Sierra Nacimiento approximately 22 km (14 mi) east, proving a structural relief of at least 3.7 km (2.2 mi) on the east side of the San Juan Basin here.

0.6

1.4 The ridge to the right is made up of the Pictured Cliffs Formation, the uppermost marine sandstone in this part of the basin. *Ophiomorpha*, pelecypod, and gastropod fossils—all indicators of a marine environment of deposition—are common in the upper portion of the Pictured Cliffs here (Fassett, 1966).

1.3

2.7 **Stay straight at four-way intersection at crest of hill.** At 9:00, the south face of Mesa Portales exposes the upper 80 m (260 ft) of the Cretaceous section, here comprising the Fruitland and Kirtland Formations. Like at Stop 3, thick, stacked sandstone sheets of the Paleocene Ojo Alamo Formation cap Mesa Portales here. The K–Pg contact at 9:00 is at an elevation of approximately 2,230 m (7,300 ft), whereas at Stop 3 (2.5 km [1.5 mi] due north of your current location), it is at 2,165 m (7,100 ft), indicating an approximate north dip at

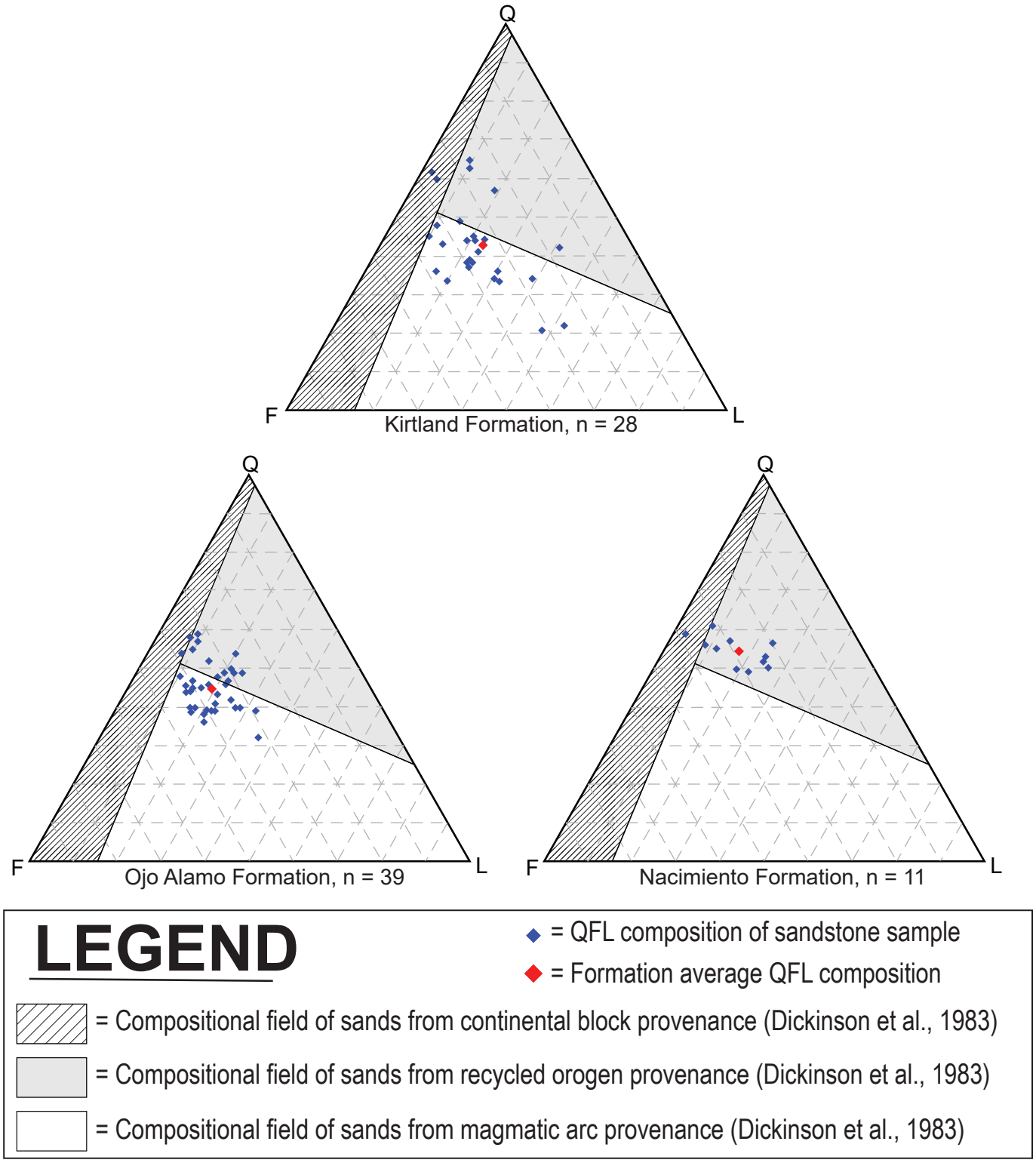

Figure 1.49. Ternary plots showing the relative abundances of quartz, feldspar, and lithic sand grains in sandstones from formations bracketing the K–Pg boundary in the San Juan Basin. Each data point represents a minimum of 300 grains counted in thin section using the Gazzi-Dickinson method. Provenance fields from Dickinson et al. (1983). Modified from Hobbs and Fawcett (2021).

1.5°. From 10:00 to 12:00, Mesa La Ventana dips toward you. The Sierra Nacimiento makes the skyline at 9:00 to 11:00. As you begin to descend the hill, the volcanic necks of the Puerco volcanic field are visible through the junipers to the right.

0.4

3.1 Powerline followed by cattle guard.

0.2

3.3 At 9:00, a small, rounded mesa lies to the west of and lower than Mesa Portales. This mesa is capped by a channel sandstone within the Fruitland Formation. Fassett (1966) placed the Pictured Cliffs Formation-Fruitland Formation contact, which represents the latest Western Interior Seaway-influenced deposition, at the base of this mesa. All deposition in the basin after this transition was strictly terrestrial. The road here, however, goes downsection into a broad valley weathered into the thick Lewis Shale, a marine unit.

0.9

4.2 Natural playa on left, called "Zambarmo lake" (Fig. 1.52). The 4 ha (10 ac) playa likely formed when the sediment-loaded, south-flowing arroyo draining the south face of Mesa Portales avulsed southwestward. The avulsion deposited enough sediment to dam the small east-flowing valley that the road occupies here, creating a natural impoundment (Fig. 1.53). Zambarmo lake must have been a long-known source of water, as it is the only lake shown on the 1932 Highway Map of Sandoval County (Fig. 1.54).

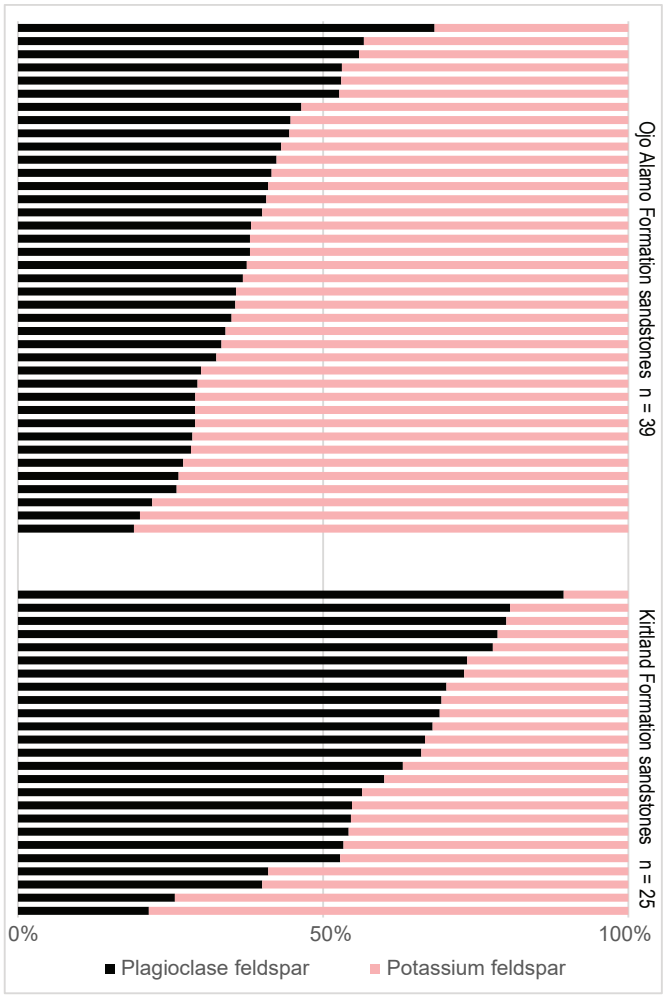

Figure 1.50. Plagioclase feldspar versus potassium feldspar proportions for sandstone samples from the Kirtland Formation (bottom) and Ojo Alamo Formation (top). From Hobbs and Fawcett (2021).

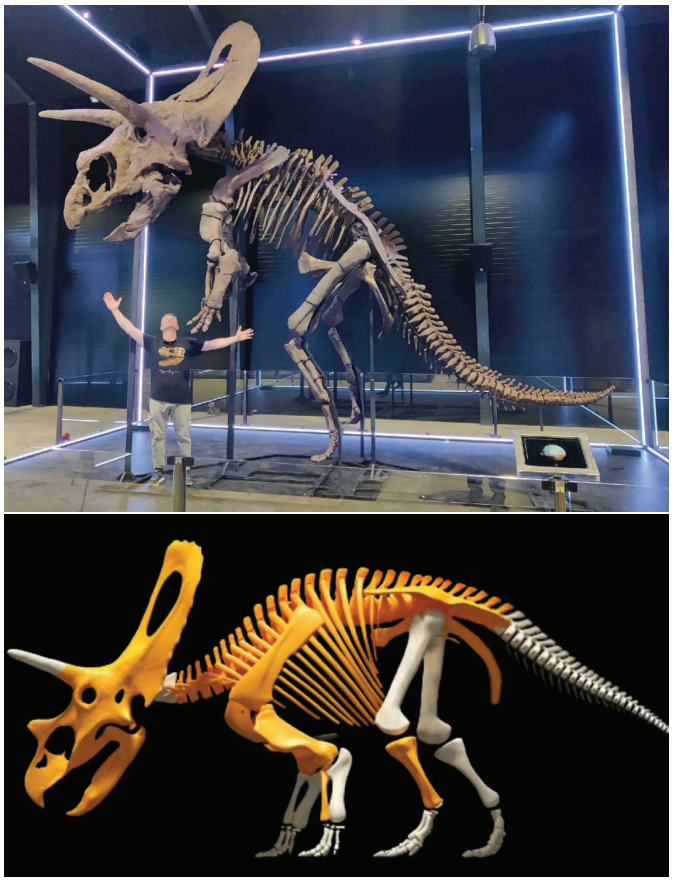

Figure 1.51. Top: The reconstructed San Juan Basin *Torosaurus* sp. skeleton on display at the Museum of Evolution in Lolland, Denmark. Note the adult *Homo sapiens* for scale. The *Torosaurus* sp. cranium is 3 m (10 ft) long. A reconstruction of this skeleton is on display in the Silver Family Geology Museum in Northrop Hall at the University of New Mexico in Albuquerque. *Photo courtesy of Amanda Cantrell.* Bottom: Diagram illustrating the fossil bones recovered in the field near Cuba, New Mexico, of the San Juan Basin *Torosaurus* sp. (in orange). The skeleton was over 75% complete. *Illustration from the Museum of Evolution, Lolland, Denmark*

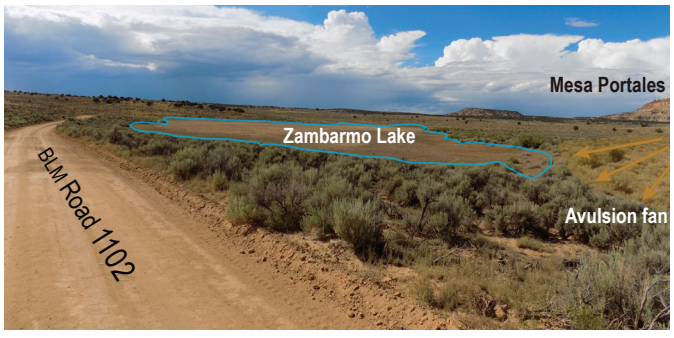

Figure 1.52. Field photograph looking northwest over Zambarmo lake.

Waypoint 1.06 [35.8675°, −107.0788°]

0.2

4.4 At 9:00, looking over the playa, notice the near-vertical fault to the left of the reentrant in Mesa Portales (Fig. 1.55). The black shale near the base of the mesa is downdropped about 12 m (40 ft) to the left. To the right of the reentrant, a large slump block displaces Ojo Alamo Formation sandstones down about 55 m (180 ft), obscuring the carbonaceous shale below it (Fig. 1.56).

0.2

4.6 **Stay left at fork.**

0.6

5.2 Road climbs a small ridge held up by platey sandy limestones in the Lewis Shale (Fig. 1.57).

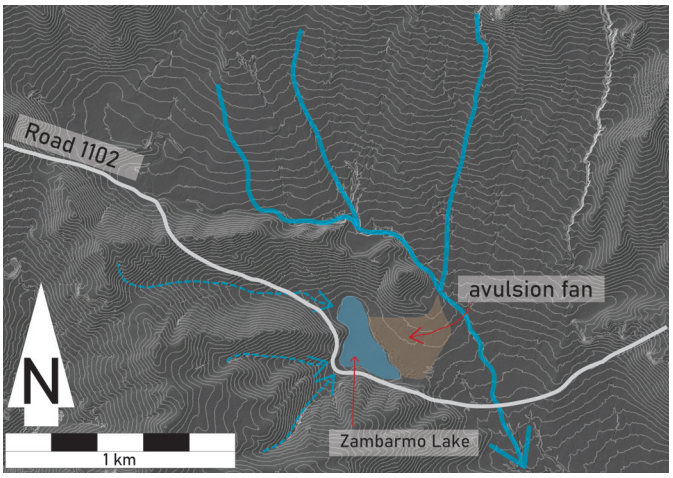

Figure 1.53. Digital hillshade map showing topographic relationships around Zambarmo lake. Contour interval is 1 m.

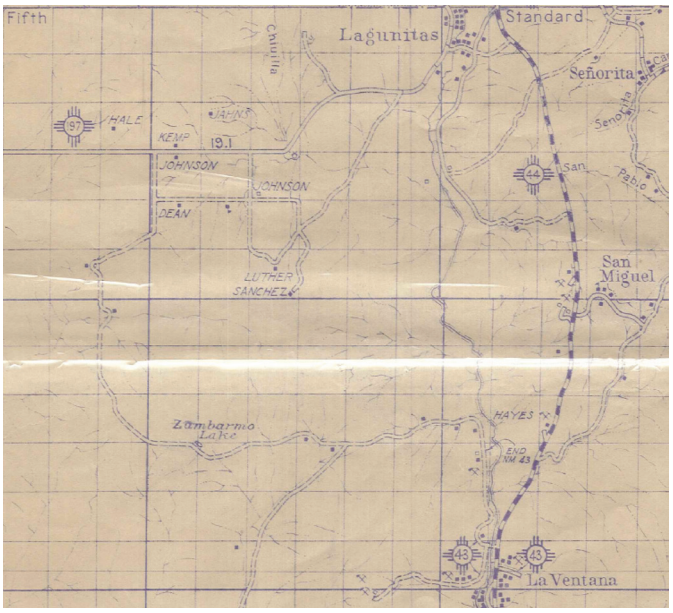

Figure 1.54. Portion of 1932 Highway Map of Sandoval County showing road log route and Zambarmo lake.

0.6

5.8 Cattle guard. **Stay straight.** Note the reddish clinker in the south face of Mesa Portales.

1.0

6.8 Descend hill. Note dip slope of La Ventana Mesa held up by arenites of the La Ventana Tongue of the Cliff House Sandstone in the distance on the right.

0.3

7.1 Road crosses the Continental Divide Trail (Fig. 1.58). If American life is getting you down, it's only a 1,064 km (660 mi) walk to old Mexico along the trail from here. The Canadian border: 3,861 km (2,394 mi). The nearest point on the actual Continental Divide is 24 km (14.4 mi) to the northwest.

1.1

8.2 **Continue straight through intersection.** Note the platey beds in the Lewis Shale (that contains so much more than just shale) to the left.

0.5

8.7 The sandstones here are the upper portions of the La Ventana Tongue of the Cliff House Sandstone. Here, the sandstones are thinner and interbedded with muddier units, and are interpreted by Fassett (1977) to represent the distal (seaward) end of shoreface sedimentation during the Campanian transgression. To the south and west, the La Ventana Tongue thickens into a massive sandbody.

0.3

9.0 Pass through the 107th meridian west. You are at the same longitude as Sheridan, Wyoming; Mazatlán, Sinaloa, Mexico; the Thwaites Glacier in Marie Byrd Land, Antarctica; and little else.

0.2

9.2 The massive sandstone at 12:00 is the Chacra bed (or Chacra tongue), a heavily exploited gas producer in the eastern basin (Fig. 1.59). The renowned USGS stratigrapher Carle H. Dane proposed the designation "Chacra sandstone" after exposures at Chacra Mesa on the south wall of Chaco Canyon (Dane, 1936). In so doing, he acknowledged Reeside's (1924) conclusion on Cretaceous shoreface sandstones in San Juan Basin: they are in fact "aggregates of successively overlapping beds which as a whole, with reference to a given chronologic plane, change their positions in the stratigraphic column from place to place." Walther's Law, writ large!

0.3

9.5 Cross cattle guard and enter private land.

0.6

10.1 At 9:00, the thick sandstone is the Chacra Tongue of the Cliff House Sandstone, a transgressive sequence deposited in the Campanian.

Figure 1.55. Photograph looking toward the north of the south face of Mesa Portales showing high-angle down-to-the-west fault (marked by white line) offsetting strata in the Kirtland Formation. Coaly layer, marked by red arrows, is offset by approximately 12 m (39 ft).

Figure 1.56. Photograph looking northeast of rockslump on south face of Mesa Portales. Relief between base of slope and crest of the mesa is 115 m (380 ft). Dashed red line marks the contact between the Kirtland Formation (Kk) and Ojo Alamo Formation (PEoa). Dashed white line marks outline of slump block.

0.7

10.8 Stay straight at crossroads with faint two track. The road to the left heads north up the Rio Puerco. The road at right provides access to the old coal mines at La Ventana 5 km (3.1 mi) south of here. The 1977 Fall Field Conference followed this route to a now-defunct bridge over the Rio Puerco. As of 2024, that road is nearly washed out (Fig. 1.60) and the route likely will be impassable the next time the NMGS Fall Field Conference visits the San Juan Basin.

0.05

10.85 Berm crossing over the artificial former channel of the Rio Puerco. In 1965, the New Mexico Department of Transportation (NMDOT) channelized a 3.4 km-long (2 mi-long) reach of the Rio Puerco here to facilitate construction of a new highway through the canyon to the south (Fig. 1.61). This bulldozer-dug channel quickly widened and deepened, leading to a near-runaway situation that threatened the very highway it was originally built to protect and delivered a considerable

Figure 1.57. Platey limestone outcrop in the Lewis Shale, near roadside at mile 5.2.

Figure 1.58. Trail marker along the Continental Divide Trail where it is crossed by the road log route at mile 7.1. The southeast side of Mesa Portales is on the skyline on the left.

Figure 1.59. Looking east toward the Chacra Tongue just left of the road at mile 9.2. The Sierra Nacimiento makes up the skyline.

Figure 1.60. Soil collapse feature along the Rio Puerco just south of the road log route. Photo looks east toward the Sierra Nacimiento up Arroyo de los Pinos.

volume of eroded sediment down the Rio Puerco (Coleman et al., 1997; Figs. 1.62 and 1.63). The NMDOT addressed the problem in the early 2000s by abandoning the artificial channel and rerouting the waters of the Rio Puerco back into their natural channel. See paper by Hobbs (this volume) on channelization and erosion on the Rio Puerco at this site.

0.15

11.0 At U.S. Route 550, **REZERO ODOMETER and turn right (south) on the paved four-lane highway**. Note the 2.5-m (8-ft)-tall wildlife fencing along the highway, installed in the past decade to protect elk (Dzéél, *Cervus canadensis*) from cars.

0.0 **Waypoint 1.07 [35.8779°, −106.9726°]**

0.1

0.1 On both sides of highway dead ahead, mesas capped by the thick La Ventana Tongue of the Cliff House Sandstone are dipping north. The southbound highway here is, therefore, heading downsection.

0.2

0.3 Note erosion on both sides of highway, which was built across an old meander of the Rio Puerco here (Fig. 1.64). The "new" artificial channelized Rio Puerco breached into this meander sometime in the late 1990s. The Rio Puerco's path on the east side of the highway here was aided by a bulldozer-widened cut through Cretaceous bedrock about 70 m (230 ft) east of the highway in order to alleviate threats to the new highway.

0.5

0.8 Bridge over the Rio Puerco. Stone steps in the channel below this bridge were installed in the early 2000s in response to engineering-induced downcutting in this reach (Fig. 1.65). On both sides of the highway, gravelly terraces of the Rio Puerco can be seen capping Cretaceous bedrock 10 to 30 m (33 to 100 ft) above the Rio Puerco.

0.4

1.2 **Waypoint 1.08 [35.8584°, −106.9693°]**

Turn left (east) onto County Road 11. For the next 3 miles, this highway runs through the watershed of Arroyo de los Pinos, a large tributary to the Rio Puerco that drains about 5 miles of the Sierra Nacimiento mountain front. After turn, note the east-sloping terraces of the Arroyo de los Pinos, which merge to the west with terraces of the Rio Puerco. The Arroyo de los Pinos is incised 11 m (36 ft) into its 19th century floodplain.

0.2

1.4 To the north (left), note a small, steeply dipping, down-to-the-west fault offsetting the Menefee Formation-La Ventana Sandstone contact (Fig. 1.66). An increase in fracture density near the fault zone is typical in steep faults in this region (see Ruf and Erslev, 2005; Hart and Cooper, 2021).

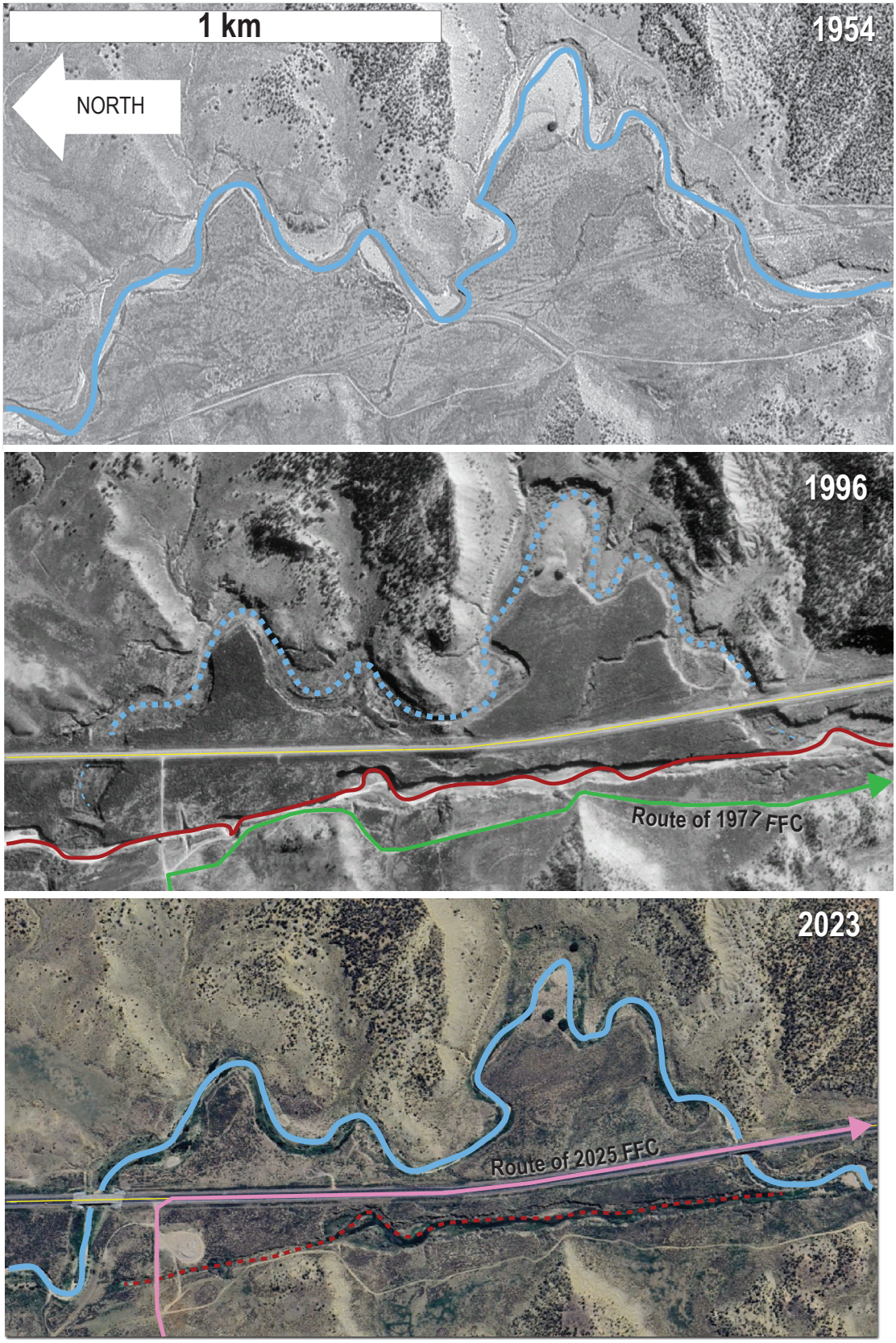

Figure 1.61. Repeat aerial photographs of the Rio Puerco's channelized reach. Top photo, from May 1954, shows the Rio Puerco prior to highway construction and channelization. Note the wider sandy bottom of the stream. Middle photo, from October 1996, shows the reach while the stream was diverted through a straight artificial channel (red line). State Road 44 (yellow line) was conveyed across the former natural channel via earthen berms. Bottom photo, from July 2023, shows the reach after the artificial channel was abandoned and the stream was redirected through its natural channel. U.S. Route 550 (yellow line) now crosses the Rio Puerco via two bridges. Routes of the 1977 (green line) and 2025 (pink line) Fall Field Conferences shown.

Such a fracture increase likely leads to the absence of sandstone observed at the fault trace atop the mesa. The high mesas to the south at 1:30 to 3:00 are La Ventana Mesa North (nearest you) and La Ventana Mesa South (farther southeast and higher), both capped by the La Ventana Sandstone and dipping toward you at 4° to 8° (Woodward and Schumacher, 1973). At 12:00, a majority of the Phanerozoic section of central New Mexico, including Pennsylvanian through Cretaceous sedimentary units, is before you on the steeply dipping to overturned drag fold along the Nacimiento fault marking the eastern margin of the San Juan Basin here. On the far side of the Nacimiento fault up to the skyline, Paleoproterozoic and Mesoproterozoic crystalline metamorphic and igneous rocks make up the highlands of the Sierra Nacimiento.

0.5

1.9 To the right are beautifully banded late Quaternary alluvial sediments of Arroyo de los Pinos exposed in vertical arroyo walls (Fig. 1.67). Red horizons here are due to deposition of increased amounts of sediment eroded from reddish Permian and Triassic sedimentary rock upstream, whereas the lighter-colored tan and brown horizons likely have provenance in Jurassic and Cretaceous units, both of which tend to be less red. Red horizons like these often are misinterpreted as buried soils by geologists lacking the knowledge requisite for pedologic studies. On the left, the contact between the Menefee Formation and La Ventana Sandstone continues near the top of the mesa on the skyline.

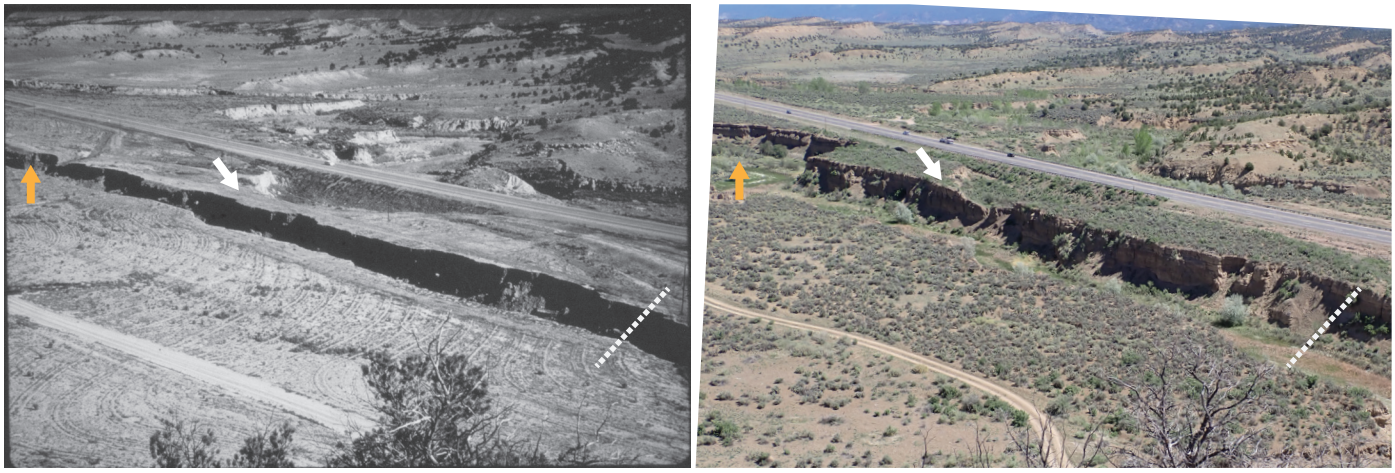

Figure 1.62. August 1967 (left) and June 2024 (right) photographs of the Rio Puerco diversion, Rio Puerco natural channel, and US 550/NM 44. Streamflow is from left to right. Arrows are placed at exactly the same locations in each photo. Orange arrow marks location of the widest meander in the diverted reach, which had not begun meandering in 1967. White arrow marks location of the abandoned meander loop in the natural channel; the western wall of that loop was breached by eastward lateral incision of the diverted reach (as predicted by Coleman et al., 1997). White dashed line marks the 51 m (167 ft) width of the diverted reach in 2024; note the narrower width of the same location in 1967. Left photo taken by Richard Hadley in August 1967. Right photo taken by Kevin Hobbs on 6 June 2024, at approximately 9:45 AM, from 35.8687°, −106.9749°.

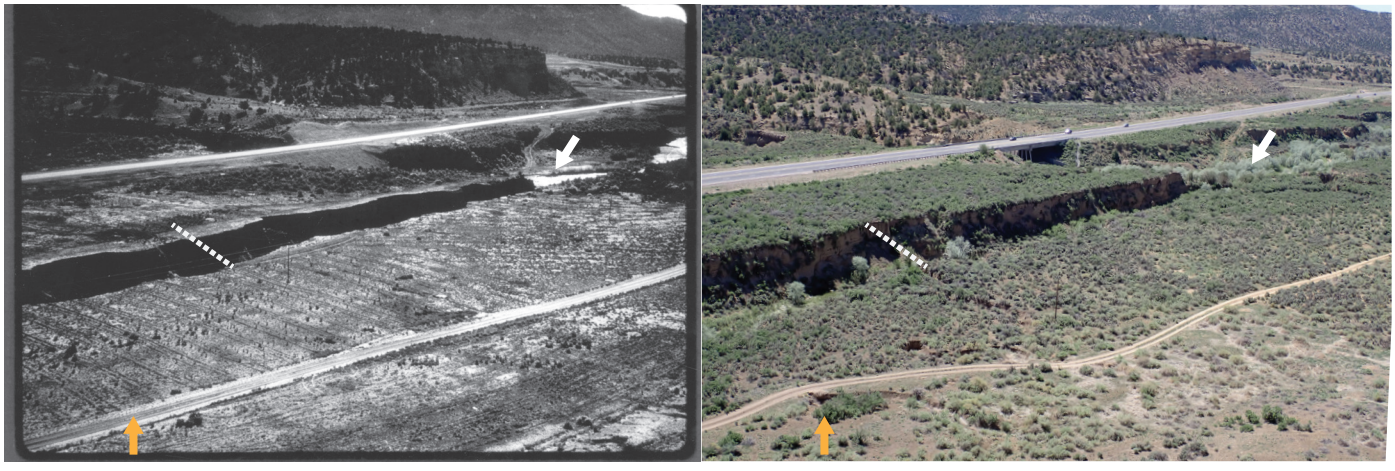

Figure 1.63. August 1967 (left) and June 2024 (right) photographs of the downstream confluence of the Rio Puerco diversion and natural channel just downstream of US 550/NM 44. Streamflow is from left to right. Note the earthen berm conveying State Road 44 across the Rio Puerco in left photo, which by 2005 was removed and replaced with the bridge seen in the right photo. Arrows are placed at exactly the same locations in each photo. Orange arrow marks location of 4-m (13-ft)-wide soil collapse sinkhole developed since 1967. White arrow marks location of the Rio Puerco streambed in 1967, which has been lowered by approximately 4 m (13 ft) since 1967. White dashed line marks the 44 m (143 ft) width of the diverted reach in 2024; note the narrower width of the same location in 1967. The diverted reach was originally 6 m (20 ft) wide when constructed in 1965. The width at this location was listed as >30 m (>100 ft) in a 1973 report (Coleman et al., 1997). Left photo taken by Richard Hadley in August 1967. Right photo taken by Kevin Hobbs on 6 June 2024, at approximately 9:45 AM, from 35.8687°, −106.9749°.

0.4

2.3 Road bends to the left (north) as it rejoins the route of the pre-1966 State Road 44 and enters a strike valley in the Menefee Formation. At 11:30, interbedded mudstones, coals, and sandstones of the Menefee Formation dip shallowly west into the basin. To the east, note the pyramidal buttes capped with fluvial sandstones within the Menefee Formation (Fig. 1.68).

0.4

2.7 Just left of straight ahead, note the anticlinal form of beds in the Menefee Formation (Fig. 1.69). Is this tectonic, or simply gravity-induced slumping related to road construction or Quaternary landscape development?

0.2

2.9 At 9:00, a massive 7-m (23-ft)-thick orange sandstone at the base of the La Ventana Tongue is deposited in a paleochannel that was eroded at least 4 m (13 ft)

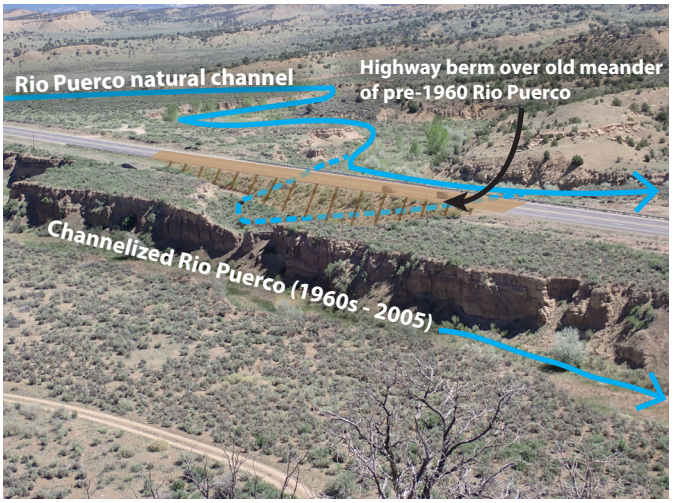

Figure 1.64. Annotated photograph of the U.S. Route 550 berm over abandoned meander in the natural channel of the Rio Puerco. View is toward the northeast.

Figure 1.65. Photograph of engineered stone steps installed in 2005 beneath the lower U.S. Route 550 bridge over the Rio Puerco. View is toward the east (upstream). Note erosion on right side of photo. Taken from Loberger et al. (2021).

Figure 1.66. Annotated photograph of the Menefee Formation-La Ventana Tongue of the Cliff House Sandstone contact on the north side of Arroyo de los Pinos just east of U.S. Route 550. The white line marks the contact. Red lines are inferred faults with arrows indicating sense of motion. The true number of faults in this fault zone is unknown; it is common for the total offset—here, about 4 m (13 ft)—to be accommodated by a number of small-offset individual faults spread across a distance about an order of magnitude greater than total offset.

Figure 1.67. Photograph of banded alluvial sediments in the Arroyo de los Pinos drainage. The source of these sediments, which are likely Holocene, is in the mountain front of the Sierra Nacimiento, shown in the background about 5 km (3.1 mi) to the east. Arroyo wall is approximately 5 m (16 ft) tall

into the underlying coaly sediments of the Menefee Formation (Fig. 1.70).

0.5

3.4 Crest of hill. Note the thickness variation in the basal sandstone of the La Ventana Sandstone to the west (left); these variations likely are due to paleotopography like that seen a half-mile back. The sandstone ridges to the east (right) are fluvial deposits of the Menefee Formation. Road enters private property.

1.0

4.4 Road descends. To the right, a dip slope of Menefee Formation sandstones with dramatic hoodoos (Fig. 1.71). Note scraggly ponderosa pines on that dip slope. At the lower end of their elevation range, New Mexico ponderosa pines prefer sites like these with shallow sandstone bedrock, presumably to exploit sandstones' propensity for high porosity and well-developed fractures into which roots can penetrate.

0.3

4.7 At left, a view to the west through a gap in the ridge exposes the steep south side of Mesa Portales 10 km (6 mi) to the west at 9:00. The large-gated compound at right, complete with an indoor pool, movie theater, sauna, and seven-car garage, was listed for sale at a cool $1.5 million in 2024. Worth it for the outcrops alone!

Figure 1.68. Photograph of pyramidal buttes capped by fluvial sandstones within the Menefee Formation in the South Fork of Arroyo de los Pinos. View is toward the southeast. The Sierra Nacimiento makes up the skyline on the left; La Ventana Mesa South in on the right. The Menefee Formation here dips about 8° to the northwest, directly toward the viewer.

Figure 1.69. Photograph of anticlinal folding in the Menefee Formation beside County Road 11 (Old State Road 44).

Figure 1.70. The Menefee Formation-Cliff House Sandstone contact at mile 2.9 showing a 4-m (13-ft)-deep paleochannel that was filled in with marine sandstones. Dashed white line marks the contact.

0.8

5.5 Crest of hill. At 1:00, note the broad north-plunging anticline defined by the mesa-capping La Ventana Sandstone, which has thinned considerably over last 4 miles.

0.8

6.3 The homes at 3:00 are built atop a 23-m (75-ft)-high terrace of San Miguel Arroyo, which heads at 2,865 m (9,400 ft) and drains approximately 8 km (5 mi) of the Sierra Nacimiento mountain front.

Figure 1.71. Hoodoos in the Menefee Formation at mile 4.9. Beds here dip about 15° to the west, perpendicular to County Road 11. Note the small ponderosa pines, which here are at the lower end of the elevation range at this latitude.

Figure 1.72. Remains of a stone house in front of a Menefee Formation outcrop.

0.1

6.4 A new culvert was installed over San Miguel Arroyo here in 2023, replacing the old wood bridge. It remains to be seen if the culvert will be sufficient for conveying maximum discharge of the arroyo…

0.1

6.5 **Waypoint 1.09 [35.9237°, −106.9414°]**

Turn right (east) immediately after the arroyo onto the Forest Road 78 (San Miguel Road).

0.2

6.7 Note the deep incision of the San Miguel Arroyo at 3:00. At 9:00, the deep red strata in the Menefee Formation have been interpreted as clinker. At 12:00, the steeply dipping Mesozoic section is seen on the lower third of the mountain front. The very white unit on the mountain front is the Jackpile Sandstone and the upper two-thirds of the mountain are Proterozoic crystalline rocks.

0.1

6.8 Cattle guard.

0.7

7.5 At left, note the remains of a stone house with a steel roof (Fig. 1.72). This house, like many others of its vintage in the upper Rio Puerco Valley, has two doors on its front wall. These Rio Puerco two-door houses should not be confused with Tudor houses found elsewhere on Planet Earth. The house sits in front of and is constructed out of sandstones of the Menefee Formation.

0.2

7.7 Note shallow syncline in the Menefee Formation hill to the left (Fig. 1.73). Woodward et al. (1973) show this syncline—and a parallel anticline about 1.6 km (1 mi) to the west—trending north-northwest for over 12 km (7.5 mi), slightly oblique to the north-trending Nacimiento fault that is 3 km (1.9 mi) east of here.

The road soon climbs a small forested ridge then bends to the south (right) into a strike valley paralleling the base of the poorly exposed Point Lookout Sandstone, which thins considerably to the north between here and Cuba.

Figure 1.73. Shallow syncline in the Menefee Formation at mile 7.7. White line marks a bedding plane; dashed where obscured by colluvium.

0.9

8.6 **Left (southeast) at road fork in a right-hand curve onto Forest Road 20.** The right fork leads to the tiny village of San Miguel, which at one time had a small smelter fed by the San Miguel mines 3.5 miles (2.2 mi) to the southeast, a one-room school, and about 130 ha (320 ac) of irrigated fields and pastures fed by springs along the mountain front to the east (Van Hart, 2013).

0.1

8.7 Hogback of sandstone of the Encinal Canyon Member of the Dakota Formation at 12:00 (Fig. 1.74). The steep, narrow nature of the canyon ahead suggests a youthful—or at least rejuvenated—landscape here on the Sierra Nacimiento mountain front. Through the gap in the hogback, Proterozoic high-grade metamorphic rocks make up the high country to the east; these rocks are on the eastern upthrown side of the Nacimiento fault system. The timing of their uplift is to be discussed at Stop 4.

Figure 1.74. View to the east up San Miguelito Canyon through a hogback formed by the Encinal Canyon Member of the Dakota Formation. The mostly forested high ridge in the background, through the gap in the hogback, is 2,775-m (9,101-ft)-tall Cerro Castrado, comprising Proterozoic quartz-feldspar gneiss, biotite gneiss, biotite-quartz-feldspar schist, and hornblende schist.

0.5

9.2 Pass through the steeply dipping Encinal Canyon Member sandstone portal. Note the orientation of beds on both sides of the road. Woodward et al. (1973) mapped at least four north-trending faults accommodating uplift of the Sierra Nacimiento just upstream and east of here (Fig. 1.75). Elsewhere along the mountain front, uplift appears to have occurred along just one major fault surface.

0.1

9.3 **Stay left at road forks to remain on Forest Road 20.** Note small cuesta of a sandstone within the Jurassic Morrison Formation at 12:00. Road soon enters a north-trending strike valley within the Morrison Formation and gains elevation.

0.8

10.1 **Waypoint 1.10 [35.9327°, −106.8994°]**

STOP 4. Road bends to right (east), and a rough two track takes off to the left (north). Park off the right side of road before bend to right. Exit vehicles, walk north, and gather at road junction for short walk and discussion of the Jurassic Todilto Formation, Cordilleran tectonics, the Morrison Formation-Dakota Formation unconformity, and mountain-front geomorphology.

This stop includes two discussions. The group will split into two halves, with one half going to Stop 4A and the other to Stop 4B. Then, the groups will swap places so that each attendee gets to visit both discussion sites. Stop 4A will investigate the San Juan Basin Phanerozoic section as a "tectonic speedometer" and how the sedimentary units we've seen today and will see tomorrow record large-scale tectonic evolution of our continent. Stop 4B will inspect a lovely outcrop of the geologic contact between the Jurassic Entrada Sandstone and Todilto Formation, then link the observed properties of those units to ongoing research into carbon sequestration in the same units in the subsurface of the San Juan Basin.

STOP 4A: Overview of a Tectonic Speedometer

Waypoint 1.11 [35.9346°, −106.9018°]

This stop is a chance to observe a thick sequence of sediments and discuss them in a context of a recorder of competing regional and local processes that controlled the generation of space. From this viewpoint we can see approximately 5 km (3.1 mi) of stratigraphy that is a record a 300-million-year evolution in settings from intracratonic to a large scale progressive flexural foreland to a dynamic basin to a broken foreland.

Five Kilometers of Record

Figure 1.76 shows the view looking to the east. On the skyline is the ~1,700 Ma (Premo et al., 2023) San Miguel Gneiss on the western edge of the Nacimiento uplift. Thicknesses, ages, and lithologies discussed are derived from the geologic map of Woodward et al. (1973). The "great unconformity" with 1,400 My of missing time record is near the tree line at the base of the slope. Approximately 300 m (1,000 ft) of Permian Abo and Yeso Formations are mapped as a depositional contact. In the tree-covered low valley is approximately 350 m (1,150 ft) of near-vertical Triassic Chinle Group with minor complications from the north-south trending Nacimiento fault. In the midground, the white ridge is approximately 100 m (330 ft) of west-dipping Jurassic Entrada Sandstone eolianites and Todilto Formation evaporites. These Jurassic units are the focus of Stop 4B.

The section to this point can be generally described as continental red beds and clastics with very slow accumulation rates (tens of meters per million years).

The slope we climbed up in the near ground consists of 260 m (850 ft) of Upper Jurassic Morrison Formation variegated continental sandstones, siltstones, and shales. The Jackpile Member of the Morrison Formation is just below the ridge we are standing on. This thickness is more than the ~100–200 m (~330–660 ft) maximum thickness to the north (Chapman and

DeCelles, 2021). The white sandstones in the near ground and on which we are standing are in Cretaceous Dakota Formation, which is ~60 m (~200 ft) thick here. The Dakota Formation sandstones mark a major change with regional marine incursions and the beginning of an order-of-magnitude acceleration of subsidence rates.

The view to the west (Fig. 1.77) is of a record of an expanding foreland section. Overlying Cretaceous Dakota Formation sands are ~600 m (~1,970 ft) of marine Mancos Shale. The first ridge is ~500 m (~1,640 ft) of the moderately dipping Upper Cretaceous Mesaverde Group, a prograding-to-the-northeast clastic coastline with the La Ventana Tongue of the Cliff House Sandstone, Menefee Formation, and Point Lookout sands thinning into the off-shore Mancos Shale. This is overlain by ~400 m (~1,310 ft) of uppermost Cretaceous marine Lewis Shale. The mesa in the midground has ~100 m (~330 ft) of another prograding clastic coastline with coals in the Upper Cretaceous Pictured Cliffs Sandstone and Kirtland and Fruitland Formations.

The Upper Jurassic and Cretaceous sections record a change from a slow subsidence rate and continental sediments to subsidence rates of hundreds of meters per million years and deposition in a continental-scale marine basin.

Another major change occurs at the top of the Cretaceous with a major unconformtiy but the continuation of rapid subsidence. The top of the Cretaceous on Mesa Portales (and in most of the San Juan Basin) is capped by ~30 m (~100 ft) of cliff forming sandstones and conglomerates of the Paleogene Kimbeto Member of the Ojo Alamo Formation. Above this and near the skyline is ~370 m (~1,210 ft) of nonmarine clastics in the Paleogene Nacimiento Formation. In the distance at the skyline the base of the nonmarine clastic Paleogene San Jose Formation is present. Rudolph et al. (this volume) estimate the San Jose Formation's original thickness was ~1,900 m (~6,230 ft) using vitrinite reflectance, well logs, and modeling. The dashed line in the sky in Figure 1.77 represents the top of the San Jose Formation that would have projected to a present-day elevation of ~4 km (~14,000 ft) ASL based on the modeling presented by Rudolph et al. (this volume), but that conclusion is challenged by stratigraphic evidence elsewhere in the basin. (Note that there has been substantial regional uplift of at least 1.5 km [0.9 mi] since the San Jose Formation was deposited in the early Eocene).

Sediment Accumulation Rates

The restored section (Fig. 1.78) has accumulated ~700

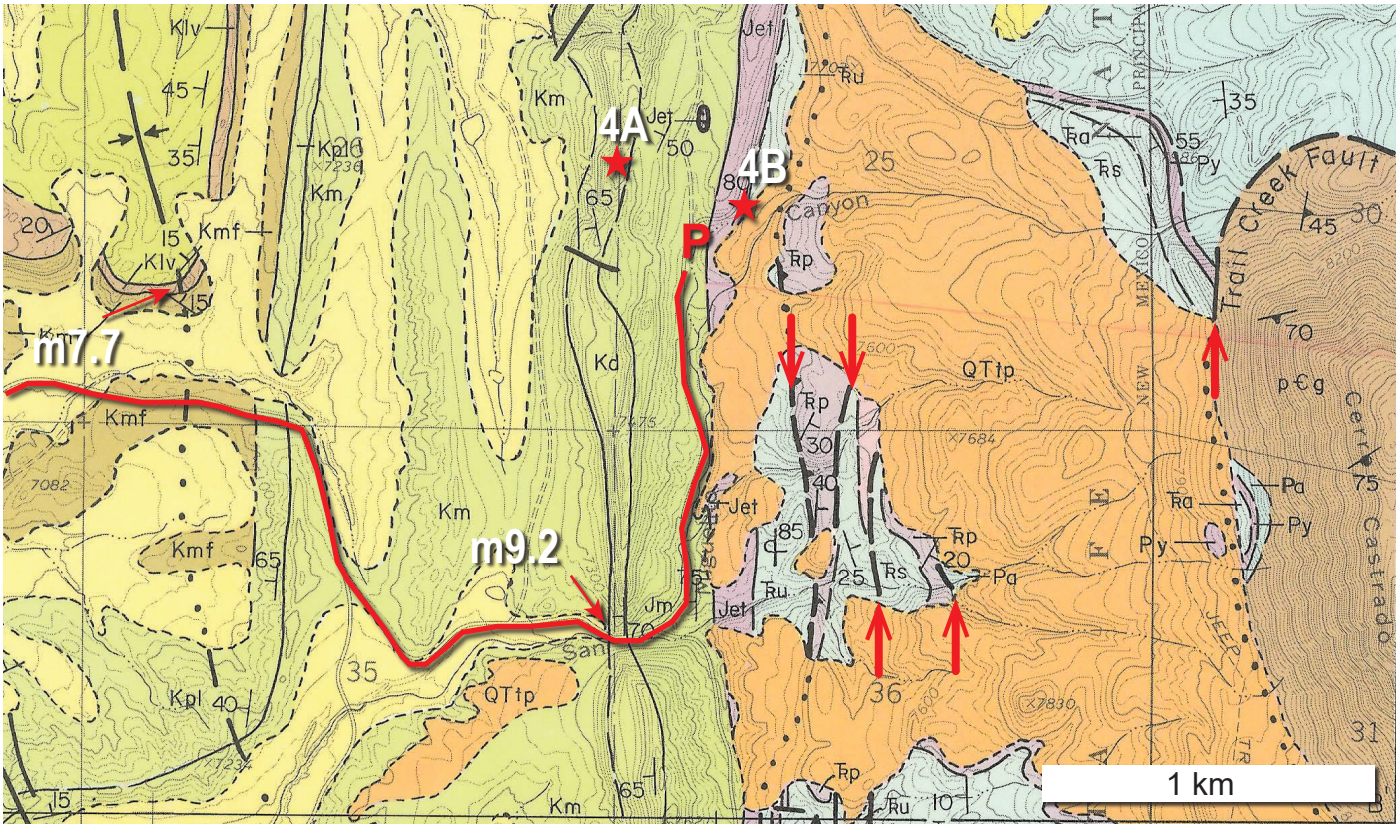

Figure 1.75. Annotated geologic map showing road log route (red line) leading to Stop 4 and the Sierra Nacimiento mountain front. Vertical red arrows mark individual faults accommodating uplift of the eastern side of the fault zone; here, only the Trail Creek fault is named. Note the repeated section of Triassic strata (repeating bands of blue and purple map units) to the southeast and east of Stop 4. Stops 4A and 4B are marked with stars. Parking area for Stop 4 marked with "P." The syncline at mile 7.7 and the Dakota Formation hogback portal at mile 9.2 are marked. The large orange polygons marked "QTtp" represent significant pediment and terrace deposits, likely the Rito Leche surface of Bryan and McCann (1936). pCg = gneiss; Pa = Abo Formation; Py = Yeso Formation; TRa = Agua Zarca Member Chinle Group; TRs = Salitral Member Chinle Group; TRp = Poleo Sandstone Member Chinle Group; TRu = upper shale member Chinle Group; Jet = Entrada Sandstone and Todilto Formations; Jm = Morrison Formation; Kd = Dakota Formation; Km = Mancos Shale; Kpl = Point Lookout Sandstone; Kmf = Menefee Formation; Klv = La Ventana Tongue Cliff House Sandstone. Modified from Woodward et al. (1973).

m (~2,950 ft) in ~150 My from Permian to Middle Jurassic while the next 100 My has almost five times the amount of sediment accumulation (~4200 m [~13,776 ft]). The lumped sediment accumulation rate for the restored section in Figure 1.78 shows Permian to Middle Jurassic very low accumulation rates (meters per million years) followed by an order of magnitude acceleration in accumulation in the Late Cretaceous and Paleogene to rates of hundreds of meters per million years. The Neogene unconformity reflects Colorado Plateau uplift.

The observed thicknesses can be divided into four phases based on accumulation rates in the context of isopach maps showing the areal distribution of subsidence. The early low accumulation Phase 0 is characterized by distal Ancestral Rocky Mountain (ARM) orogenic and epeirogenic patterns. Phase 1 shows systematic subsidence from crustal warping in front of a progressing crustal load. Phase 2 has high subsidence, but a much broader regional subsidence pattern dominated. Phase 3 has local high subsidence rates accompanied—and perhaps partially driven—by local uplifts.

Processes that Generate Space

The orogenic processes that generate space can be thought of as crustal, related to the crust's strength and applied loads (flexure), and mantle lithospheric interaction caused by convection (dynamic). The processes are end members and not mutually exclusive. They often overlap in time and space.

Crustal Flexure

The crust has a strength. When a load is applied or removed, it bends in a predictable way (Turcotte and Schubert, 2002). Figure 1.79 shows a rift model with a flank uplift and a flexural trough. This is the result of a load removed by a crustal normal fault and the crust rebounding. The Sandia Mountains of the Rio Grande rift system are a classic rift flank uplift with the Estancia Valley to the east its flexural trough. In the foreland model, a thrust load creates a foredeep, forebulge, and a shallow backbulge. The shape of the space created is a function of the load and the strength of the crust. The depression of the Pacific crust around the Hawaiian Islands load is a classic example of a flexural foreland. Figure 1.80A is a representation

Figure 1.76. Photograph looking east from Stop 4A showing rocks representing the intracratonic (Phase 1) to progressive flexural foreland (Phase 2) systems. View looking to the east-southeast. On the skyline are the Precambrian crystalline basement rocks (pC) of the western edge of the Nacimiento uplift. Approximately 300 m (1,000 ft) of Permian Abo and Yeso (Pay) Formations are mapped as a depositional contact near the tree line at the base of the slope. In the tree-covered low valley is approximately 350 m (1,150 ft) of near-vertical Triassic Chinle Group deposits (TRc) with minor thickness complications from the north-south trending Nacimiento fault. In the midground, the white ridge is approximately 100 m (330 ft) of west-dipping Jurassic Entrada Sandstone and Todilto Formations (Jet). This is stop 4B. The section to this point can be describe as continental red beds and clastics with very slow accumulation rates (tens of centimeters per million years). The slope we climbed up in the near ground is 260 m (850 ft) of Upper Jurassic Morrison Formation (Jm) containing variegated continental sandstones, siltstones, and shales. The white sandstones in the near ground and on which we are standing is approximately 60 m (200 ft) of Cretaceous Dakota Formation (Kd).

The observed section is interpreted to be the result of intracratonic processes from the Permian until Middle Jurassic then change to a progressive flexural foreland system with the Morrison, a backbulge-to-forebulge deposit, and the Dakota representing the entry into a distal foredeep (see text for discussion). The dashed white lines mark approximate contacts between units. The black toothed line marks the approximate location of the easternmost fault of the Nacimiento fault system. General geology interpretations modified from Woodward et al. (1973).

of a simple foreland in front of an isolated basement cored uplift referred to as Laramide style uplift. These foreland basins generated by local uplifts are generally tens of kilometers wide.

A linear load that advances hundreds of kilometers will create a basin system that will systematically advance the flexural foreland subsidence zones like a wave. Figure 1.80B is a diagram showing the zones of a progressing flexural foreland basin system. A point that is in the foredeep today was once in the backbulge. The load is the entire orogenic wedge, not just the thrust belt. The thrust belt foredeeps are typically 150 to 300 km (94 to 188 mi) wide depending on the strength of the crust. This model was developed by DeCelles and Giles (1996) to explain the sequence of sediments in front of the Sevier thrust belt to the north in Utah and Wyoming where they have documented 150–300 km (94–188 mi) of advance of a progressing flexural basin foreland system (Price and Mountjoy, 1970; DeCelles and Coogan, 2006).

Geodynamic

Mantle flow generates topography in addition to crustal processes. Hager and Richards (1989) defined dynamic topography as topography generated by flow (convection) in the mantle. The relief of midocean ridges and ocean trenches are simple examples of dynamic topography. Dynamic subsidence is characterized by 600 to 1,000-km (375 to 625-mi) wave length basins with synchronous subsidence. Synchronous 2 km subsidence of the Permian Basin across 800 km (500 mi) is an example of dynamic subsidence (Rudolph 2023). Figure 1.80C illustrates a ~1,000 km (~625 mi)-wide dynamically subsiding basin above a flattening subducting slab.

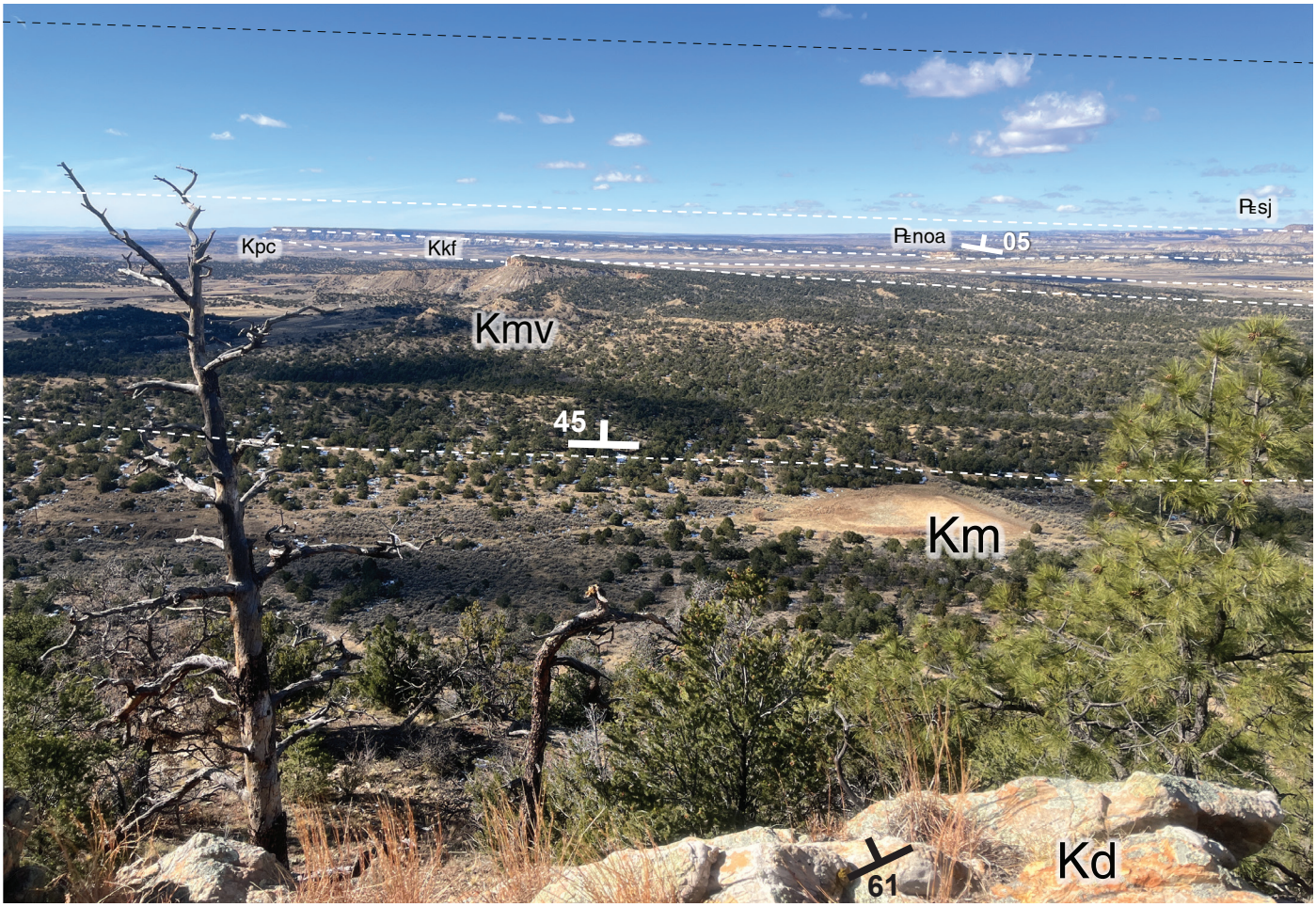

Figure 1.77. Photograph looking west from Stop 4A showing rocks representing the progressive flexural foreland (Phase 1) to dynamic subsidence (Phase 2) to broken foreland (Phase 3) systems. View looking to the west into expanding foreland section. Overlying the Cretaceous Dakota Formation are ~600 m (~1,970 ft) of marine Mancos Shale (Km). The first ridge is ~500 m (~1,640 ft) of the moderately dipping Mesaverde Group (Kmv), deposits of a prograding clastic coastline. This is overlain by ~400 m (~13,120 ft) of Cretaceous marine Lewis Shale (Kl). The mesa in the midground has ~100 m (~330 ft) of another prograding clastic coastline with coals in the Upper Cretaceous Pictured Cliffs (Kpc) and Kirtland and Fruitland Formations (Kkf) overlain by ~400 m (~1,310 ft) of cliff forming fluvial sandstones and conglomerates of the Paleocene Kimbeto Member of the Ojo Alamo Formation (seen at Stop 3) and valley-forming fluvial siliciclastic Nacimiento Formation (combined into PEnoa) (seen at Stop 2). At the skyline, the base of the fluvial siliciclastic Paleogene San Jose Formation (PEsj) is present. The dashed line in the sky represents the restored top of the Chuska Sandstone at ~3500 m (~11,1480 ft) ASL. From modeling and wells, the original San Jose Formation thickness is estimated to have been ~1,900 m (~6,230 ft) (see text). The Morrison and Dakota section records an eastward progressing flexural basin system. During deposition of the upper Mancos Shale and Mesaverde Group, this changes to a 600 km (375 mi) wavelength uniform subsidence pattern attributed to dynamic processes. The Ojo Alamo Formation makes a change to enhanced local subsidence due to local uplifts as the foreland is broken. See Figure 1.61 and text for explanation.

Broken Foreland

Broken foreland basins (Horton et al. 2022) are foreland systems with local basement-cored uplifts disturbing the foreland (Fig. 1.81). Broken forelands are unusual but not uncommon. They are thought to be caused by reactivation of inherent weak zones in the crust by end loading and/or basal stresses from a downgoing slab (Horton et al., 2022; Weil and Yonkee, 2023).

Genetic Analysis

A genetic analysis of our four phases divides them into different tectonic settings. Phase 0: Permian to Middle Jurassic is characterized by low accumulation rates reflecting distal ARM and intracratonic processes. Phase 1: Late Jurassic to Early-middle Cretaceous exhibits slow subsidence, a hiatus, then the beginning of accelerating subsidence reflecting the distal end of an advancing flexural wave of backbulge basin to forebulge of the Sevier orogeny. Phase 2: Late Cretaceous rapid subsidence but the pattern has changes from a distal foreland with a narrow foredeep (100–200 km [63–126 mi]) with a progressing acceleration of accommodation to a broad (600 km [375 mi]) area of synchronous rapid sedimentation representing dynamic subsidence. Phase 3: Paleocene broken foreland with local uplifts creating loads that drive local flexural subsidence and possibly continued dynamic subsidence.

Phase 0: Permian to Middle Jurassic—Intracratonic

The basal unconformity and Permian section are interpreted as distal ARM influences followed by intracratonic slow accumulation with no simple systematic pattern is interpreted to have had minor influence from processes at the craton margin.

Phase 1: Late Jurassic to Mid Cretaceous—Flexural Foreland Basin System

This phase is dominated by distal impacts of the North

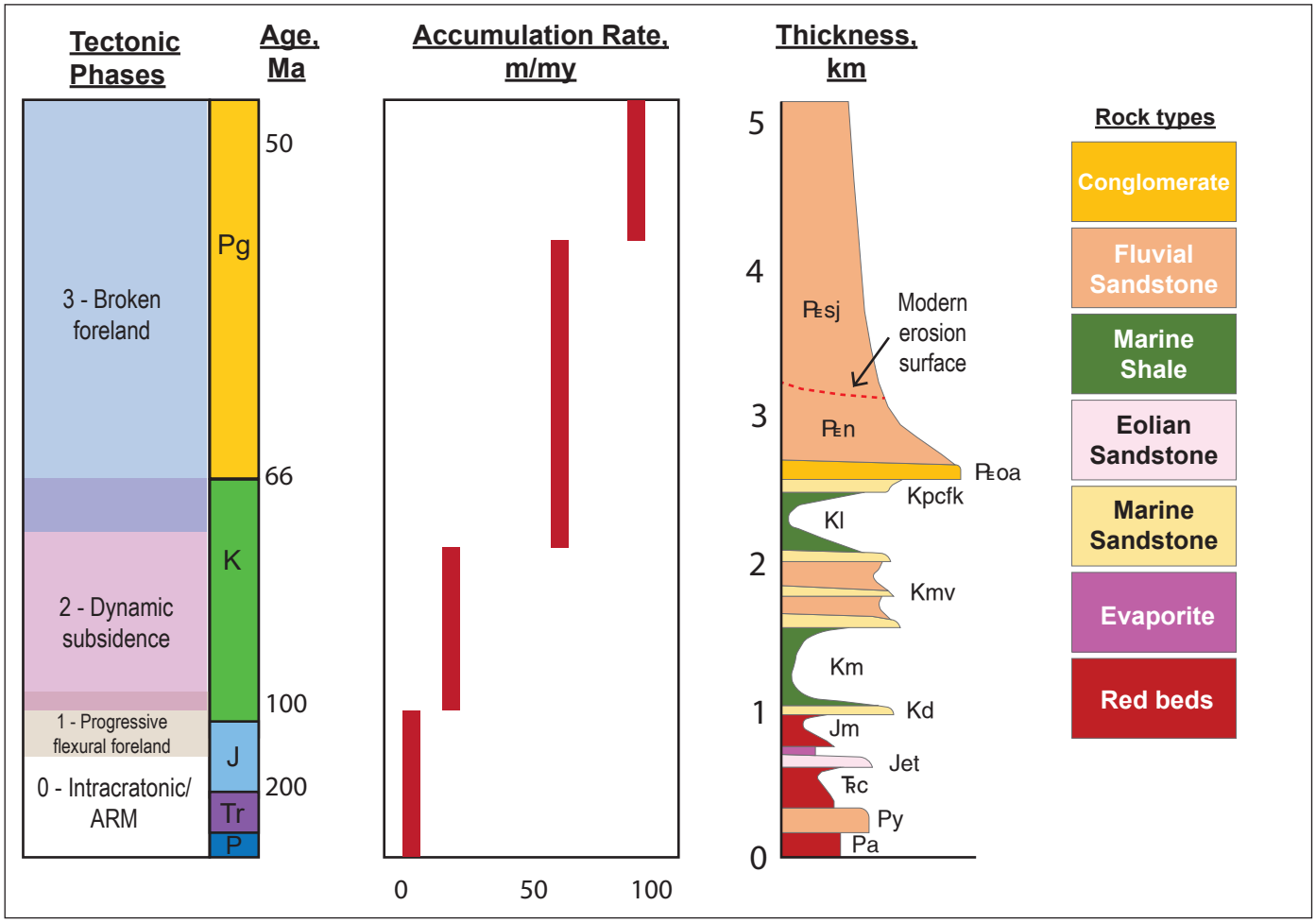

Figure 1.78. Eastern San Juan Basin sediment thickness, the "Tectonic Speedometer." Sediment thickness and accumulation rates for the observed section at Stop 4A. The simplified restored section diagram in thickness is in the center of the diagram. The vertical red lines show accumulation rates broadly averaged by tectonic phase. From the Permian until the Middle Jurassic, accumulation was low and then accelerated in the Cretaceous. The erosion reflects Neogene Colorado Plateau uplift. Phase 0 (Permian to Middle Jurassic) was typified by low accumulation rates reflecting intracratonic processes. Phase 1 (distal progressive flexural foreland, Late Jurassic to Late Cretaceous) was slow then began to accelerate reflecting the advancing flexural wave of backbulge to forebulge of the Sevier orogeny. Phase 2 (dynamic subsidence, Late Cretaceous into the Paleogene) had continued rapid subsidence but the pattern has changed from a narrow foredeep (100 to 200 km [63 to 126 mi]) with a progressing acceleration of accommodation to a broad (600 km [375 mi]) area of synchronous rapid subsidence. Phase 3 (broken foreland, Paleogene) had proximal local uplifts creating loads that drove small-scale flexural subsidence. The colored boxes representing the different phases are shown to overlap each other because dominance of any one process is thought to be transitional.

American Cordillera. A well-established progressive flexural foreland system developed in the northwest and a more complicated convergent system became established to the south. During the Late Jurassic, the Sevier thrust belt was active to the west (Decelles and Giles, 1996; Yonkee and Weil, 2015) and a backarc rift was active to the south (Lawton et al., 2020; Chapman and DeCelles, 2021). The geologic history to the south is less constrained than to the west because of the overprint by multiple younger events. Lawton et al. (2022) show that the Late Jurassic rift system was buried by an advancing foreland basin system. The subduction continued and arc persisted but a systematically advancing foredeep is not as clearly identified. The arc itself was later translated north and is now the Peninsular Ranges near Los Angeles, California. Creation of high-resolution subsidence curves in the Morrison Formation and more revelations from the south could better clarify the competing influences.

The accumulation patterns of the Morrison Formation have been interpreted as the distal end of an advancing flexural foreland basin system driven by the eastward encroachment of the Sevier orogenic front. Cenomanian isopach maps show this location on the distal end of a classic flexural foreland pattern with a narrow foredeep near the Sevier orogenic front (Decelles and Giles, 1996; Painter and Carrapa, 2013; Yonkee and Weil, 2015). Painter and Carrapa's (2013) Cenomanian isopach map (Fig. 1.82) is representative of this period. The space generation during this time interval was dominated by crustal processes with a progressive flexural foreland system moving into the area and is illustrated in Figure 1.83. Complicating the situation is the probability of influence from the south where a back-arc rifting event could impose a rift flank basin on the distal fore bulge basin (Chapman and Decelles, 2021). By the mid Cretaceous, the back-arc rift system is overlain by a foreland system. There is a load to the south in addition to a progressing flexural foreland system to the northwest. Further work is needed to elucidate the details of geological effects from the southern rifting-influenced tectonics versus those from western flexural foreland-influenced tectonics.

Phase 2: Late Cretaceous—Dynamic Subsidence

Rapid subsidence picked up during this time, but the pattern is shifted to a 600-km (375-mi)-wide bowl shape (Painter and Carrapa, 2013; DeCelles, 2014; Yonkee and Weil, 2015). Painter and Carrapa's (2013) Campanian isopach (Fig. 1.82) is representative of this time. It shows no foredeep; instead, a broad basin with synchronous subsidence centered in eastern Wyoming, ~400 km (~250 mi) in front of the Sevier orogenic wedge. This broad area calls for a deeper cause. Reconstructions of subducted slabs based on mantle imaging put a flattened slab containing an oceanic rise in the area under this basin (Liu et al., 2010) The arrow on Figure 1.82 shows the direction of the subducting slab. Subduction and the orogenic wedges load were still active (Yonkee and Weil, 2015). The geodynamic forces created by the flattened slab overwhelmed the crustal flexural processes to dominate the subsidence pattern. In Figure 1.83, a comparison of the Phase 1 basin cross section to Phase 2 basin cross section illustrates the change in subsidence pattern.

Phase 3: Latest Cretaceous to Paleocene—Broken Foreland

The San Juan Basin proper formed as a local flexural basin (Figure 1.80A) in a broader foreland basin system. The Nacimiento uplift to the east created a load that can account for the continued rapid subsidence. This is the subject of the first two stops tomorrow where we see evidence of the beginning of the broken foreland in the latest Cretaceous. The cross section in Figure 1.81 is lithospheric-scale schematic representation of this time.

Figure 1.83 shows the change from basin-wide flexural-dominated Phase 1 to Phase 2 when dynamic processes dominated. In Phase 3, a broken foreland developed where local uplifts and flexure dominated over dynamic and broad flexural processes.

The transitions and relationships between the dominance of mechanisms are emerging areas of study. Recent dating of the nonmarine strata, seismic data interpretations, and thermochronology show that the orogenic wedge was still active but

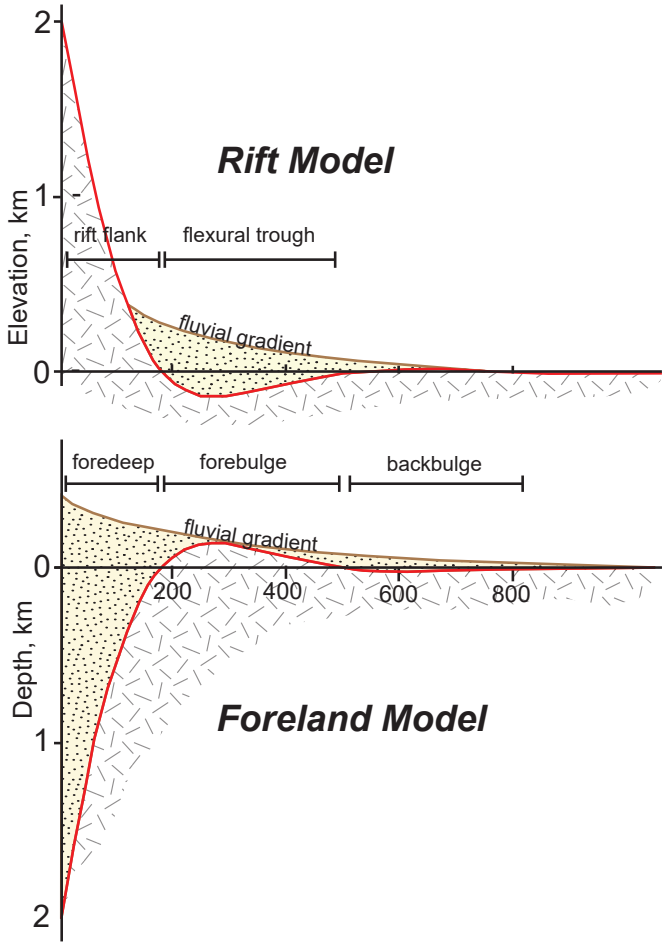

Figure 1.79. Schematic diagram of rift and foreland flexure from Chapman and Decelles (2022) illustrating basins (yellow stipple below fluvial gradient) formed by flexure of the lithosphere. The two flexural profiles are analytical solutions to flexure of a "broken" plate (Turcotte and Schubert, 2002). The rift model has a rift flank uplift and a flexural trough. The foreland model has a foredeep, forebulge, and a backbulge basin. The physics are similar to the deflection at end of a diving board just before and after a dive.

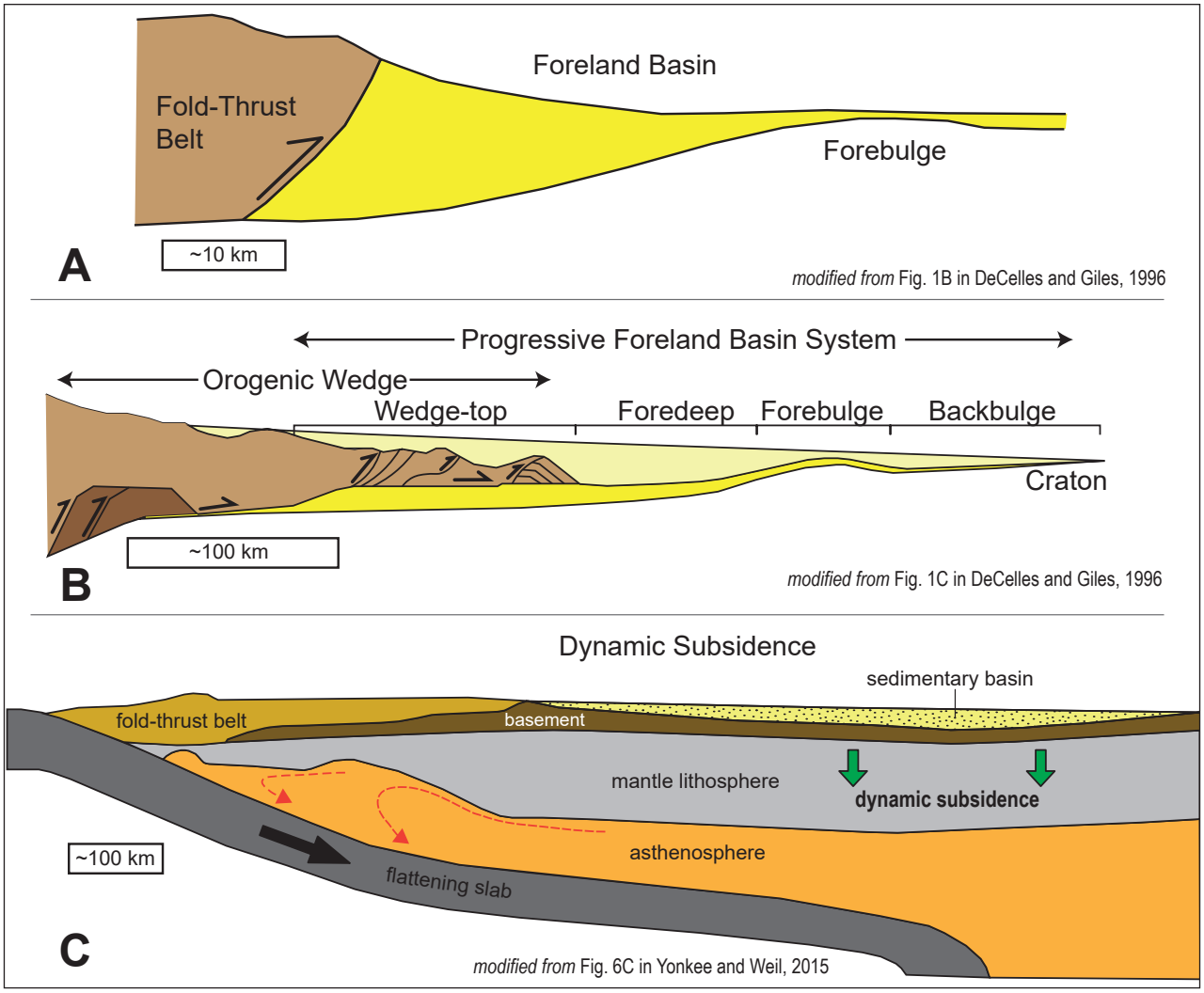

Figure 1.80. Flexural versus geodynamic processes. A: simple foreland basin. B: progressive flexural foreland basin system. C: geodynamic driven subsidence. A and B are controlled by crustal strength and a load. C is controlled by asthenosphere flow. A: Simple foreland basins form via crustal processes where a basin results due to a crustal load (thrust fault) imposed on the crust. The depth and width of the basin is a function of crustal strength (DeCelles and Giles, 1996). B: Progressive flexural foreland basin system advances in front of an advancing orogenic load. A migrating area of accelerating subsidence is a defining characteristic. The rate that the flexural wave advances is controlled by the rate that the orogenic wedge advances (DeCelles and Giles, 1996). C: Dynamic subsidence is created by the geodynamic of flow in the asthenosphere. It is characterized by long (500 to 1,000 km [310 to 620 mi]) wavelengths and synchronous timing (Yonkee and Weil, 2015). During an orogenic event, all these processes can be active simultaneously to some degree, but at different times one process dominates the generation of space.

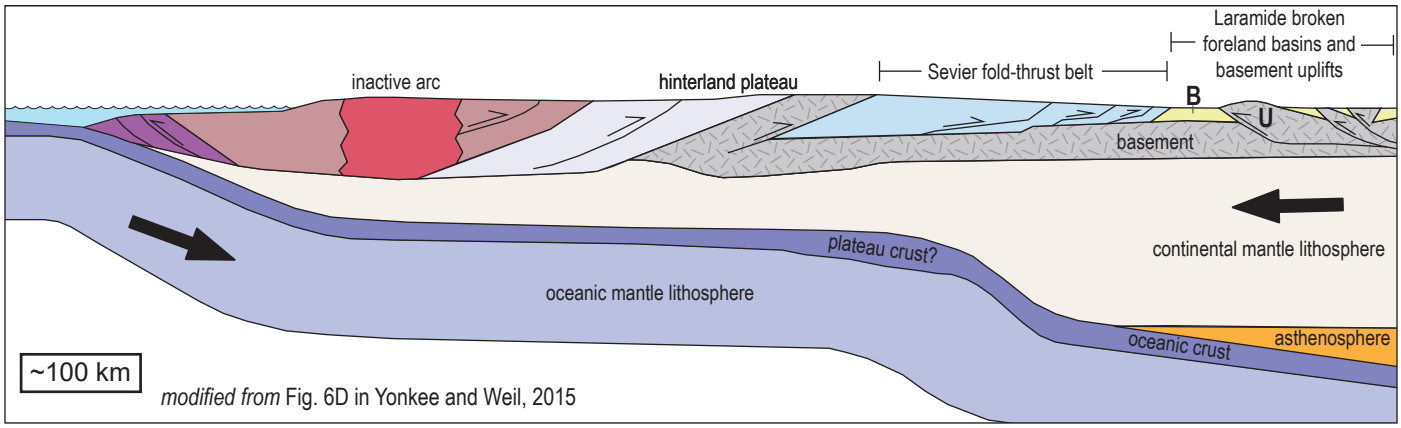

Figure 1.81. Schematic cross section of broken foreland model representing the Western Cordillera at approximately 55 Ma. Broken foreland basin system had local basement uplifts (U) that created local basin subsidence (B) in addition to broader processes. The driving mechanism is thought to be reactivation of preexisting weak crustal zones by end loading from the orogenic wedge and/or basal load from the downgoing lithospheric slab.

not advancing and had no foredeep at this time (Yonkee and Weil, 2015). Geodynamic forces should also be active into the Eocene. Isopach maps and subsidence studies (Rudolph et al., this volume) show the beginning of broken foreland structures in the Late Cretaceous. 3D analysis of reconstructed isopachs of the Paleogene maps would help distinguish dynamic from broad and local flexural controls. Many questions remain with regards to the final stages of San Juan Basin contractional tectonics: What is the relationship between flat slab subduction and crustal weakening? How do geodynamic processes overwhelm crustal processes?

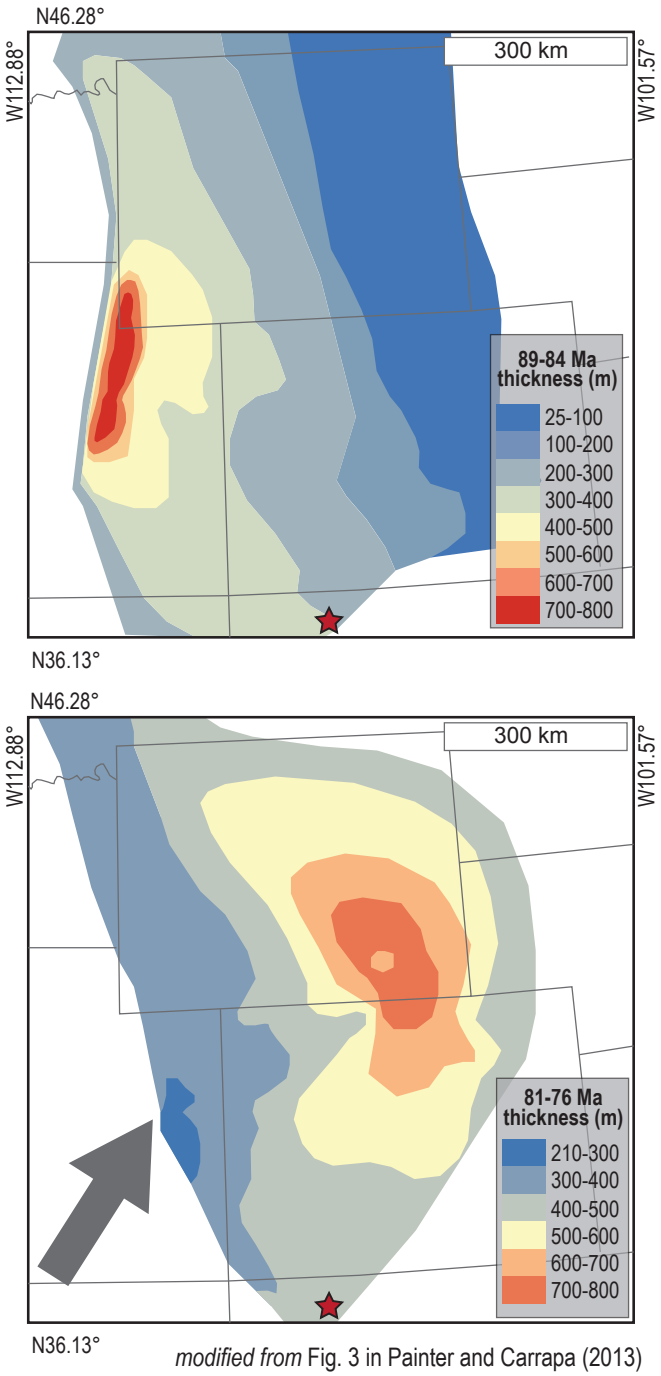

Figure 1.82. Flexural versus dynamic foreland isopachs. Top: Isopach map of the Late Cretaceous (89 to 84 Ma) deposits representative of the Phase 1 progressive flexural foreland system. Bottom: Isopach of the latest Cretaceous (81 to 76 Ma) deposits representative of the Phase 2 dynamic subsidence dominant system. The red star marks the San Juan Basin. Arrow indicates motion direction of the subducted oceanic plate beneath North America in the Late Cretaceous. Modified from Painter and Carrapa (2013).

Paleogeographic Maps

A review of Blakey's paleogeographic maps (Fig. 1.84) conveys a feel for the temporal changes in continental paleogeography caused by the evolution of the western margin. Phase 0 would have been hot and dry with very little topography. The Triassic Chinle paleogeography shows a mostly passive craton margin and a flat terrain of small rivers and ergs.

At the beginning of Phase 1 (e.g., Late Jurassic Morrison Formation time), the conditions are still hot and dry, but the rivers and depositional systems are organized and systematic. To the west is the retro arc of the Sevier orogeny with a flexural foreland system. To the south is the McCoy-Bisbee-Sabinas back arc rift system. Here we are on the edge of Sevier back bulge basin and a McCoy-Bisbee-Sabinas rift flank basin.

By the end of Phase 1 in the Late Cretaceous when the Dakota Formation and Mancos Shale were being deposited in the San Juan Basin, the Sevier orogenic deformation front has advanced eastward some ~250 km (~156 mi), pushing a progressive flexural basin system to the east. The generation of space has overwhelmed the sediment supply creating the Cretaceous seaway. The region has progressed from backbulge basin to forebulge to the beginning of a foreland basin. Northern New Mexico would have been sitting in a shallow, muddy seaway. To the south the rift system was replaced by highlands. Offshore to the southwest, the Shatsky oceanic rise was heading northeastward toward the trench.

By Phase 2, latest Cretaceous Mesaverde Group time, we would have been on a beach as the geodynamic forces from the subducting Shatsky rise have overpowered the flexural forces from the still active but not advancing Sevier orogeny. The change from a flexural shape with maximum space created near the deformation front to a broad gentle bowl shape allowed the shoreline to prograde far into the seaway.

By Phase 3, Paleogene Nacimiento Formation time, the seas have retreated from most of the interior of North America. The San Juan Basin was a local basin on coalescing alluvial and fluvial systems coming off a rising highlands bordering the basin. The flat slab with the Shatsky rise has proceeded farther northeastward facilitating the contractional reactivation of crustal weak zones creating local uplifts with corresponding flexural basins breaking up the foreland.

Sevier versus Laramide

Recognizing the late Mesozoic to early Cenozoic deformation as a continuum of strain from the convergence of the Pacific oceanic crust and North American continental crust, is it appropriate to call these two different orogenic events? In the mid-1800s, the pioneering Western geologist Gilbert (1876) recognized "orographic disturbances" of basement-cored uplifts associated with the Cretaceous–Tertiary (as it was then called) boundary and its importance relative to the

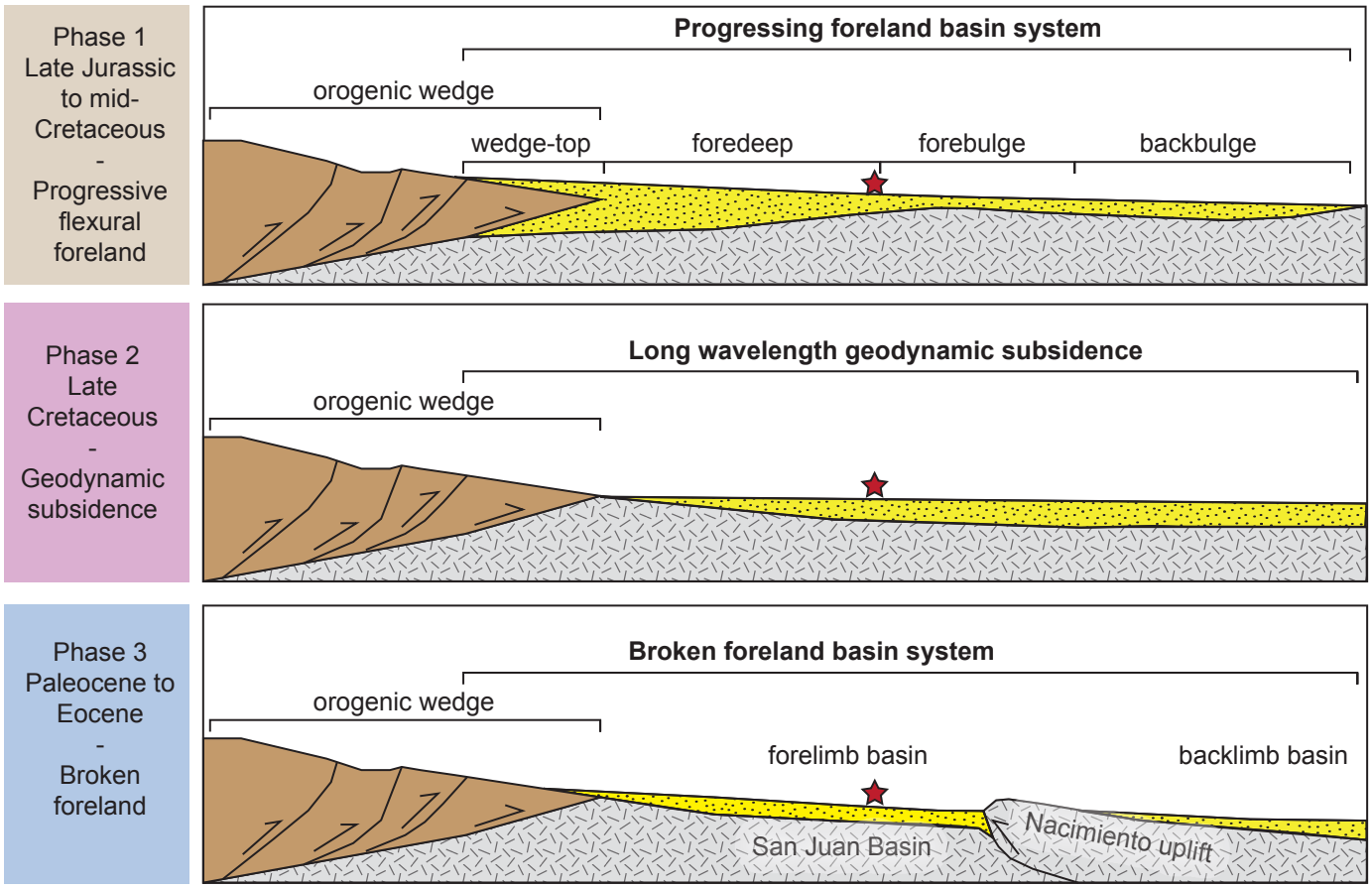

Figure 1.83. Evolution of Cordilleran foreland. Schematic structural cross sections showing the evolution form Phase 1 distal progressive flexural foreland basin system to Phase 2 dynamic subsidence to Phase 3 broken foreland. The red star is the approximate location of the San Juan Basin. Modified from figure 1 in Horton et al. (2022).

distribution of coal. Blackwelder (1914) defined the Laramide orogeny as Maastrichtian to middle Eocene basement-involved deformation east of the "thin-skinned fold belt." Blackwelder recognized an older orogeny to the west called the Jurassic "Nevadan." For this reason, he proposed the western United States was different from the "Cordilleran revolution" being recognized in Canada and South America. Armstrong (1968) defined the Sevier orogeny as a large system of thrusts that "had virtually ceased by the time the Laramide orogeny began east of the Sevier belt in latest Cretaceous time."

Much of Blackwelder's (1914) discussion centered on vertical versus horizontal tectonics. The thought was that the old thin-skinned fold belt stopped and the basement-cored uplifts began. The deformation was too wide and diachronous to be "belonging to one great system instead of two or three systems" (Blackwelder, 1914).

Since the 1970s, new data show that the two orogenies overlap in time and space. Some basement-cored uplifts like the Moxa arch in Wyoming were active as early as the Campanian, synchronous with the Phase 1. Part of the Moxa arch extends under and into the fold belt as the LaBarge platform. New seismic techniques demonstrate the features are physically connected with basement-cored foreland uplifts detaching into the same midcrustal weak layers as the fold belts (Worthington et al., 2015; Erslev et al., 2022).

We now know the fold belt was active during the breakup of the foreland. Dating the nonmarine wedge top deposits with magnetostratigraphy and detrital thermochronology shows that thrust belt deformation continued in the Paleocene after the thrust front stopped advancing. Seismic interpretations in the fold belt show offsets of Eocene strata.

Globally, the depression in front of an orogeny is recognized as part of that orogenic system.

We now know that the Sevier orogeny and the Laramide orogeny overlapped in time and space. Is it time to change what we call them? Suggestions: Call it all Sevier orogeny and use Laramide for a distinct structural style. Or Laramide phase of the Sevier or something else? American Cordillera?

STOP 4B: The Jurassic Entrada Sandstone and Todilto Formations

Waypoint 1.12 [35.9331°, −106.8981°]

The Jurassic Entrada Sandstone is an eolianite present in the San Juan Basin. Although the Entrada Sandstone in the San Juan Basin has yielded only limited, local success from a petroleum resource perspective, its utility as a disposal zone has been realized and is currently being further studied for carbon sequestration potential. The sealing capability of the

overlying Todilto Limestone is a one of the key elements in the storage capacity of the Entrada Sandstone.

The Entrada Sandstone was deposited in an eolian environment during the Jurassic, covering the area that later became the San Juan Basin. The thickness of the Entrada Sandstone varies from 30 to 76 m (100 to 250 ft). Porosity trends follow structural depth. Deeper parts of the San Juan Basin exhibit nearly zero electric log derived porosity; updip/upstructure along the Chaco Slope, the Entrada Sandstone has porosity as much as 25% and permeability from 180–430 md (Vincelette and Chittum, 1981). Stratigraphic traps are formed by the topography of the Entrada erg with overlying, sealing Todilto Formation limestone and anhydrite facies.

The Todilto Formation is present throughout the San Juan Basin and is composed of evaporite and limestone facies. It acts as the seal for Entrada Sandstone reservoir (production and injection) traps. The organic-rich limestone facies of the Todilto Formation are the source and provide the seal for the underlying Entrada Sandstone oil fields. The limestone facies of the Todilto Formation varies from <6 to 42 m (<20 to 140 ft; Ridgely and Hatch, 2013).

There are nine oil fields in the south-central San Juan Basin with cumulative production of 5.764 million barrels of oil (MMBO) 0.498 billion cubic feet (BCF) of natural gas with only four wells currently active (Enverus, 2025).

High-salinity formation water is commonly produced with oil and gas and disposed of in nearby disposal wells targeting nonaquifer or petroleum-bearing reservoir pore space. In the San Juan Basin, Jurassic sandstones including the Entrada Sandstone have been utilized for oil and gas wastewater disposal. There are currently six wells to dispose of saltwater into the Entrada Sandstone permitted in the San Juan Basin (Enverus, 2025).

In the western San Juan Basin, a (now defunct) cryogenic plant originally operated by Anadarko split methane from the associated hydrogen sulfide and carbon dioxide fraction of produced natural gas. Rather than venting these gases to the atmosphere, an acid gas injection (AGI) well, the Pathfinder AGI #1 (30-045-35172), was drilled ~4 km (~2.5 mi) northwest of Kirtland, New Mexico, and operated from 2010 to 2019. The composition of the injected gas was ~80% CO_2 and 20% H_2S (NMOCD, 2025). The Pathfinder AGI #1 well has been temporarily abandoned after the closure of the gas processing plant.

The U.S. Department of Energy (DOE) and the U.S. National Energy Technology Laboratory (NETL) fund CarbonSAFE projects to provide for the design and building of large-scale carbon sequestration projects. Through CarbonSAFE grants, New Mexico Tech (NMT), New Mexico Bureau Geology and Mineral Resources (NMBGMR), New Mexico Petroleum Recovery Research Center (PRRC), and Sandia and Los Alamos National Laboratories have partnered with private companies to study San Juan Basin carbon sequestration with the goal of storing 50 million metric tons of CO_2 per year, mainly in the Entrada Sandstone.

After stop, return to vehicles, turn cars around and retrace the route back to County Road 11.

3.6

13.7 **Turn right (north) and continue north on County Road 11 at junction of San Miguel Road and County Road 11**.

0.2

13.9 The 250-m (820-ft)-high south face of Mesa de Cuba, 10 km (6 mi) distant, is visible at 10:30. The place on the left looks tired.

1.0

14.9 Crest of hill. Before you is the broad valley of San Pablo Arroyo, which heads at approximately 2,900 m (9,500 ft) elevation at Eureka Mesa and drains approximately 8 km (5 mi) of the Sierra Nacimiento mountain front. The valley here is eroded into the thick, soft, Cretaceous Lewis Shale, hence its great width.

0.8

15.7 **Stay straight**. The road to the right leads to San Pablo, another tiny community like San Miguel to south. San Pablo is located along the southernmost perennial stream draining the Sierra Nacimiento in this area. The community supported a small coal mine in the steeply dipping Menefee Formation that supplied homes and the small smelter at San Miguel (Van Hart, 2013). One of the best-preserved examples of a northern New Mexico Spanish colonial house is in San Pablo, currently operated as a bed-and-breakfast.

0.2

15.9 Another new culvert, this one over Señorito Creek. At 9:00, on the broad alluvial plain of Señorito Creek, is a 1,200-m (3,900-ft) graded dirt landing strip. One wonders who needed to land their plane here?

0.7

16.6 Old bridge (as of summer 2024) over Arroyo Hondo, whose headwaters were captured by the steeper Nacimiento Creek 6 km (3.8 mi) northeast of here. Likely due to its decapitation, Arroyo Hondo is far less incised than adjacent streams and seems underfit for its valley. At 2:30, the site of the Nacimiento Mine is plainly visible.

0.9

17.5 Crest of hill. From 9:30 to 11:00, there are good outcrops of the mudstones and sandstones of the Late Cretaceous Kirtland Formation on steep slopes ~300 m (~1,000 ft) to the west.

0.8

18.3 Cross an arroyo with the vernacular name Lagunitas Arroyo. Like Arroyo Hondo to the south, this drainage appears to have been beheaded by Nacimiento Creek, and, as is evident to the left, is largely unincised. At 3:00, the Menefee Mining Corporation operates a humate processing plant at the site of a former sawmill and incinerator.

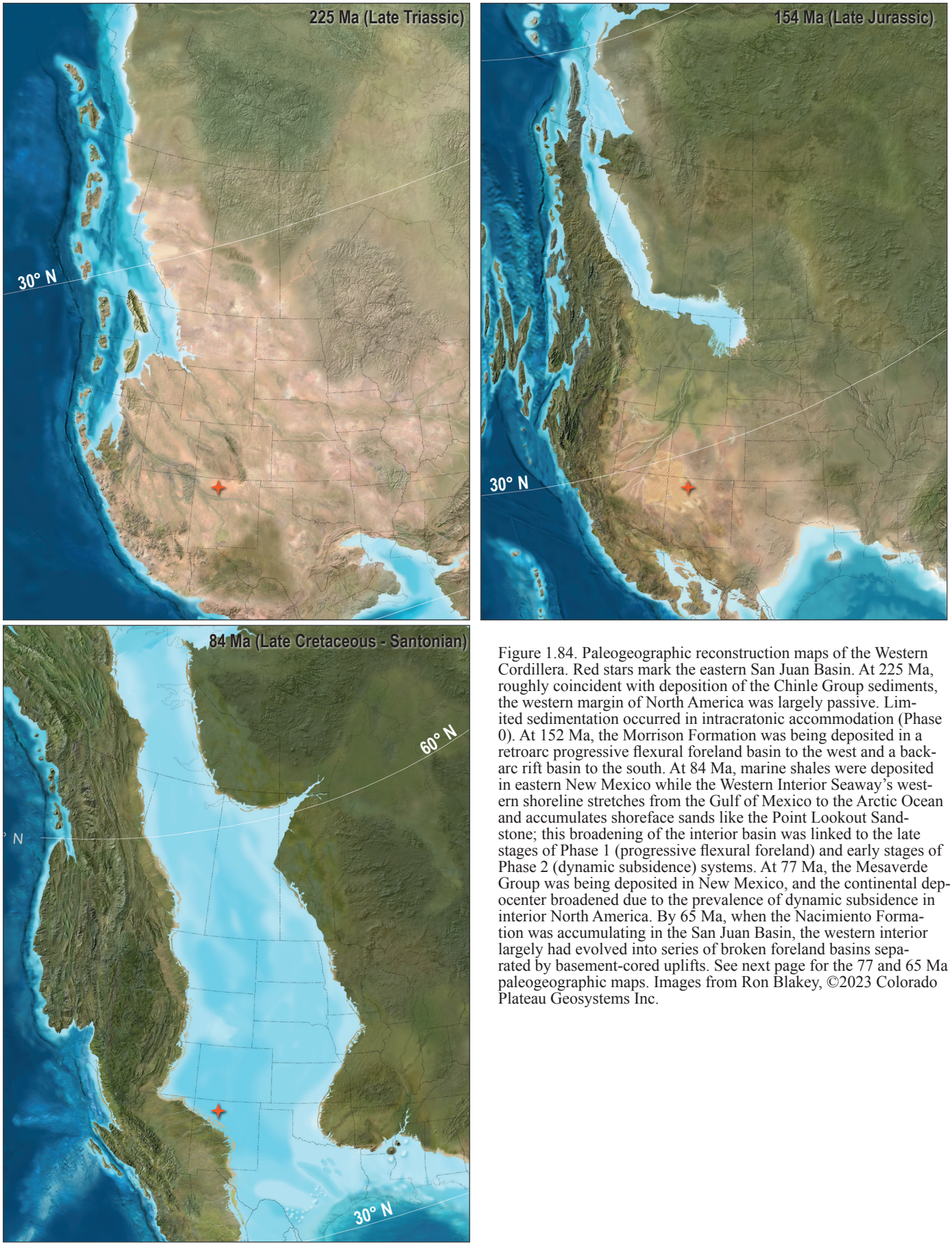

Figure 1.84. Paleogeographic reconstruction maps of the Western Cordillera. Red stars mark the eastern San Juan Basin. At 225 Ma, roughly coincident with deposition of the Chinle Group sediments, the western margin of North America was largely passive. Limited sedimentation occurred in intracratonic accommodation (Phase 0). At 152 Ma, the Morrison Formation was being deposited in a retroarc progressive flexural foreland basin to the west and a back-arc rift basin to the south. At 84 Ma, marine shales were deposited in eastern New Mexico while the Western Interior Seaway's western shoreline stretches from the Gulf of Mexico to the Arctic Ocean and accumulates shoreface sands like the Point Lookout Sandstone; this broadening of the interior basin was linked to the late stages of Phase 1 (progressive flexural foreland) and early stages of Phase 2 (dynamic subsidence) systems. At 77 Ma, the Mesaverde Group was being deposited in New Mexico, and the continental depocenter broadened due to the prevalence of dynamic subsidence in interior North America. By 65 Ma, when the Nacimiento Formation was accumulating in the San Juan Basin, the western interior largely had evolved into series of broken foreland basins separated by basement-cored uplifts. See next page for the 77 and 65 Ma paleogeographic maps. Images from Ron Blakey, ©2023 Colorado Plateau Geosystems Inc.

0.3
18.6 As we continue upsection, the first outcrops of the Paleogene Ojo Alamo Sandstone appear on the small mesa here.

0.3
18.9 **Stay straight**. The turnoff to the left leads to the Sandoval County Fairgrounds. The name of the road gives you a hint as to the biggest attraction at the fair.

0.1
19.0 Sandoval County Soil and Water Conservation District office at left.

0.9
19.9 The curiously named Southern All Around Road enters at right. Just ahead on the left is the last Ojo Alamo Sandstone outcrop before entering "downtown" Cuba, which is built upon alluvium of the Rio Puerco and its tributaries.

0.2
20.1 Cuba Ranger Station of the Santa Fe National Forest. The Cuba Ranger District is noncontiguous and stretches 80 km (50 mi) from the Jicarilla Apache Nation and the Chama River canyon in the north to the northern border of Jemez Pueblo in the south. Dead ahead is the Cuban Lodge, one of several old-fashioned motels operating in Cuba.

0.1
20.2 **Right turn (north) onto U.S. Route 550.**

0.2
20.4 The Cuba Laundromat at left.

0.2
20.6 Cattle-Lack Feed store at right. The man that will pun will pick a pocket.

0.2
20.8 At right, a liquor store, then a grocery. Visit in the order of your choosing.

0.2
21.0 Downtown Cuba. Located at an incredible intersection of abundant natural resources—game, irrigable land, perennial water, timber, and travel routes—Cuba has been the site of human occupation for at least four millennia (Post, 1994).

0.3
21.3 Bridge over Rio Puerco.

0.4
21.7 **Right turn (east) onto Los Pinos Road. Return to Circle A Ranch**.

End of Day 1 Road Log

Chamisa (Ch'ildiilyésiits'óóz, *Ericameria nauseosa*) growing in the engine compartment of a 1959 Studebaker pickup buried in the alluvium of Escavada Wash.